Synthesis of Non-Isocyanate Polyurethanes from Waste-Derived Fish Oil

by

© Courtney M. Laprise

A thesis submitted to the
School of Graduate Studies
in partial fulfillment of the requirements for the degree of

Master of Science (M.Sc.)

Department of Chemistry
Memorial University of Newfoundland
St. John's, Newfoundland and Labrador, Canada

July, 2019

St. John's Newfoundland

Abstract

Waste-derived fish oil (FO) can be epoxidized, reacted with CO_2 to produce cyclic carbonates, then reacted with an amine to form non-isocyanate polyurethane materials. The FO used was previously extracted from the by-products produced at fish processing plants, including heads, bones, skin and viscera. Extracting oil from these waste products and using it as a feedstock reduces the amount of waste generated by fish processing plants. Three different methods were used for the epoxidation of the FO: (i) oxidation by *3*-chloroperoxybenzoic acid, (ii) oxidation by hydrogen peroxide and acetic acid, catalyzed by sulfuric acid, and (iii) oxidation by hydrogen peroxide catalyzed by formic acid. A gate-to-gate life cycle assessment of the epoxidation methods was performed, showing the formic acid reaction is the greenest route to the formation of FO epoxides. Synthesized FO epoxides were reacted with CO_2 to yield FO cyclic carbonates. The optimum conditions used 3.9 mol% tetrabutylammonium bromide and 2.0 mol% ascorbic acid (vitamin C) with respect to epoxy-groups in the starting material to form cyclic carbonates with a conversion of 90%. The products were characterized by ^{1}H and ^{13}C NMR spectroscopy, IR spectroscopy, and TGA. The FO carbonates were used to produce sustainable, bio-sourced polyurethanes. Using a biomass-derived amine, non-isocyanate polyurethane materials were synthesized and preliminary studies towards their degradation in aqueous solutions was performed. This process could lead to new opportunities in waste management, producing valuable materials from a resource that is otherwise underutilized.

Acknowledgements

First of all, I would like to thank my supervisors and committee members, Dr. Francesca Kerton, Dr. Christopher Kozak, and Dr. Kelly Hawboldt for the opportunity to work on such an interesting project, as well as all of the support with research and writing throughout my project. They were always available to answer questions and made the research enjoyable and interesting. I also want to thank Dr. Kelly Hawboldt's research group, who provided me with the waste-derived fish oil throughout my project.

I want to give a large thank you to current and past Green Chemistry and Catalysis group members who helped me through the rough times over my degree. Especially over the last year of my program, they were very helpful, supportive, and gave great life advice. I would also like to thank NSERC, the School of Graduate Studies, and the Memorial University Department of Chemistry Dr. Liqin Chen Graduate Award for funding.

Lastly, but most importantly, I would like to thank my family and close friends who encouraged me and helped me complete this tremendous accomplishment. Without their support and the occasional shoulder to lean on, I would not be where I am today. In the hardest times, they were there for me, and provided me with the help I needed to keep going.

Table of Contents

List of Tables

List of Figures

List of Schemes

List of Abbreviations and Symbols

ADP:	abiotic depletion potential
AP:	acidification potential
BIOACC:	bioaccumulation
BPh_3:	triphenylborane
$CaCO_3$:	calcium carbonate
CALB:	lipase B from *Candida antarctica*
CH_2Cl_2:	dichloromethane
CH_3COOH:	acetic acid
ChCl:	choline chloride
ChCl-OxA:	choline chloride-oxalic acid deep eutectic solvent
CLSO:	carbonated linseed oil
CO_2:	carbon dioxide
CpLIP:	Lipase/acyltransferase from *Candida parapsilosis*
CSBO:	carbonated soybean oil
DES:	deep eutectic solvent
DHA:	docosahexaenoic acid
DMC:	dimethyl carbonate
EDX:	energy dispersive X-ray
EFO:	epoxidized fish oil
ELSO:	epoxidized linseed oil
EMO:	epoxidized methyl oleate
EOA:	epoxidized oleic acid
EPA:	eicosapentaenoic acid

ESBO:	epoxidized soybean oil
ETFO:	epoxidized tablet fish oil
$FeCl(O_2N_2)$:	iron(III) amino-bis(phenolate) complex
FO:	fish oil
GC-MS:	gas chromatography mass spectrometry
GW:	global warming potential
h:	hour(s)
H_2O_2:	hydrogen peroxide
ha:	hectare
HCOOH:	formic acid
INGTP:	human toxicity by ingestion potential
INHTP:	human toxicity by inhalation potential
IR:	infrared
IS:	internal standard
K_2HPO_4:	potassium phosphate dibasic
KCl:	potassium chloride
KH_2PO_4:	potassium phosphate monobasic
K_{OC}:	soil sorption coefficient
K_{OW}:	octanol-water partition coefficient
LCA:	life cycle assessment
MC:	Middle Cove Beach, NL
m-CBA:	3-chlorobenzoic acid
m-CPBA:	3-chloroperoxybenzoic acid
$MgCl_2$:	magnesium chloride

$MgSO_4$:	magnesium sulfate
min:	minute(s)
MO:	methyl oleate
MOF:	metal organic framework
Na_2SO_3:	sodium sulfite
NaCl:	sodium chloride
$NaHCO_3$:	sodium bicarbonate
NIPU:	non-isocyanate polyurethane
NMR:	nuclear magnetic resonance
OA:	oleic acid
OD:	ozone depletion potential
OxA:	oxalic acid
PBDE:	polybrominated diphenyl ether
PER:	persistence
PPNCl:	bis(triphenylphosphine)iminium chloride
PU:	polyurethane
SEM:	scanning electron microscope
SF:	smog formation potential
T:	temperature
t:	time
TBAB:	tetrabutylammonium bromide
TBAI:	tetrabutylammonium iodide
TFO:	tablet fish oil
T_g:	glass transition temperature

Chapter 1: Introduction

1.1 Green Chemistry

Green chemistry is a large, interdisciplinary field, that is governed by the same core ideas. These overarching ideas involve reducing the hazard and environmental impact of chemistry, both in the processes used and the products synthesized. This is through preventing primary pollution, instead of waste treatment. In an effort to better define green chemistry, Anastas and Warner outlined principles that would inherently make chemistry safer for both humans and the environment (**Figure 1.1**).[1] These principles are a good set of guidelines to perform safer and greener chemistry.

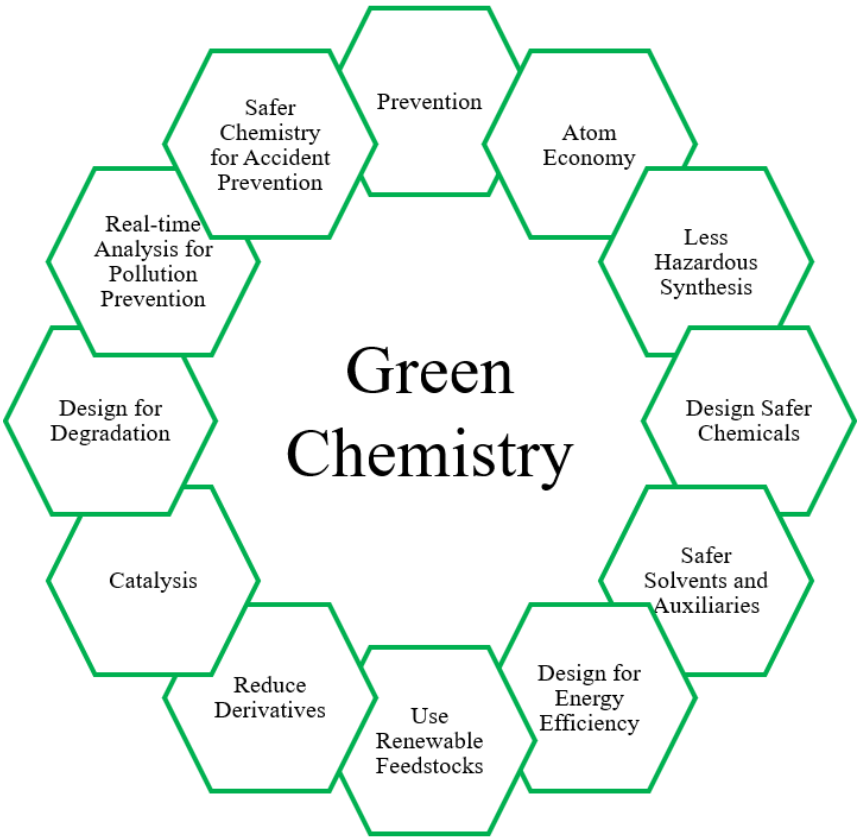

Figure 1.1. The 12 principles of green chemistry.

Even before the advent of these principles, metrics that could be used for the qualitative determination of the greenness of a reaction have been proposed. In 1991, Trost introduced the concept of atom economy, which is the percentage of atoms in all reagents used that are in the final desired product.[2] Before this, metrics like stereoselectivity or regioselectivity were considered more important. In theory, a 100% atom economic reaction would indicate that all reagents are combining to form the product, with no by-products and therefore, in theory, no waste is generated. Atom economy assumes stoichiometric quantities of the reagents, a 100% yield, and ignores the solvents or chemicals used in the workup of the reaction. Atom economy can therefore be misleading in the true environmental impact of a reaction but is a good initial indicator.

In 1994, Sheldon introduced the concept of environmental- or E-factor, which is a ratio of the mass of waste to the mass of product produced, excluding water.[3] The reasoning for excluding water was that it could lead to a large skewing of the E-factors,[4] but ignoring the amount of water can skew the E-factors to appear more favourable for the process, appearing to generate less waste. In the specialty chemicals sector, the cost of waste can approach 40% of production costs, and in cases where highly hazardous waste has to be disposed of, this can become the most significant component of manufacturing costs.[5] An accurate depiction of the amount of waste generated by a process is therefore very important. In the pharmaceutical industry, the trend is to include water in the calculation of the E-factor.[4] The introduction of the E-factor allowed for the inclusion of solvents and auxiliary chemicals in the determination of the amount of waste generated, and therefore the greenness of the reaction. The metric was inspired by the fine chemical industry in the

1980s, specifically a pharmaceutical plant that was shut down when the cost of waste disposal approached that of its generated income.[4] While the E-factor is a quick calculation that can be easily performed, it should not be relied on as a clear indication of the greenness of a reaction, especially when comparing multiple routes to a desired product, as it does not take into account the toxicity or hazard of the reagents used or the waste produced.

Further improving on this idea of accounting for waste and comparing methods with respect to their environmental impact, a life cycle assessment (LCA) of a route can be performed. Performing an LCA allows for a comparison of processes based on many different environmental and health factors. LCAs have been around in many different forms, with the first partial LCAs dating as far back as the late 1960s and early 1970s, before becoming the standardized process today.[6] This standardization gives goals and guidance on defining the scope, developing the LCA, and the interpretation of the results.[7] Defining the scope of the assessment will determine how detailed and complex the assessment will be. An LCA can include all stages of production of a product, including the production of all components that are included in the process of interest, or include processes which occur after the production and distribution of the product such as its recycling or disposal. Performing an LCA with this level of detail requires a large amount of time and data, both of which may be difficult to obtain. If an LCA is being performed in order to compare multiple processes, one of which is in the research or development phase, a full scale LCA may be too difficult to perform as the required data is not readily available.[8] A simpler LCA can be performed by ignoring the pre- and post-production details and only focusing on the process itself, or a gate-to-gate LCA. Using this method,

the processes can be compared using the same parameters, while requiring less data and time.

In 2011, Mercer, Andraos and Jessop introduced a method to perform an LCA that simplifies it for use in undergraduate or graduate level green chemistry courses.[9] It follows the standards and conventions of an LCA, on a gate-to-gate level, using nine different metrics for the comparison of different processes. This route was used for the determination of the greenest route for the formation of the fish oil (FO) based epoxides in Section 2.2.3.

1.2 Conventional Polyurethane Synthesis

Polyurethanes (PU) were first reported in 1947 by Otto Bayer, and were synthesized through the reaction of an isocyanate with a polyol.[10] In the reaction, the hydroxyl groups of the polyol react with the isocyanate functional group forming a urethane linkage (**Scheme 1.1**). Since their discovery, PUs have been produced industrially for the production of foams, coatings, adhesives, and elastomers.[11] PU foams are created through the addition of small amounts of water, which reacts with the isocyanate group to form carbon dioxide (CO_2) and an unstable carbamic acid (**Scheme 1.2**).[12] By 2021, the projected worldwide consumption of PUs will be over 79 billion USD.[13] Industrially, the isocyanates used are formed from amines using phosgene, a toxic gas, which is in turn derived from chlorine and carbon monoxide.[14] Isocyanates themselves are highly toxic and water sensitive, leading to many special safety precautions that must be implemented. Several industrially used diisocyanates are known to have negative impacts on human health, and the formed PUs can break down into carcinogenic aromatic amines.[14,15]

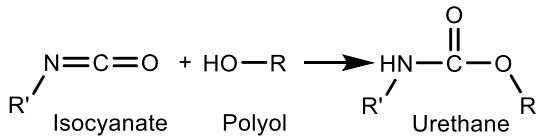

Scheme 1.1. Urethane formation from a polyol and isocyanate.[12]

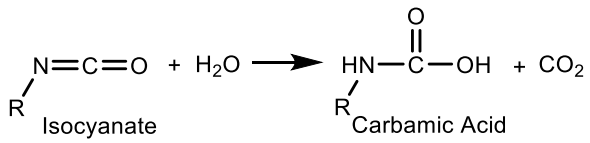

Scheme 1.2. Reaction of isocyanate with water to form self-blown polyurethane foams.[12]

PU polymers and blown foams, while they are widely used in the furniture and automotive industry, are easily ignited, burn quickly, and evolve large amounts of smoke and toxic gases.[16] To mitigate their high flammability, flame-retardant additives are commonly added, many of which are polybrominated diphenyl ethers (PBDEs) that have serious health hazards and are considered persistent organic pollutants. Because of this, alternatives have been widely studied,[17] but much more work needs to be done before PUs can be considered harmless to human health and the environment.

The synthesis of PUs can be made safer and better for the environment by invoking the principles of green chemistry. One way that PU synthesis has been made safer is via use of an overall greener reaction process and by utilizing biomass-derived chemicals. Generally, the polyol is derived from plant-based biomass which is then reacted with an isocyanate for curing. Polyols that are derived from vegetable oils are frequently used, as they can be easily synthesized with a varying number of hydroxyl groups depending on the amount of unsaturation, or using oils with large amounts of ricinoleic acid, a natural polyol.

In 2000, Javni et al. synthesized several vegetable oil-based polyols by first epoxidizing the oils, then converting the epoxy groups to hydroxyl groups.[18] The formed polyols could then be reacted with a modified diphenyl methane diisocyanate to give a partly bio-derived PU. Many vegetable oils were epoxidized and used to form polyols, including olive, peanut, canola, corn, soybean, safflower, and sunflower oil. Castor oil is a natural polyol, as it is composed of mostly ricinoleic acid (**Figure 1.2**). While the other vegetable oils are derived from edible plants, 80% of the world's supply of castor oil is produced from non-edible plants,[19] allowing for a stable feedstock without impacting food production. The castor oil-based PU showed a higher stability than that of soybean oil, and under air, showed a greater thermal stability than the conventional polyoxypropylene-based PU.[18]

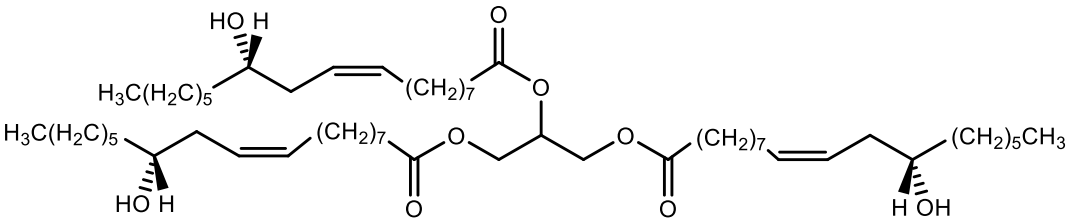

Figure 1.2. Structure of the major component of castor oil.[14]

Soybean oil is a commonly used bio-based oil for the production of PU materials as the unsaturated double bonds in the fatty acids can be converted to hydroxyl functionalities for use in conventional PU synthesis (**Figure 1.3**). In 2011, Tan et al. used a commercially available soybean oil-based polyol to form PU foams.[20] Using polymeric methylenediphenyl diisocyanate, a chain extender, gelation catalyst, blowing catalyst and a silicone surfactant, soybean-based PU foams could be synthesized that had a higher glass

transition temperature (T_g) than their petroleum-based counterparts. The foams were similar in density and cellular morphology, but foams with 100% soybean oil-derived polyol aged much faster due to their higher gas permeation.

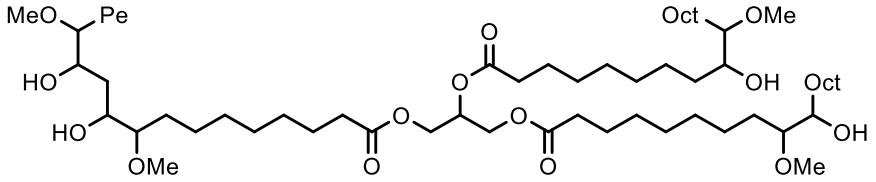

Figure 1.3. Structure of soybean oil-derived polyol.

In 2016, Alagi et al. synthesized soybean oil-based polyols by reacting soybean oil with 2-mercaptoethanol for different reaction times.[21] By differing the reaction time, the number of primary hydroxy functional groups could be controlled, and therefore so could the amount of branching in the PU. The resulting polyol could then be reacted with a prepolymer formed from reacting another diol with 4,4'-methylenebis(cyclohexyl isocyanate) but unfortunately this isocyanate is toxic and a chronic health hazard.

These materials, while incorporating biomass-derived polyols, still use isocyanates to produce PU materials, which is the main health hazard in their production. Many of the commonly used isocyanates are asthmagens or serious skin irritants.[15] Two of the most commonly used isocyanates, methyl diphenyl diisocyanate and toluene diisocyanate (**Figure 1.4**), are known carcinogens[22] that are highly toxic, with low LC_{50} values (**Table 1.1**).[23] In order to make the synthesis of PU materials greener, not only does biomass need to be incorporated, but the use of isocyanates needs to be avoided.

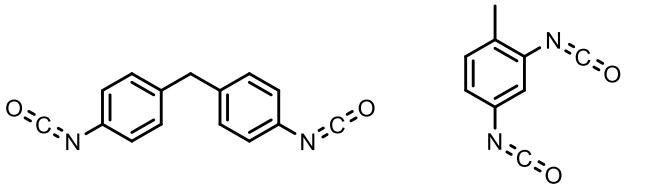

Figure 1.4. Structures of methyl diphenyl diisocyanate and toluene diisocyanate.

Table 1.1. LC_{50} values of two industrially used isocyanates.

Isocyanate	LC_{50} (ppm)
Methyl diphenyl diisocyanate	36.0
Toluene diisocyanate	49.0

1.3 Green Route to Plant Oil-Based Non-Isocyanate Polyurethanes

Reducing the use of isocyanates and moving towards utilizing bio-based materials has been of large interest for several decades, as it circumvents the use of toxic compounds in the production of industrially important materials.[24,25] The number of publications on biomass and renewable feedstocks has been rapidly increasing, with over 25,000 published in 2018 (**Figure 1.5**). As shown in Section 1.2, biomass-derived chemicals can be incorporated into the production of PU materials through the conventional isocyanate route, but in order to completely remove the use of toxic isocyanates and phosgene, a different route must be used.

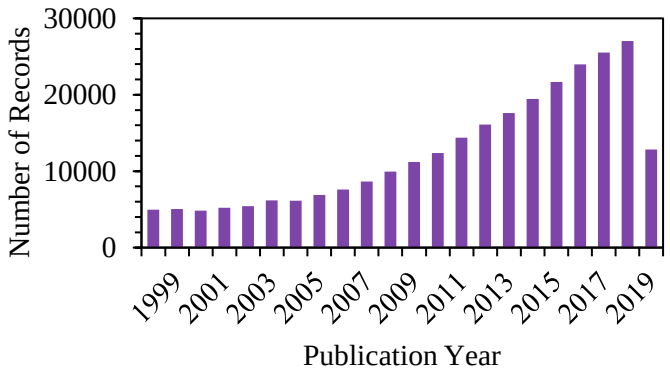

Figure 1.5. Number of publications per year on biomass and renewable feedstocks (From Web of Science (21/06/2019), articles, topic = biomass OR renewable AND feedstock).

In 1979, the very first isocyanate-free synthesis of a PU material was reported, becoming the first true non-isocyanate PU (NIPU).[26] The material was produced through a polycondensation reaction of diols with biscarbamates (**Scheme 1.3**). This removed the use of isocyanates as a reactant but formed low molecular weight by-products. Another route to form NIPU materials is through a polyaddition reaction of an organic cyclic carbonate with an amine (**Scheme 1.4**). This polyaddition route to form NIPUs is preferable to the polycondensation reaction as it is better characterized in the literature, is more economic as solvents and catalysts are not required, by-products are minimal, and the final material can be post-functionalized due to the presence of the hydroxyl group.[27] These hydroxyl groups make these materials polyhydroxyurethanes (PHUs), which are a subset of the NIPU classification. The polyaddition reaction can be performed using biomass-derived cyclic carbonates, therefore removing isocyanates while still incorporating biomass into the material. Soybean oil-derived cyclic carbonates were first synthesized in 2004, and were subsequently used to make NIPU materials by curing with ethylenediamine.[28]

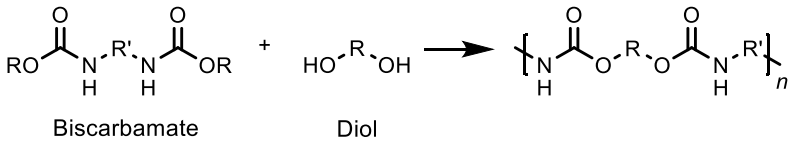

Scheme 1.3. Polycondensation reaction forming non-isocyanate polyurethane.

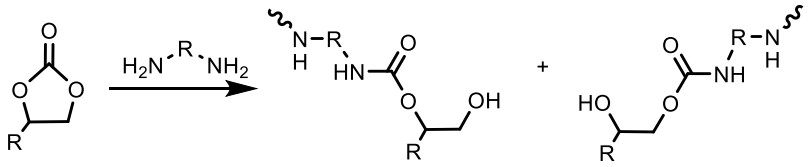

Scheme 1.4. Polyaddition reaction of cyclic carbonate with an amine forming non-isocyanate polyurethane.

Since the first synthesis of soybean oil-derived cyclic carbonates, many other vegetable-based oils have been used including linseed,[29,30] cottonseed,[31] and sunflower[32,33] oils. These bio-based cyclic carbonates are synthesized through the coupling of CO_2 and epoxides, which are in turn derived from oxidizing the vegetable-based oils. Vegetable-based oils, such as soybean oil, are very intriguing starting materials for NIPU synthesis, as they are a potentially renewable resource that is non-toxic. Soybean oil, which is one of the most widely used bio-derived oils for NIPU synthesis, had a worldwide production of over 330 million tonnes in 2016, with the largest producers being USA, Brazil and Argentina (**Figure 1.6**).[34] The production of land-based crops uses large amounts of land space, and therefore competes with food production for land space. In 2016, the amount of arable land on Earth was 1.4 billion ha,[34] much of which is being lost to pollution or erosion due to overuse and use of fertilizers.[35] In order to not compete with food production and not overuse land for growing crops, ocean-based biomass is an attractive alternative. A

start-up out of Berkeley, California focuses on using triglycerides from algal oils for synthesizing polyols that can then be reacted with isocyanates to make PU materials for surfboards.[36] This allows for the use of biomass-derived materials to be incorporated into PU without using large amounts of land space to grow crops. In a similar manner, oils derived from fish can be a green alternative to land-based crops for the synthesis of NIPU materials.

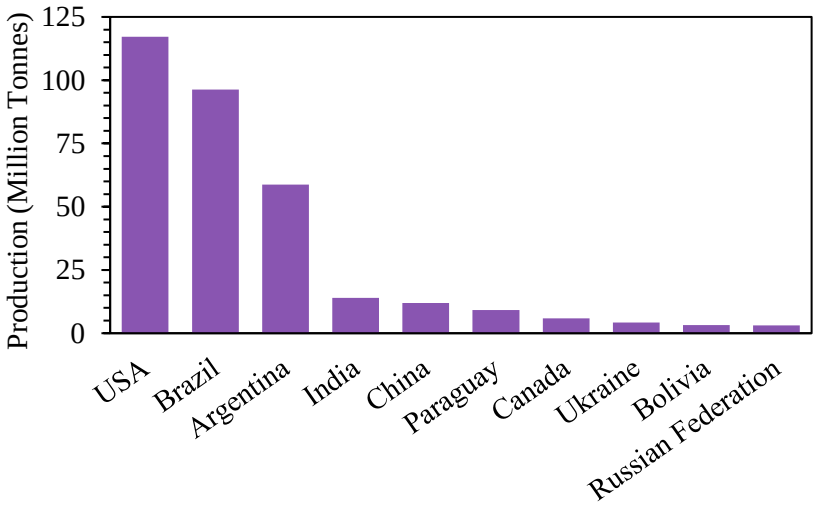

Figure 1.6. Soybean production by country.[34]

Fish processing generates large amounts of waste that is presently used to produce low cost fertilizers or dumped at sea.[37] With approximately 50 wt.% of the total catch being discarded as waste,[38] there is a large amount of material available for use as a feedstock for NIPU synthesis. With increasing production in the aquaculture industry to meet the growing demands of a growing population, the amount of waste produced will also increase. This waste will need to be disposed of, at a cost to the industry. Since 1991, the total finfish production in Canada has steadily increased (**Figure 1.7**), and in Atlantic

Canada alone, the waste from the industry reached over 418,000 metric tonnes per year in 2002.[39] The amount of recoverable oil from this waste varies considerably depending on the species, season, and tissue present in the waste material, but can account for up to 50% of the waste material.[37] By utilizing this material for the production of NIPUs, it does not compete with food production or use large amounts of land space.

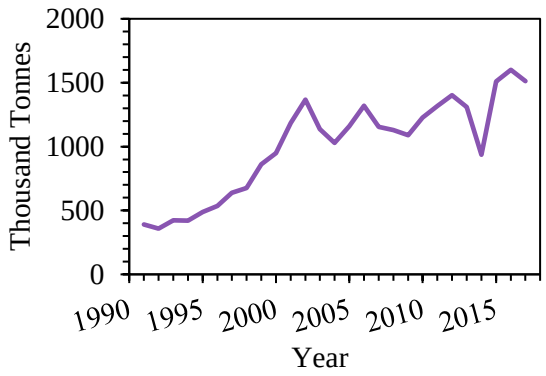

Figure 1.7. Total Canadian finfish production per year from 1991-2017.[40]

Within this thesis, the literature route for the formation of bio-based NIPUs was followed for the formation of waste-derived FO-based NIPUs,[29,33,41] with the oil first oxidized to form epoxidized FO (EFO), followed by a 100% atom economical reaction between the epoxide and CO_2, forming a cyclic carbonate, or carbonated FO (CFO). In the final step, the NIPU is formed by reacting the cyclic carbonate with an amine (**Scheme 1.5**).

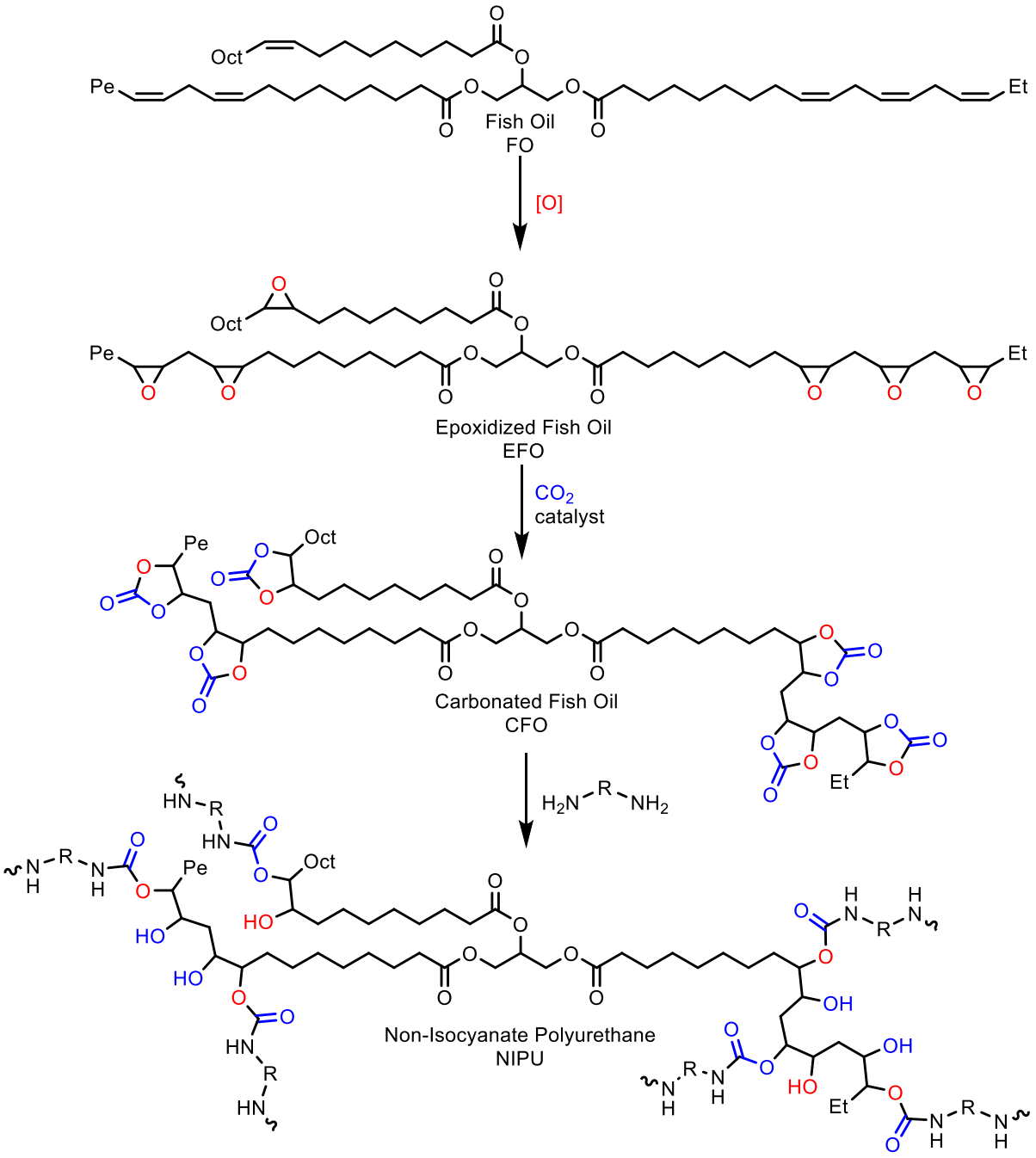

Scheme 1.5. Synthesis of NIPU from waste-derived FO.

1.3.1 Methods Used for Synthesis of Bio-Derived Epoxides

Many biomass-derived oils have been used for the synthesis of epoxides, using a variety of catalysts and reaction conditions. In 2013, Saithai et al. reported using lipase B from *Candida antarctica* (CALB), or a lipase/acyltransferase from *Candida parapsilosis* (CpLIP) with hydrogen peroxide (H_2O_2) for the formation of epoxidized soybean oil (ESBO).[42] They also performed a chemical epoxidation using H_2O_2 and formic acid (HCOOH), catalyzed by sulfuric acid (H_2SO_4), for comparison with the enzymatic epoxidation reactions. Using the different methods, ESBO with varying numbers of epoxide groups were synthesized, ranging from 4.60 to 2.25 per molecule, with the highest conversion being 78%. The formed ESBO was analyzed for the content of free fatty acids. When HCOOH and H_2SO_4 were used the product had a low free fatty acid content, at less than 0.6%, while the reaction with CpLIP had a free fatty acid content of 46% to 48%. The formed epoxides could then be used to form copolymers with methyl methacrylate.

Bhalerao and co-workers used CALB, as a catalyst for the ultrasound assisted formation of ESBO.[43] Within 5 h, they achieved a conversion of 91.2% to the epoxide. Without the use of ultrasound, the conversion to the epoxide dropped to 27.6% within the same reaction time. The reaction uses toluene as a reaction solvent, which is highly flammable and a health hazard, but the reaction allows for recycling of the catalyst. The solid catalyst could be recovered by a simple filtration, washed with toluene and reused six times, with a slight decrease to 59% relative conversion after the sixth reuse.

Simple carboxylic acids, such as HCOOH and acetic acid (CH_3COOH), are commonly used as catalysts for the epoxidation of biomass-derived oils. In 2018, Meadows

et al. used HCOOH or CH_3COOH with H_2O_2 to compare their relative reactivities towards synthesizing ESBO.[44] In the aqueous phase of the reaction, the carboxylic acid used reacts with H_2O_2 to form a peracid, either performic or peracetic acid. This further reacts with the double bonds in the organic phase to oxidize them and form the desired epoxide groups. A comparison of HCOOH with CH_3COOH at different reaction times and concentrations of H_2O_2 showed that HCOOH was the more effective oxygen carrier, achieving higher conversions to the epoxide. Under optimized conditions, the ESBO was formed with 98% conversion of the alkenes within 6 h using a molar ratio of oil:formic acid:H_2O_2 of 2:1:4.

In 2002, Marks and Larock used 0.5 mol% of methyltrioxorhenium, 12.0 mol% of pyridine, and 150 mol% of H_2O_2 to fully epoxidize capelin FO over 6 h.[45] A FO ethyl ester was also epoxidized, using 0.34 mol% of methyltrioxorhenium, 8.15 mol% of pyridine, and 1.03 equivalents of H_2O_2, in an 86% yield. The FOs were also reacted with Wilkinson's catalyst, $[RhCl(PPh_3)_3]$, to conjugate the polyunsaturated fatty acids in the FO, followed by the epoxidation reaction. While the conjugation of the oils occurred in high yields, epoxidation of these conjugated FOs resulted in only partial epoxidation and the ^{13}C and ^{1}H nuclear magnetic resonance (NMR) spectra were too difficult to interpret. Except the limited examples just discussed, FO has otherwise not been investigated to produce epoxides.

1.3.2 Catalysts Used for Coupling of Bio-Derived Epoxides and CO_2

Utilizing CO_2 as a chemical reactant poses a challenge, as it is a very stable small molecule,[46] and therefore requires a catalyst in order to activate it for reaction. While the rising concentration of CO_2 in the Earth's atmosphere will require policy changes and

changes in regulations, it is possible for chemistry and catalysis to contribute to the reduction of CO_2 in the atmosphere via its capture and utilization.[47,48] While one carbon capture and utilization process will not fix the problem alone, each use for CO_2 can contribute to the solution. Utilizing CO_2 for various syntheses is highly attractive, especially from a green chemistry perspective. CO_2 is non-toxic, non-flammable, inexpensive, and readily available. The potential environmental benefits of using CO_2 are very attractive but capturing and using an inert molecule like CO_2 will require large amounts of energy that may offset the potential benefits. In order to properly assess the true impact of a carbon capture and utilization process, an LCA on the full life cycle of the material is required.[49,50]

A wide range of catalysts have been synthesized and reported for the activation of CO_2 for the production of cyclic carbonates.[51,52] In 2015, Alves et al. developed a series of organic molecules for the synthesis of carbonated linseed oil (CLSO) from epoxidized linseed oil (ELSO) and CO_2.[30] Tetrabutylammonium bromide (TBAB) was used as the organo-catalyst (**Figure 1.8**), with a hydrogen bond donor (HBD) used as an activator for the reaction. A series of 17 HBDs were tested, with the four best activators being 1,3-bis(2-hydroxyhexafluoroisopropyl)benzene (HBD1), hexafluoro-2-(*p*-tolyl)isopropanol (HBD2), perfluoro-*tert*-butanol (HBD3) and pyrocatechol (HBD4) (**Figure 1.9**). The reaction to form CLSO was performed using 2.2 mol% of both TBAB and the HBD, at 120 °C and a pressure of 50 bar of CO_2. Quantitative conversion could be obtained after 10 h, without using any organic solvents, but relatively high temperatures and pressures were

used, and so there is a need to develop more efficient catalysts that would be active under milder conditions.

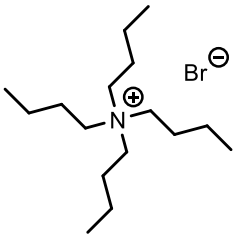

Figure 1.8. Structure of organo-catalyst TBAB.

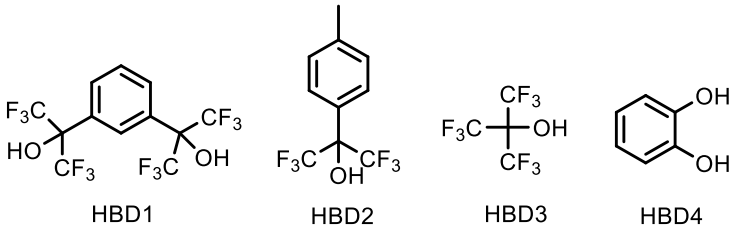

Figure 1.9. HBDs used for the synthesis of CLSO from ELSO and CO_2.

Büttner and co-workers reported an iron-based catalyst for the synthesis of cyclic carbonates from a wide range of epoxides.[53] Using tetra-*n*-octylphosphonium bromide as the catalyst, a wide range of iron salts were tested for use as a cocatalyst, with iron(III) chloride giving a high conversion, as well as the highest selectivity for the cyclic carbonate. Using 2 mol% of tetra-*n*-octylphosphonium bromide, 0.25 mol% of iron(III) chloride, at 100 °C and 50 bar CO_2, for 24 h, 5 different vegetable oil-derived cyclic carbonates, based on linseed, soybean, and sunflower oil, were prepared with quantitative conversions of the epoxide groups to carbonates.

In 2016, Kerton and co-workers reported the use of several iron(III) amino-bis(phenolate) complexes for the synthesis of cyclic carbonates from CO_2 and several epoxides.[54] The iron complexes used were synthesized from several different ligands, producing a range of catalysts with different activities towards cyclic carbonate formation (**Figure 1.10**). Using several co-catalysts and reaction conditions, the catalysts were tested using propylene oxide. The catalyst with *t*-butyl groups as both substituents on the phenolate rings showed promising activity towards the formation of cyclic carbonates, with a 74% conversion of propylene oxide using 0.025 mol% of the iron catalyst, 0.1 mol% TBAB, at 100 °C and 20 bar CO_2 for 22 h.

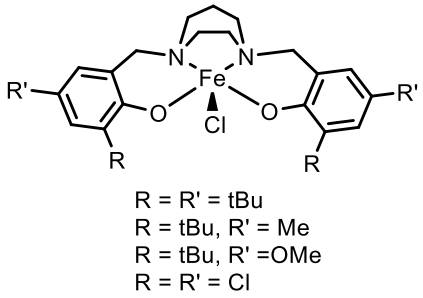

Figure 1.10. Iron(III) amino-bis(phenolate) complexes reported by Kerton and co-workers.[54]

In 2016, Babu et al. reported the use of a metal organic framework (MOF) for the room temperature formation of cyclic carbonates from propylene oxide.[55] A micro-mesoporous MOF, UMCM-1-NH_2, was used along with TBAB for the reaction at 1 bar CO_2 and room temperature for 24 h. The MOF contained an amine functionality, as well as Zn_4O clusters, both of which are thought to be important in the mechanism for the reaction. The reaction produced the desired cyclic carbonate in a 90% conversion. When performed

with either the MOF or TBAB alone, neither produced a significant amount of product. A reaction was also performed with a mixture of the catalyst precursors, and did not show any catalytic activity, showing the importance of the environment that the porous MOF provides for reaction.

1.3.3 Methods Used for Synthesis of Non-Isocyanate Polyurethanes from Cyclic Carbonates

NIPU materials can easily be formed from cyclic carbonates by reacting them with an amine. The amine ring-opens the cyclic carbonate and forms a urethane linkage with a hydroxyl group. In 2012, Bähr and Mülhaupt reported the preparation of linseed and soybean oil based NIPU materials.[29] The CLSO used had a higher carbonate content than the CSBO. By mixing the two carbonates in different mass ratios, the carbonate content was varied between 20.8 wt% and 26.7 wt%. The resulting mixtures were cured using ethylenediamine, 1,4-butanediamine, or isophorone diamine, a cycloaliphatic amine. The materials produced varied in their mechanical properties, with the highest T_g at 60 °C using CLSO alone with isophorone diamine. The materials were tested for swelling in water, and due to the high number of hydroxyl groups, the water uptake was significant. With the increasing carbonate content, and therefore increasing number of hydroxyl groups, the amount of water absorbed also increased. This was reduced when the more hydrophobic isophorone diamine was used.

Bähr and co-workers reported the use of cyclic limonene dicarbonate for the formation of NIPU materials (**Scheme 1.6**).[56] Limonene is a sustainable and bio-derived

chemical that is produced by many plants, and can be extracted from waste citrus fruits.[57,58] Despite this, limonene and other terpenes have not been widely investigated for the formation of NIPU materials.[56] In the synthesis of limonene-derived linear NIPUs, the cyclic carbonate was reacted with different amines: 1,4-butanediamine, 1,6-hexamethylenediamine, 1,12-dodecanediamine, and isophorone diamine. Polyfunctional amines were also used to form branched NIPU networks. When a hyperbranched amine, Lupasol® was used, the resulting NIPU was very stiff and brittle with a T_g ranging from 55 °C to 62 °C. Linear NIPUs made with isophorone diamine gave the highest T_g at 70 °C.

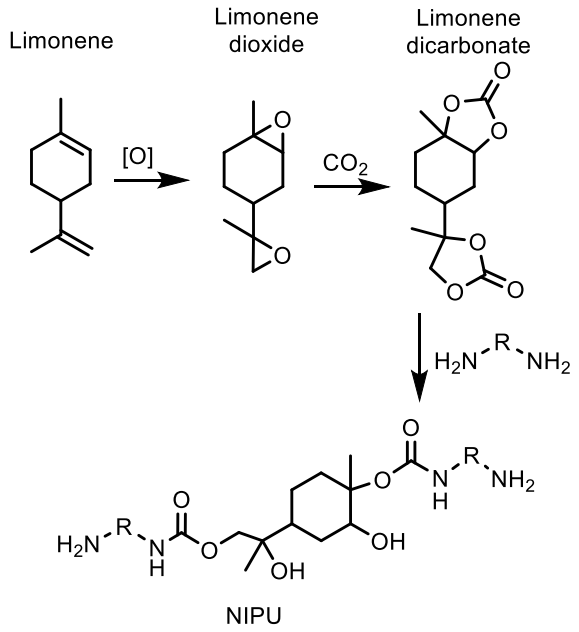

Scheme 1.6. Formation of NIPU from limonene.[56]

In 2016, Grignard et al. reported the formation of NIPU foams derived from CSBO and an amino-terminated polymer.[59] 1,3-Bis(hydroxyhexafluoroisopropyl)benzene was used as a catalyst for the formation of CSBO, and was not removed from the product before

formation of the NIPU as it also catalyzes the reaction between the cyclic carbonate and amine. The resulting CSBO-based NIPUs had T_g values in the range of –2 °C to –5 °C. The foaming process of the NIPU materials involved saturating the polymer with CO_2 at 40 °C and 100 or 300 bar for 3 h, then cooling the reactor to 0 °C before depressurizing. The foaming then occurred by heating the CO_2 saturated sample at 80 °C or 100 °C. The resulting foams have potential applications as insulation and do not require the use of harmful foaming agents.

To create a fully bio-derived NIPU coating, Mahendran et al. used CLSO and a bio-based amine, NC-540, which is derived from cashew nut shell liquid.[60] The cyclic carbonate and amine were mixed in a range of mixing ratios and cured at different temperatures. The film with a CLSO:amine mixing ratio of 1:0.75 that was cured at 100 °C showed the best performance as a coating, with the least amount of swelling in dichloromethane. The film also had a void-free high gloss coating, while samples cured at lower temperatures showed a diminished gloss value. The formed films were 100% bio-derived materials that could be used to replace PU coating where high gloss and scratch resistance is required.

1.4 Objectives for Thesis

The main objective for this thesis was to synthesize a green alternative to conventional PU materials that also improves on the environmental impact of those derived from vegetable oils. Current methods for the epoxidation of oils use a wide range of conditions and catalysts, which may be used in a large excess, or performed at high

temperatures for extended periods of time. Therefore, the objective was to use environmentally friendly methods to epoxidize the FO, that did not require large amounts of reagents, a long reaction time, or high temperature.

Cyclic carbonate formation is generally performed at both high temperature and pressure, while using various catalysts. Another aim, therefore, was to optimize the reaction conditions for the formation of CFO, using lower temperatures, lower pressures, a green catalyst, and therefore less energy. The final step in the literature route to bio-based NIPU materials is reaction with an amine, which is often toxic and not bio-derived. Another objective of this thesis was to use bio-derived amines to increase the amount of bio-based material incorporated into the NIPU network. This could also increase the degradability of the NIPU material, which is the final aim of this thesis.

1.5 References

(1) Anastas, P. T.; Warner, J. C. *Green Chemistry: Theory and Practice*; Oxford University Press: New York, 1998.

(2) Trost, B. M. The Atom Economy - A Search for Synthetic Efficiency. *Science*. **1991**, *254* (5037), 1471–1477.

(3) Sheldon, R. A. Consider the Environmental Quotient. *Chemtech* **1994**, 38–47.

(4) Sheldon, R. A. The E Factor 25 Years on: The Rise of Green Chemistry and Sustainability. *Green Chem.* **2017**, *19* (1), 18–43.

(5) Lancaster, M. Waste: Production, Problems and Prevention. In *Green Chemistry: An Introductory Text*; Royal Society of Chemistry: Cambridge, UK, 2002.

(6) Guineé, J.; Heijungs, R.; Huppes, G.; Zamagni, A.; Masoni, P.; Buonamici, R.; Ekvall, T.; Rydberg, T. Life Cycle Assessment: Past, Present, and Future. *Environ. Sci. Technol.* **2011**, *45* (1), 90–96.

(7) Horne, R. E. Life Cycle Assessment: Origins, Principles and Context. In *Life Cycle Assessment: Principles, Practice and Prospects*; Horne, R., Grant, T., Verghese, K., Eds.; CSIRO: Collingwood, 2009.

(8) Tufvesson, L. M.; Tufvesson, P.; Woodley, J. M.; Börjesson, P. Life Cycle Assessment in Green Chemistry: Overview of Key Parameters and Methodological Concerns. *Int. J. Life Cycle Assess*. **2013**, *18* (2), 431–444.

(9) Mercer, S. M.; Andraos, J.; Jessop, P. G. Choosing the Greenest Synthesis: A Multivariate Metric Green Chemistry Exercise. *J. Chem. Educ*. **2012**, *89* (2), 215–220.

(10) Bayer, O. Das Di-Isocyanat-Polyadditionsverfahran (Polyurethane). *Angew. Chemie*. **1947**, *59*, 257–288.

(11) Cornille, A.; Guillet, C.; Benyahya, S.; Negrell, C.; Boutevin, B.; Caillol, S. Room Temperature Flexible Isocyanate-Free Polyurethane Foams. *Eur. Polym. J*. **2016**, *84*, 873–888.

(12) Gama, N. V.; Ferreira, A.; Barros-Timmons, A. Polyurethane Foams: Past, Present, and Future. *Materials*. **2018**, *11*.

(13) Plastics Insight. Market value forecast of polyurethane worldwide from 2016 to 2021 (in billion U.S. dollars). https://www.statista.com/statistics/720449/global-polyurethane-market-size-forecast/ (accessed July 2, 2019).

(14) Blattmann, H.; Fleischer, M.; Bähr, M.; Mülhaupt, R. Isocyanate- and Phosgene-Free Routes to Polyfunctional Cyclic Carbonates and Green Polyurethanes by Fixation of Carbon Dioxide. *Macromol. Rapid Commun*. **2014**, *35* (14), 1238–1254.

(15) Karol, M. H.; Kramarik, J. A. Phenyl Isocyanate is a Potent Chemical Sensitizer. *Toxicol. Lett*. **1996**, *89* (2), 139–146.

(16) Wang, C.-Q.; Lv, H.-N.; Sun, J.; Cai, Z.-S. Flame Retardant and Thermal Decomposition Properties of Flexible Polyurethane Foams Filled with Several Halogen-Free Flame Retardants. *Polym. Eng. Sci*. **2014**, *54* (11), 2497–2507.

(17) United States Environmental Protection Agency. *Flame Retardants Used in Flexible Polyurethane Foam: An Alternatives Assessment Update*; 2015.

(18) Javni, I.; Petrović, Z. S.; Guo, A.; Fuller, R. Thermal Stability of Polyurethanes Based on Vegetable Oils. *J. Appl. Polym. Sci*. **2000**, *77* (8), 1723–1734.

(19) Sawpan, M. A. Polyurethanes from Vegetable Oils and Applications: A Review. *J. Polym. Res*. **2018**, *25* (8).

(20) Tan, S.; Abraham, T.; Ference, D.; Macosko, C. W. Rigid Polyurethane Foams from a Soybean Oil-Based Polyol. *Polymer*. **2011**, *52*, 2840–2846.

(21) Alagi, P.; Choi, Y. J.; Hong, S. C. Preparation of Vegetable Oil-Based Polyols with Controlled Hydroxyl Functionalities for Thermoplastic Polyurethane. *Eur. Polym. J.* **2016**, *78*, 46–60.

(22) Furtwengler, P.; Avérous, L. Renewable Polyols for Advanced Polyurethane Foams from Diverse Biomass Resources. *Polym. Chem*. **2018**, 4258–4287.

(23) Varma, D. R.; Mulay, S. Methyl Isocyanate: The Bhopal Gas. In *Handbook of Toxicology of Chemical Warfare Agents*; Gupta, R. C., Ed.; Elsevier Academic Press: London, 2009; pp 293–312.

(24) Maisonneuve, L.; Lamarzelle, O.; Rix, E.; Grau, E.; Cramail, H. Isocyanate-Free Routes to Polyurethanes and Poly(Hydroxy Urethane)s. *Chem. Rev*. **2015**, *115*, 12407–12439.

(25) Noreen, A.; Zia, K. M.; Zuber, M.; Tabasum, S.; Zahoor, A. F. Bio-Based Polyurethane: An Efficient and Environment Friendly Coating Systems: A Review. *Prog. Org. Coatings*. **2016**, *91*, 25–32.

(26) Yamazaki, N.; Iguchi, T.; Higashi, F. The Reaction of Diphenyl Carbonate with Amines and Its Application to Polymer Synthesis. *J. Polym. Sci. Part A Polym. Chem.* **1979**, *17*, 835–841.

(27) Datta, J.; Włoch, M. Progress in Non-Isocyanate Polyurethanes Synthesized from Cyclic Carbonate Intermediates and Di- or Polyamines in the Context of Structure–Properties Relationship and from an Environmental Point of View. *Polym. Bull*. **2016**, *73* (5), 1459–1496.

(28) Tamami, B.; Sohn, S.; Wilkes, G. L. Incorporation of Carbon Dioxide into Soybean Oil and Subsequent Preparation and Studies of Nonisocyanate Polyurethane Networks. *J. Appl. Polym. Sci*. **2004**, *92* (2), 883–891.

(29) Bähr, M.; Mülhaupt, R. Linseed and Soybean Oil-Based Polyurethanes Prepared via the Non-Isocyanate Route and Catalytic Carbon Dioxide Conversion. *Green Chem*. **2012**, *14* (2), 483–489.

(30) Alves, M.; Grignard, B.; Gennen, S.; Detrembleur, C.; Jerome, C.; Tassaing, T. Organocatalytic Synthesis of Bio-Based Cyclic Carbonates from CO_2 and Vegetable Oils. *RSC Adv*. **2015**, *5* (66), 53629–53636.

(31) Zheng, J. L.; Burel, F.; Salmi, T.; Taouk, B.; Leveneur, S. Carbonation of Vegetable Oils: Influence of Mass Transfer on Reaction Kinetics. *Ind. Eng. Chem. Res*. **2015**, *54* (43), 10935–10944.

(32) Doley, S.; Sarmah, A.; Sarkar, C.; Dolui, S. K. In Situ Development of Bio-Based Polyurethane-Blend-Epoxy Hybrid Materials and Their Nanocomposites with Modified Graphene Oxide via Non-Isocyanate Route. *Polym. Int*. **2018**, *67* (8), 1062–1069.

(33) Doley, S.; Dolui, S. K. Solvent and Catalyst-Free Synthesis of Sunflower Oil Based Polyurethane through Non-Isocyanate Route and Its Coatings Properties. *Eur. Polym. J*. **2018**, *102*, 161–168.

(34) Food and Agriculture Organization of the United Nations. FAOSTAT http://www.fao.org/faostat (accessed July 2, 2019).

(35) Milman, O. Earth Has Lost a Third of Arable Land in Past 40 Years, Scientists Say. *The Guardian*. 2015.

(36) Tullo, A. H. C&EN's 2018 10 Start-Ups to Watch. *Chemical & Engineering News*. 2018.

(37) Kerton, F. M.; Liu, Y.; Omari, K. W.; Hawboldt, K. Green Chemistry and the Ocean-Based Biorefinery. *Green Chem.* **2013**, *15*, 860–871.

(38) Hawboldt, K.; Adeoti, I. A. Fish Processing Waste Streams as a Feedstock for Fuels. In *Fuels, Chemiclas and Materials from the Oceans and Aquatic Sources*; Kerton, F. M., Yan, N., Eds.; Wiley, 2017; pp 229–276.

(39) AMEC Earth & Environmental Limited. Management of Wastes From Atlantic Seafood Processing Operations. *Rep. Environ. Canada Atl. Reg.* **2003**.

(40) Fisheries and Oceans Canada. Aquaculture: Production Quantities and Values http://www.dfo-mpo.gc.ca/stats/aqua/aqua-prod-eng.htm (accessed July 2, 2019).

(41) Javni, I.; Doo, P. H.; Petrović, Z. S. Soy-Based Polyurethanes by Nonisocyanate Route. *J. Appl. Polym. Sci.* **2008**, *108* (6), 3867–3875.

(42) Saithai, P.; Lecomte, J.; Dubreucq, E.; Tanrattanakul, V. Effects of Different Epoxidation Methods of Soybean Oil on the Characteristics of Acrylated Epoxidized Soybean Oil-Co-Poly(Methyl Methacrylate) Copolymer. *Express Polym. Lett.* **2013**, *7* (11), 910–924.

(43) Bhalerao, M. S.; Kulkarni, V. M.; Patwardhan, A. V. Ultrasound-Assisted Chemoenzymatic Epoxidation of Soybean Oil by Using Lipase as Biocatalyst. *Ultrason. Sonochem.* **2018**, *40*, 912–920.

(44) Meadows, S.; Hosur, M.; Celikbag, Y.; Jeelani, S. Comparative Analysis on the Epoxidation of Soybean Oil Using Formic and Acetic Acids. *Polym. Polym. Compos.* **2018**, *26* (4), 289–298.

(45) Marks, D. W.; Larock, R. C. The Conjugation and Epoxidation of Fish Oil. *J. Am. Oil Chem. Soc.* **2002**, *79* (1), 65–68.

(46) Aresta, M.; Dibenedetto, A. Utilisation of CO_2 as a Chemical Feedstock: Opportunities and Challenges. *Dalt. Trans.* **2007**, 2975–2992.

(47) Tappe, N. A.; Reich, R. M.; D'Elia, V.; Kühn, F. E. Current Advances in the Catalytic Conversion of Carbon Dioxide by Molecular Catalysts: An Update. *Dalt. Trans.* **2018**, *47* (38), 13281–13313.

(48) Kätelhön, A.; Meys, R.; Deutz, S.; Suh, S.; Bardow, A. Climate Change Mitigation Potential of Carbon Capture and Utilization in the Chemical Industry. *Proc. Natl. Acad. Sci.* **2019**, *23*, 11187–11194.

(49) von der Assen, N.; Jung, J.; Bardow, A. Life-Cycle Assessment of Carbon Dioxide Capture and Utilization: Avoiding the Pitfalls. *Energy Environ. Sci.* **2013**, *6* (9), 2721.

(50) von der Assen, N.; Bardow, A. Life Cycle Assessment of Polyols for Polyurethane Production Using CO_2 as Feedstock: Insights from an Industrial Case Study. *Green Chem.* **2014**, *16* (6), 3272–3280.

(51) North, M.; Pasquale, R.; Young, C. Synthesis of Cyclic Carbonates from Epoxides and CO_2. *Green Chem*. **2010**, *12* (9), 1514–1539.

(52) Shaikh, R. R.; Pornpraprom, S.; D'Elia, V. Catalytic Strategies for the Cycloaddition of Pure, Diluted, and Waste CO_2 to Epoxides under Ambient Conditions. *ACS Catal*. **2018**, *8*, 419–450.

(53) Büttner, H.; Grimmer, C.; Steinbauer, J.; Werner, T. Iron-Based Binary Catalytic System for the Valorization of CO_2 into Biobased Cyclic Carbonates. *ACS Sustain. Chem. Eng*. **2016**, *4* (9), 4805–4814.

(54) Alhashmialameer, D.; Collins, J.; Hattenhauer, K.; Kerton, F. M. Iron Amino-Bis(Phenolate) Complexes for the Formation of Organic Carbonates from CO_2 and Oxiranes. *Catal. Sci. Technol*. **2016**, *6* (14), 5364–5373.

(55) Babu, R.; Kathalikkattil, A. C.; Roshan, R.; Tharun, J.; Kim, D. W.; Park, D. W. Dual-Porous Metal Organic Framework for Room Temperature CO_2 fixation via Cyclic Carbonate Synthesis. *Green Chem*. **2015**, *18* (1), 232–242.

(56) Bähr, M.; Bitto, A.; Mülhaupt, R. Cyclic Limonene Dicarbonate as a New Monomer for Non-Isocyanate Oligo- and Polyurethanes (NIPU) Based upon Terpenes. *Green Chem*. **2012**, *14* (5), 1447–1454.

(57) Lopresto, C. G.; Petrillo, F.; Casazza, A. A.; Aliakbarian, B.; Perego, P.; Calabrò, V. A Non-Conventional Method to Extract D-Limonene from Waste Lemon Peels and

Comparison with Traditional Soxhlet Extraction. *Sep. Purif. Technol*. **2014**, *137*, 13–20.

(58) Negro, V.; Mancini, G.; Ruggeri, B.; Fino, D. Citrus Waste as Feedstock for Bio-Based Products Recovery: Review on Limonene Case Study and Energy Valorization. *Bioresour. Technol*. **2016**, *214*, 806–815.

(59) Grignard, B.; Thomassin, J. M.; Gennen, S.; Poussard, L.; Bonnaud, L.; Raquez, J. M.; Dubois, P.; Tran, M. P.; Park, C. B.; Jerome, C.; et al. CO_2-Blown Microcellular Non-Isocyanate Polyurethane (NIPU) Foams: From Bio- and CO_2-Sourced Monomers to Potentially Thermal Insulating Materials. *Green Chem.* **2016**, *18* (7), 2206–2215.

(60) Mahendran, A. R.; Wuzella, G.; Aust, N.; Müller, U. Synthesis, Characterization, and Properties of Isocyanate-Free Urethane Coatings from Renewable Resources. *J. Coatings Technol. Res*. **2014**, *11* (3), 329–339.

Chapter 2: Synthesis and Characterization of Epoxides Derived from Fish Oil and Related Unsaturated Starting Materials

2.1 Introduction

Epoxides based on renewable feedstocks, such as vegetable oils, have been produced for over 30 years[1] and are thought to be sustainable, biodegradable[2,3] products that are important intermediates for the synthesis of cyclic carbonates and non-isocyanate polyurethanes (NIPU). As demonstrated in Chapter 1, triglycerides present in biomass-derived oils can be a valuable starting material for the formation of these non-petroleum-derived epoxides. Marks and Larock[4] previously used rhodium and rhenium-based catalysts to conjugate and epoxidize the triglycerides present in both Norway fish oil (FO) ethyl esters and capelin FO, showing that FO can be a possible substitute for land-based biomass. The capelin FO contained approximately 4.5 carbon-carbon double bonds per triglyceride, identical to the waste-derived FO used herein that also contains 4.5 carbon-carbon double bonds, as determined by ^{1}H nuclear magnetic resonance (NMR) spectroscopy. The goal for this chapter was to synthesize epoxidized FO (EFO) through environmentally friendly and sustainable methods which adhere to the principles of green chemistry.

FO used in this work was extracted by the Hawboldt group within the Department of Process Engineering at Memorial University of Newfoundland, from Atlantic salmon (*Salmo salar Linnaeus*) offcuts by a modified fishmeal process.[5] The produced FO is composed of approximately 70.48 ± 2.09% triglycerides with 8.43 ± 0.95% free fatty acids. The fatty acid profile for the FO is complex with the major fatty acids being oleic (18:1ω-

9, 31.44 ± 1.64%), linoleic (18:2ω-6, 15.36 ± 0.51%), palmitic (16:0, 14.02 ± 0.77%), and palmitoleic (16:1ω-1, 6.92 ± 0.11%) acid. Model compounds oleic acid (OA) and methyl oleate (MO) are therefore used to represent the FO as they are the most abundant and simplest unsaturated fatty acid present within the FO triglycerides. This differs from soybean oil, which is mostly polyunsaturated fatty acids, with linoleic acid being the most abundant fatty acid.[6] For comparison to the extracted FO, nutritional tablet FO (TFO), which contains only triglycerides of docosahexaenoic acid (DHA, 22:6ω-3) and eicosapentaenoic acid (EPA, 20:5ω-3), was also studied.

Three routes for the formation of epoxides were used and optimized for both the model substrates, MO and OA (**Scheme 2.1**), as well as the two FO substrates (**Scheme 2.2**). These different routes will be outlined in Section 2.2.1, with a comparison of the environmental footprint of each route in Section 2.2.3. These routes include epoxidation using 3-chloroperoxybenzoic acid (*m*-CPBA), hydrogen peroxide (H_2O_2) catalyzed by sulfuric acid (H_2SO_4), and H_2O_2 catalyzed by formic acid (HCOOH).

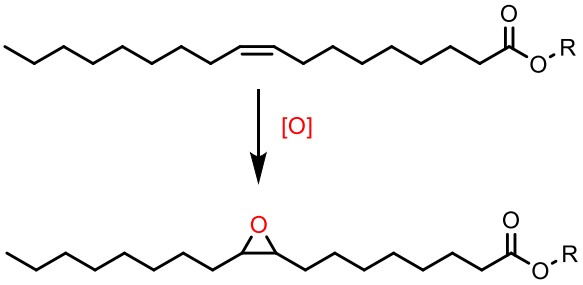

Scheme 2.1. Schematic for the conversion of MO (R = Me) and OA (R = H) to their respective epoxide.

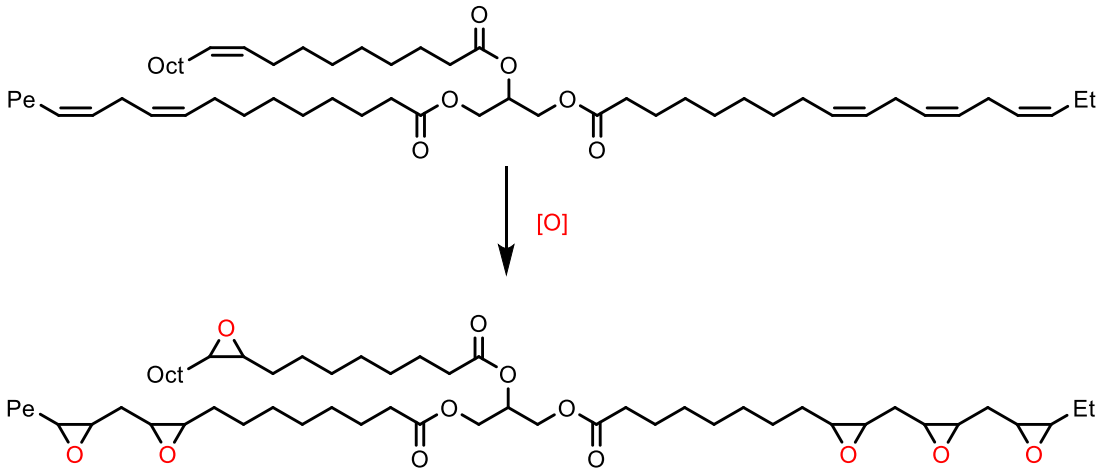

Scheme 2.2. Schematic for the conversion of FO triglycerides to epoxides.

2.2 Results and Discussion

2.2.1 Assessment of Routes to Epoxides

2.2.1.1 Epoxidation by 3-Chloroperoxybenzoic Acid

The epoxidation of the oils was performed following a literature method.[7] The oil was dissolved in 40 mL of dichloromethane (CH_2Cl_2), cooled to 0 °C, and *m*-CPBA slowly added, before stirring at room temperature for 11 h. After cooling and gravity filtration, the collected organic phase was washed three times with a sodium sulfite (Na_2SO_3) solution, three times with a saturated sodium bicarbonate ($NaHCO_3$) solution, and once with a sodium chloride (NaCl) solution. After drying over anhydrous magnesium sulfate ($MgSO_4$) and filtration, the CH_2Cl_2 was removed under reduced pressure to give the epoxidized product. This reaction gave excellent conversions of the double bonds to the desired epoxide.

The summarized reaction conditions are presented in **Table 2.1** below. MO and FO were epoxidized, obtaining a conversion of 90% and 96-99%, respectively. The synthesized EFO showed an increase in viscosity from the FO (0.0530 ± 0.0001 Pa·s) to 0.0962 ± 0.0017 Pa·s. Plots for the rheology measurements of the oils are presented in the Appendix (**A2**, **A3**). Epoxidation of OA through this method gave a viscous white oily mixture that could not be filtered and purified, allowing no product to be isolated.

Table 2.1. Experimental conditions for epoxidation by *m*-CPBA.

Substrate	Oil (g)	*m*-CPBA (g)	Time (h)	Conversion to Epoxide (%)[a]
Methyl Oleate	1.43	0.93	11	90
Oleic Acid[b]	2.01	1.75	12	-
Fish Oil	1.53	2.00	12	96
	1.50	1.99	12	99

[a]Determined by ^{1}H NMR spectroscopy. [b]Product could not be isolated.

The *m*-CPBA reaction proceeds through a concerted mechanism with a cyclic intermediate (**Scheme 2.3**), causing the stereochemistry of the starting epoxide to be maintained during the reaction. The starting unsaturated fatty acids all contain *cis*-oriented double bonds, and therefore form the *cis*-oriented epoxides.

Using *m*-CPBA for the epoxidation of the fatty acids gives a high conversion to the desired epoxide, but in terms of atom efficiency, this route is not ideal. The only reagent used besides the oil is *m*-CPBA, and it is only providing one oxygen towards the product, leaving the rest of the molecule as waste. Calculating the atom efficiency for the

epoxidation of MO through this method gives 66%. While it gives a high conversion, in terms of green chemistry, it uses a hazardous chemical, a large amount of solvent for the reaction, and has a low atom efficiency. The overall impact on health and the environment will be explored in more detail and compared with the other epoxidation methods in Section 2.2.3.

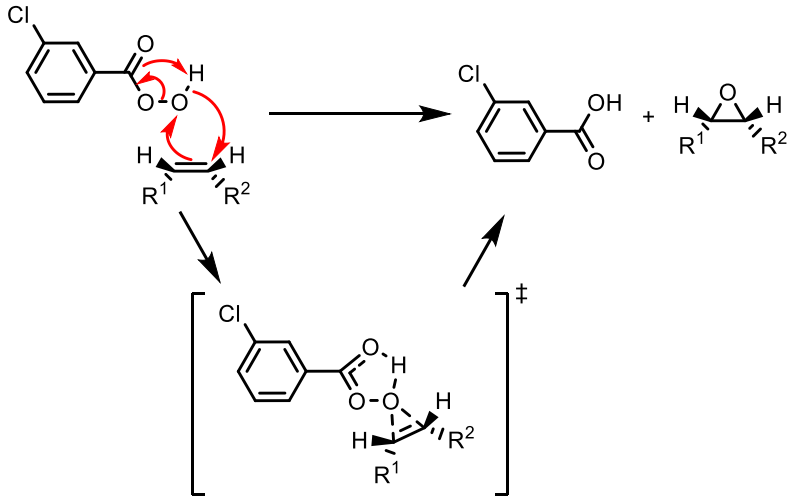

Scheme 2.3. Mechanism of the formation of epoxides from *m*-CPBA.[8]

2.2.1.2 Optimization of Sulfuric Acid Catalyzed Epoxidation

Following a literature method that utilizes H_2O_2 as the oxidant,[9] the oils used in this thesis were epoxidized. The oils were dissolved in heptane, and acetic acid (CH_3COOH) was added before heating to the desired reaction temperature in an oil bath. An acidified H_2O_2 solution was then added dropwise over 1 h with stirring. Upon complete addition, the reaction mixture was stirred and heated for the desired reaction time and then cooled to 0

°C. The organic layer was washed with deionized water, dried over $MgSO_4$ and filtered. After removing the solvent, the desired epoxide was collected.

The summarized experimental conditions and conversions achieved for each substrate are presented in **Table 2.2** below. For MO a conversion of the double bonds to the epoxide of 76% was obtained at 60 °C. Increasing the temperature slightly to 65 °C did not significantly increase the conversion, so the lower temperature was used for further reactions. The epoxidation of OA occurred with a similar conversion of 85% under the same conditions. Waste-derived FO was epoxidized with a conversion of 61% in 18 h at 60 °C. In the ^{1}H NMR spectrum for the formed product (**Figure 2.6**) there is a new peak at 3.39 ppm that corresponds to the formation of a polyol side product, which is formed at a 39% conversion. Reducing the reaction time to 12 h, the conversion to the epoxide is increased to 89%, with the conversion to the polyol reduced to 5%. Reducing the temperature to 50 °C significantly reduced the conversion to the epoxide to 60% with 0.95% conversion to the polyol.

TFO was epoxidized for 18 h at 60 °C, giving a yellow oil that showed no visible epoxide groups by ^{1}H NMR spectroscopy. Evidence for the formation of hydroxyl groups is provided by IR analysis and is discussed later in this chapter (Section 2.2.2.3.). Since the product formed hydroxyl groups, this indicates over-oxidation and ring-opening of the epoxide. In order to reduce the amount of polyol produced, the reaction time was lowered to 15.25 h, increasing the conversion to the desired epoxide to 65%. By ^{1}H NMR spectroscopy, this product showed no formation of the undesired hydroxyl groups.

Table 2.2. Experimental conditions for epoxidation by H_2O_2 catalyzed by H_2SO_4.

Substrate	alkene:CH_3COOH: H_2O_2 [a]	H_2SO_4 (wt.%) [b]	T (°C)	t (h)	Conversion to Epoxide (%)[c]
Methyl Oleate	1:0.42:1.50	0.60	60	18	76
	1:0.42:1.50	0.76	65	18	84
Oleic Acid	1:0.42:1.56	0.84	60	18	85
Fish Oil	1:0.91:3.23	1.2	60	18	61
	1:1.00:3.05	1.2	60	12	89
	1:1.06:3.06	0.96	50	12	60
Tablet Fish Oil	1:0.67:1.92	0.82	60	18	-
	1:0.69:1.84	0.75	60	15.25	65

[a]mole ratio of double bonds within substrate:CH_3COOH:H_2O_2. [b]Weight % relative to mass of oil used. [c]Determined by ^{1}H NMR spectroscopy.

The acid catalyzed epoxidation of the oils using H_2O_2 and CH_3COOH proceeds through a concerted mechanism (**Scheme 2.4**) that is similar to that for the *m*-CPBA epoxidation, with the stereochemistry of the starting epoxide maintained during the reaction, forming *cis*-oriented epoxides. This method gave lower conversions than that using *m*-CPBA, but optimized conditions for MO, OA, and FO still gave high conversions above 84%. The atom efficiency is improved in this method compared with using *m*-CPBA, as the oxygen that is being incorporated into the product is coming from H_2O_2. For the epoxidation of MO the atom efficiency is 95%, as both the CH_3COOH and the H_2SO_4 are catalysts and are not included in the calculation. This reaction appears to be much greener, but it includes the use of H_2SO_4, which is highly corrosive. The overall impact on health and the environment will be explored in more detail and compared with the other epoxidation methods in Section 2.2.3.

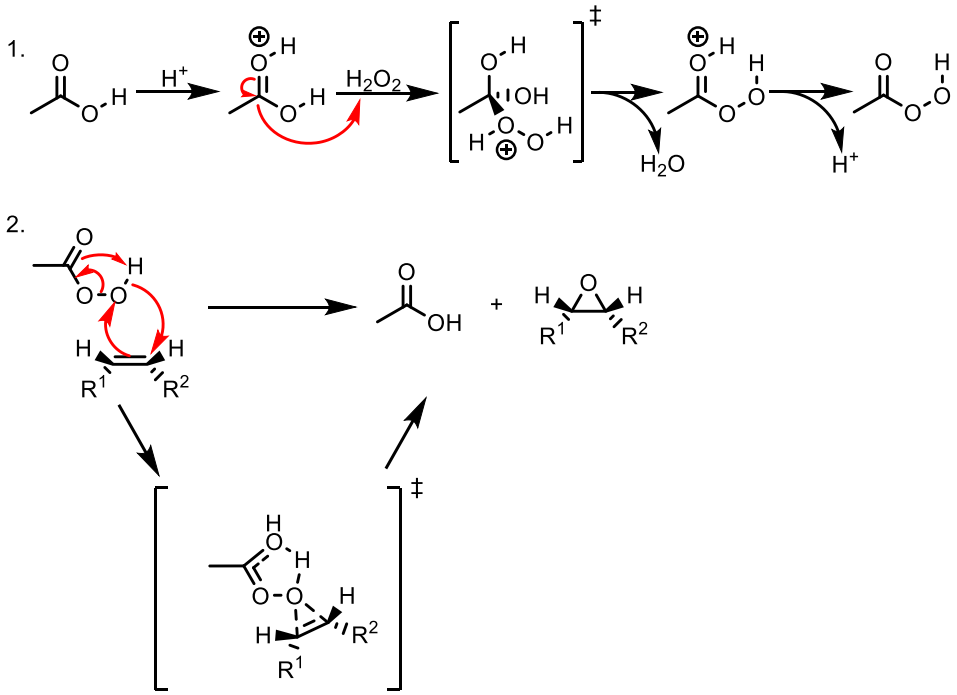

Scheme 2.4. Mechanism of the acid catalyzed formation of epoxides using H_2O_2 and acetic acid.[8]

2.2.1.3 Optimization of Formic Acid Catalyzed Epoxidation

The final method used in this work for the epoxidation of FO and related chemicals uses HCOOH and H_2O_2. The oil and HCOOH were heated to 40 °C followed by dropwise addition of H_2O_2 over 1 h with stirring. In some reactions, a previously reported deep eutectic solvent (DES) catalyst composed of choline chloride (ChCl) and oxalic acid (OxA)[10] was added with the HCOOH. Once the addition of H_2O_2 was complete, the reaction mixture was heated to the desired reaction temperature and stirred for the desired reaction time. The contents were then cooled to 0 °C, dissolved in CH_2Cl_2 or dimethyl carbonate (DMC), and the organic layer washed with deionized water, dried over $MgSO_4$, and filtered. After removing the solvent, the desired epoxidized product was collected.

The summarized reaction conditions are presented in **Table 2.3** below. The model substrate, MO, was epoxidized using the DES catalyst giving a conversion of 71% to the epoxide. To test the capability of the ChCl-OxA catalyst, OA was epoxidized without the DES in a series of reactions from 1 to 4 h, giving a maximum conversion of 85% after 4 h.

The waste-derived FO was first epoxidized with the DES catalyst added, for 8 and 9 h, giving a conversion of 82% and 75%, respectively. As with OA, a series of reactions were performed without ChCl-OxA for 1 to 5 h, with the highest conversion of 94% obtained after 5 h, which was higher than when ChCl-OxA was present. TFO was epoxidized using ChCl-OxA for 8 h to compare with the other substrates, giving a conversion of 65%. With HCOOH alone, the epoxidation of TFO was performed for 1 to 5 h, with the highest conversion of 84% obtained after 4 h. The reaction performed for 5 h had a 76% conversion to the desired product, potentially due to conversion of the epoxide to a polyol. For all substrates, a higher conversion was achieved without the use of ChCl-OxA, so only HCOOH and H_2O_2 were used for subsequent reactions.

The HCOOH catalyzed epoxidation of the substrates using H_2O_2 proceeds through the same mechanism as with CH_3COOH and H_2SO_4, keeping the stereochemistry of the double bonds the same and therefore forming *cis*-oriented epoxides. The atom efficiency of the reaction is the same as that for the CH_3COOH epoxidation, at 95%, as it still uses only H_2O_2 for the reaction, with the carboxylic acid acting as the catalyst. The HCOOH catalyzed reaction removes the use of H_2SO_4, a strong mineral acid. In the case of OA, FO, and TFO, a higher or equivalent conversion to the epoxide was achieved using HCOOH.

The overall impact on health and the environment will be explored in more detail and compared with the other epoxidation methods in Section 2.2.3.

Table 2.3. Experimental conditions for epoxidation by H_2O_2 catalyzed by formic acid.

Substrate	alkene:HCOOH: H_2O_2 [a]	ChCl-OxA (wt.%) [b]	t (h)	Conversion to Epoxide (%)[c]
Methyl Oleate	1:0.76:1.71	2.8	8	71
Oleic Acid	1:0.65:1.72	0	1	38
	1:0.71:1.68	0	2	62
	1:0.73:1.68	0	3	77
	1:0.73:1.66	0	4	85
Fish Oil	1:1.61:3.48	4.3	8	82
	1:1.57:3.48	4.3	9	75
	1:1.48:3.66	0	1	56
	1:1.51:3.37	0	3	76
	1:1.56:3.50	0	4	86
	1:1.54:3.52	0	5	94
Tablet Fish Oil	1:0.99:2.37	3.9	8	65
	1:0.96:1.63	0	1	56
	1:1.07:1.70	0	3	76
	1:1.20:1.71	0	4	84
	1:0.98:1.45	0	5	76

[a]mole ratio of double bonds within substrate:HCOOH:H_2O_2. [b]Weight % relative to mass of oil used. [c]Determined by ^{1}H NMR spectroscopy.

Similar methods using HCOOH and H_2O_2 have been reported in the literature for the epoxidation of other bio-based oils.[11–14] The reaction conditions of these methods are presented in **Table 2.4** for comparison to the HCOOH catalyzed reaction with FO. The optimized reaction temperature for the epoxidation of FO was 50 °C, which is similar to reaction temperatures reported in the literature. The reaction time of 5 h is much shorter

than the 22 h required by Campanella et al., for the conversion of soybean oil,[12] or the 72 h required by Audic et al. for broccoli oil.[11] In 2013, Hazmi et al. epoxidized jatropha oil, from a flowering plant native to the American tropics, as an intermediate to the formation of polyols using lower molar ratios of HCOOH and H_2O_2, but only achieved conversions of 59.5 to 61.5%.[13] The conditions used in this work are similar to those reported in 2018 by Meadows et al. for the conversion of soybean oil into its corresponding epoxide, which required 6 h to achieve a 98% conversion.[14] The ratio of reagents used is based on the moles of oil used, with no mass loadings reported, and so is difficult to directly compare to the ratios used in this thesis. The conditions used in the work reported herein for FO achieves a high conversion of 94% while maintaining a low reaction temperature and time, while also using less H_2O_2 than literature conditions that require longer reaction times.

Table 2.4. Comparison of literature conditions for the formation of bio-based epoxides.

Reference	Substrate	T (°C)	t (h)	alkene:HCOOH: H_2O_2 [a]	Conversion (%)
Campanella et al., 2011	Soybean oil	40	22	1:2:10	complete
Hazmi et al., 2013	Jatropha oil	65	5	0.1:0.4:1.7	59.5-61.5
Audic et al., 2014	Broccoli oil	40	72	1:2:20	complete
Meadows et al., 2018	Soybean oil	50	6	1[b]:0.5:2	98
This Work	Fish oil	50	5	1:1.54:3.52	94

[a] mole ratio of double bonds within substrate:HCOOH:H_2O_2. [b]Per mol of oil used.

2.2.2 Characterization of Epoxides

2.2.2.1 ^{1}H and ^{13}C NMR Data

NMR spectra of the model compounds MO and OA, as well as the corresponding epoxides synthesized in this work, have been previously reported and the ^{1}H and ^{13}C NMR data found herein are consistent with those reported in the literature.[9] Representative ^{1}H and ^{13}C NMR spectra for MO and its corresponding epoxide, are shown in **Figure 2.1** and **Figure 2.2**. The ^{1}H NMR spectrum for MO, **Figure 2.1**, contains a triplet at 0.87 ppm representing the terminal methyl group (H_{18}). A complex pattern of peaks appearing from 1.2 to 1.7 ppm represents the methylene protons from the carbon chain, with the protons on the carbon β to the carbonyl (H_2) represented by a triplet centered at 2.30 ppm. A broad peak at 2.01 ppm represents the allylic protons (H_8 and H_{11}) in the molecule. A singlet at 3.66 ppm represents the hydrogens (H_{19}) from the methyl ester group and the peak at 5.33 ppm corresponds to the olefinic protons (H_9 and H_{10}). In the ^{1}H NMR spectrum for EMO, these same peaks appear, with a new peak at 2.89 ppm, which represents the formation of the epoxide (H_9, H_{10}). The conversion of the double bonds to the corresponding epoxide was determined from the ratio of the epoxide protons to the sum of the epoxide protons plus the remaining olefinic protons.

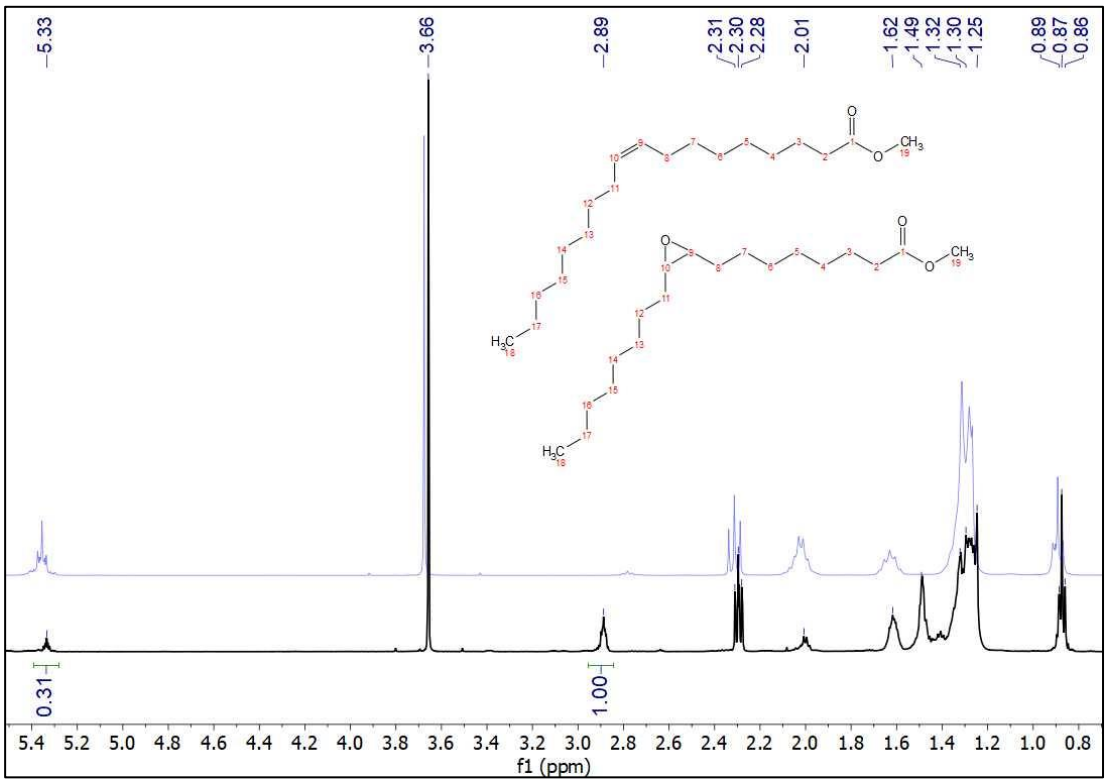

Figure 2.1. ^{1}H NMR spectra of MO (top, blue) and EMO (bottom, black) in $CDCl_3$.

The ^{13}C NMR spectra for MO and EMO, **Figure 2.2**, contain a peak at 14.2 ppm, corresponding to the terminal methyl of the carbon chain (C_{18}). Peaks from 22.8 to 34.2 ppm represent the methylene carbons in the carbon chain (C_2-C_8, C_{11}-C_{17}). The peak at 51.6 ppm in both spectra represents the methyl of the ester group (C_{19}). Peaks at 130.1 ppm and 129.9 ppm represent the olefinic carbons (C_9, C_{10}), which are reduced in size in the spectrum for EMO. A peak at 174.4 ppm corresponds to the carbonyl carbon in both MO and EMO (C_1). The ^{13}C NMR spectrum for EMO contains two new peaks at 57.3 ppm and 57.4 ppm, which corresponds to the formation of the epoxide (C_9, C_{10}).

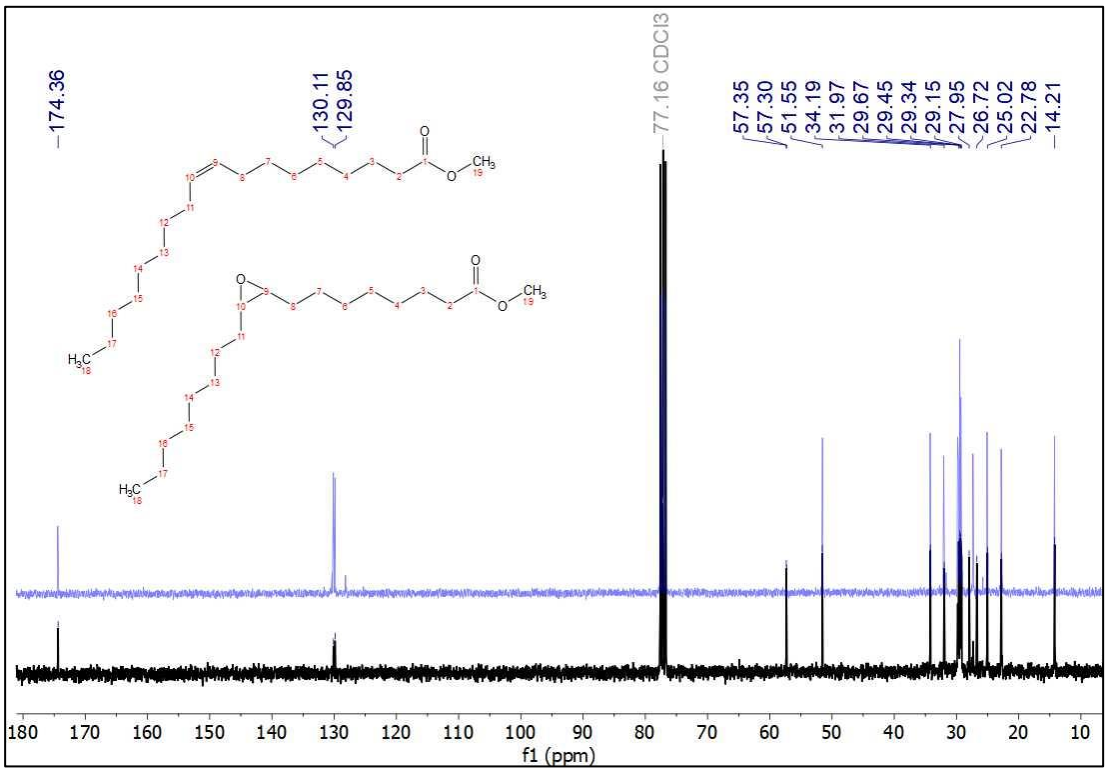

Figure 2.2. ^{13}C NMR spectra of MO (top, blue) and EMO (bottom, black) in $CDCl_3$.

Representative ^{1}H and ^{13}C NMR spectra are given for OA and EOA in **Figure 2.3** and **Figure 2.4**. The ^{1}H NMR spectrum for OA, **Figure 2.3**, contains a triplet centered at 0.88 ppm, representing the terminal methyl protons (H_{18}). A complex set of peaks from 1.27 to 1.34 ppm corresponds to the methylene protons in the carbon chain, with the carbon β to the carbonyl group represented by a triplet at 2.35 ppm (H_2), and the carbon γ to the carbonyl group represented by a peak at 1.64 ppm (H_3). The allylic protons are represented by a peak at 2.00 ppm in the spectrum for OA, which moves to 1.50 ppm in the spectrum for EOA. A peak at 5.34 ppm represents the olefinic protons (H_9, H_{10}). The ^{1}H NMR spectrum for EOA shows a new broad peak at 2.91 ppm, which corresponds to the formation of the epoxide (H_9, H_{10}).

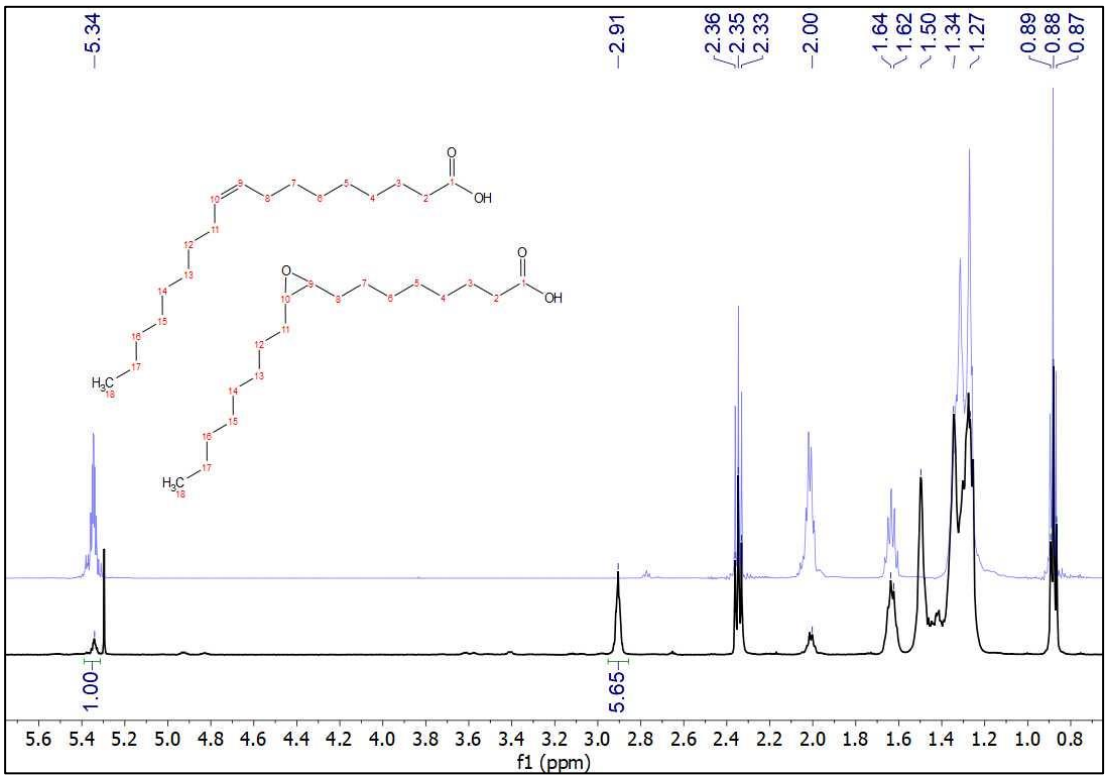

Figure 2.3. ^{1}H NMR spectra of OA (top, blue) and EOA (bottom, black) in $CDCl_3$.

The ^{13}C NMR spectrum for OA, **Figure 2.4**, contains a peak at 14.2 ppm, corresponding to the terminal methyl of the carbon chain (C_{18}). Peaks from 22.8 to 34.1 ppm represent the methylene carbons in the carbon chain (C_2-C_8, C_{11}-C_{17}). Peaks at 129.8 ppm and 130.1 ppm represent the olefinic carbons (C_9, C_{10}), which are reduced in size in the ^{13}C NMR spectrum for EOA. A peak at 180.0 ppm represents the carbonyl carbon in both OA and EOA (C_1). In the ^{13}C NMR spectrum for EOA, new peaks appear at 57.4 ppm and 57.5 ppm, corresponding to the formation of the epoxide (C_9, C_{10}).

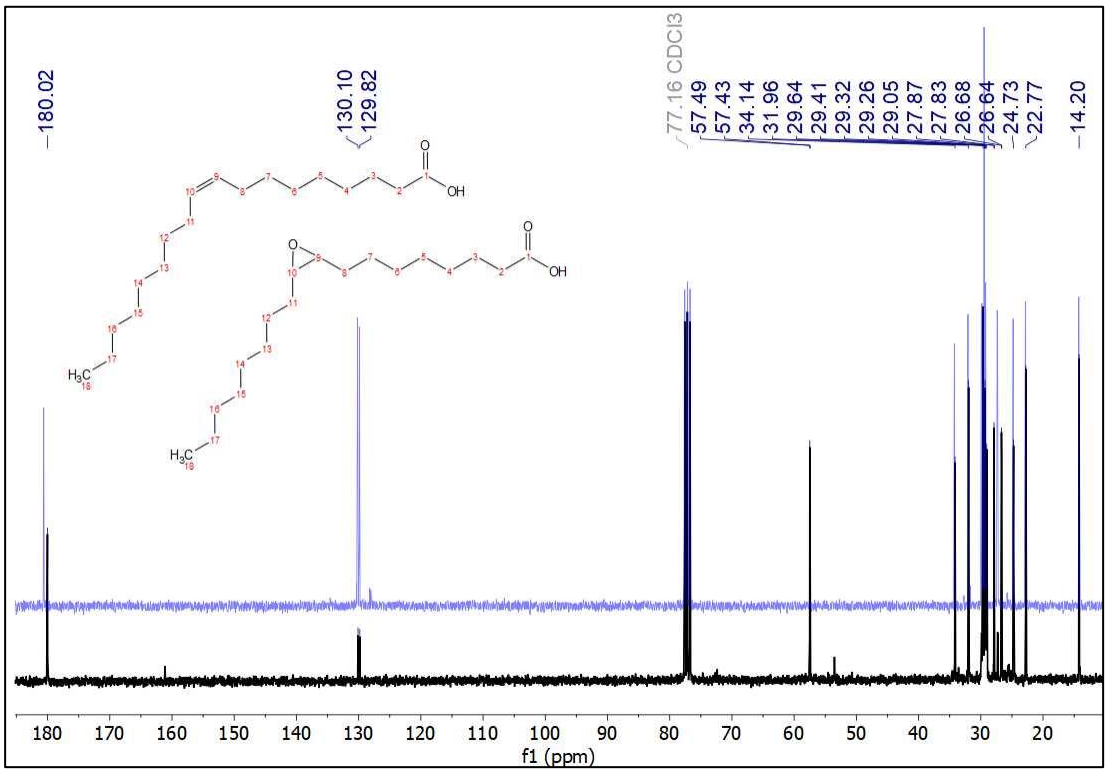

Figure 2.4. ^{13}C NMR spectra of OA (top, blue) and EOA (bottom, black) in $CDCl_3$.

In 1993, Aursand et al. extracted lipids from Atlantic salmon white muscle and performed an extensive NMR study on the lipids.[15] Their assignment of peaks is consistent spectroscopically for both ^{1}H and ^{13}C NMR spectra of the waste-derived FO and TFO used in this work. EFO synthesized in this work is similar to the vegetable oil-based epoxides, and their spectroscopic characterization using both ^{1}H and ^{13}C NMR data are consistent with those reported in the literature.[12,16] Representative ^{1}H and ^{13}C NMR spectra are given for both FO and EFO in **Figure 2.5** and **Figure 2.7**. The ^{1}H NMR spectrum for FO, **Figure 2.5**, contains a triplet at 0.87 ppm that corresponds to the terminal methyl group for all fatty acids except ω-3 fatty acids, which appear at 0.97 ppm. Peaks from 1.24 to 1.32 ppm correspond to protons of the methylene groups. A peak at 1.61 ppm represents the protons

on the carbon β to the carbonyl group for all fatty acids except DHA. The peak centered on 2.02 ppm corresponds to the protons on the allylic carbons. Peaks from 2.28 to 2.31 ppm correspond to the protons on the carbon β to the carbonyl group for all fatty acids except for DHA, which appears as a small peak at 2.38 ppm. Peaks around 2.80 ppm correspond to protons on allylic carbons between two double bonds, which shifts upfield after epoxidation. Peaks from 4.11 to 4.30 ppm and 5.25 ppm represent the protons in the glycerol chain of the triglyceride, on the methylene and methine carbons, respectively. The peaks around 5.32 ppm correspond to the olefinic protons. The ^{1}H NMR spectrum for EFO shows new peaks from 2.80 to 3.19 ppm, which corresponds to the formation of the epoxide.

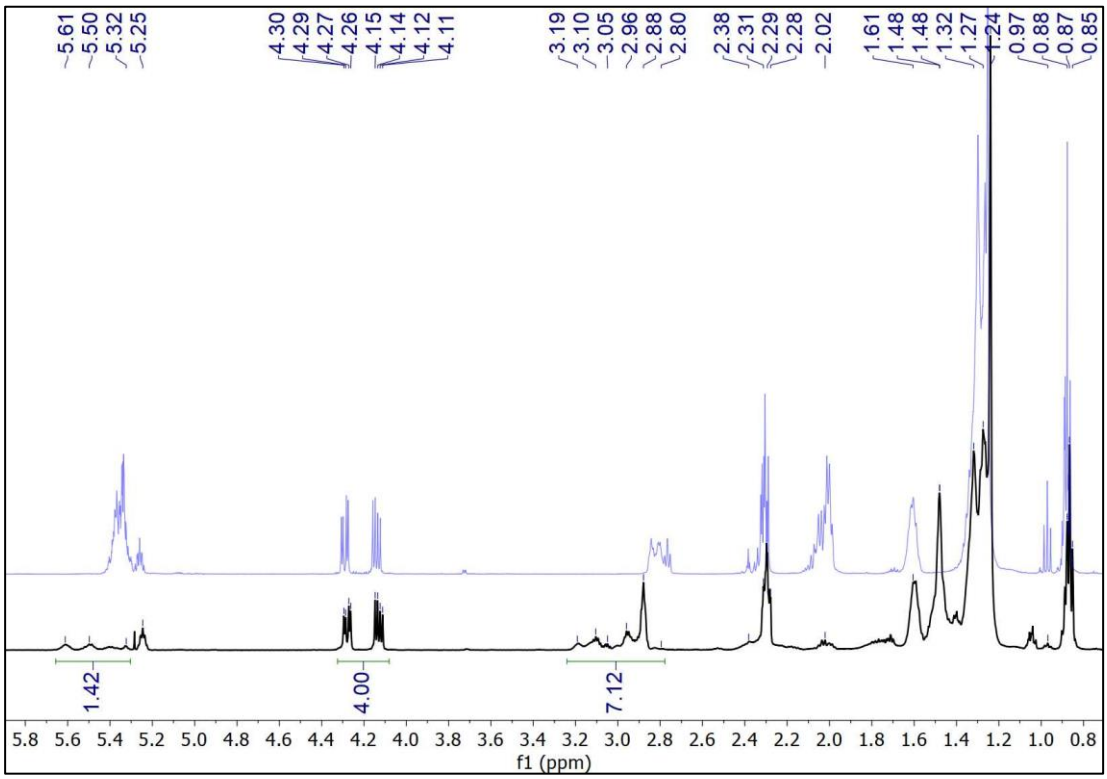

Figure 2.5. ^{1}H NMR spectra of waste-derived FO (top, blue) and EFO (bottom, black).

In an 18 h reaction using the H_2SO_4 catalyzed epoxidation of FO, the FO was over-oxidized, and a new peak appeared in the ^{1}H NMR spectrum (**Figure 2.6**) at 3.39 ppm. This corresponds to the formation of an undesired polyol from the epoxide.[17] This was also confirmed by infrared (IR) spectroscopy.

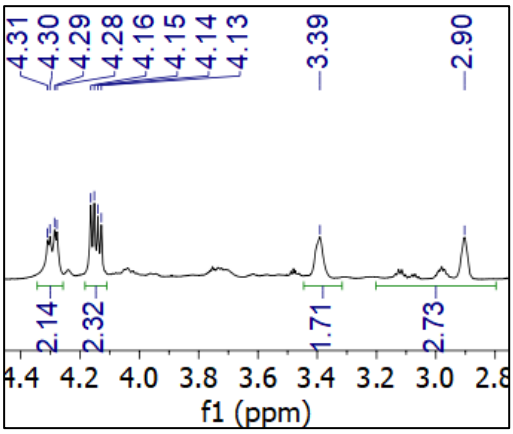

Figure 2.6. ^{1}H NMR spectrum of over-oxidized EFO sample with polyol formation.

The ^{13}C NMR spectrum for FO, **Figure 2.7**, contains a peak at 14.2 ppm, which corresponds to the terminal methyl of the fatty acid carbon chain. Peaks from 22.7 to 34.2 ppm represent the methylene carbons of the carbon chain. The peaks at 62.2 ppm and 69.0 ppm represent the carbons in the glycerol of the triglyceride, the methylene and methine carbons, respectively. Peaks from 128.0 to 132.2 ppm represent the olefinic carbons in the fatty acid. Peaks which occur between 172.9 ppm and 173.4 ppm correspond to the carbonyl carbons of different fatty acids present in the FO. In the ^{13}C NMR spectrum for EFO, the same peaks appear, with new peaks around 57.3 ppm that correspond to the formation of the epoxide groups.

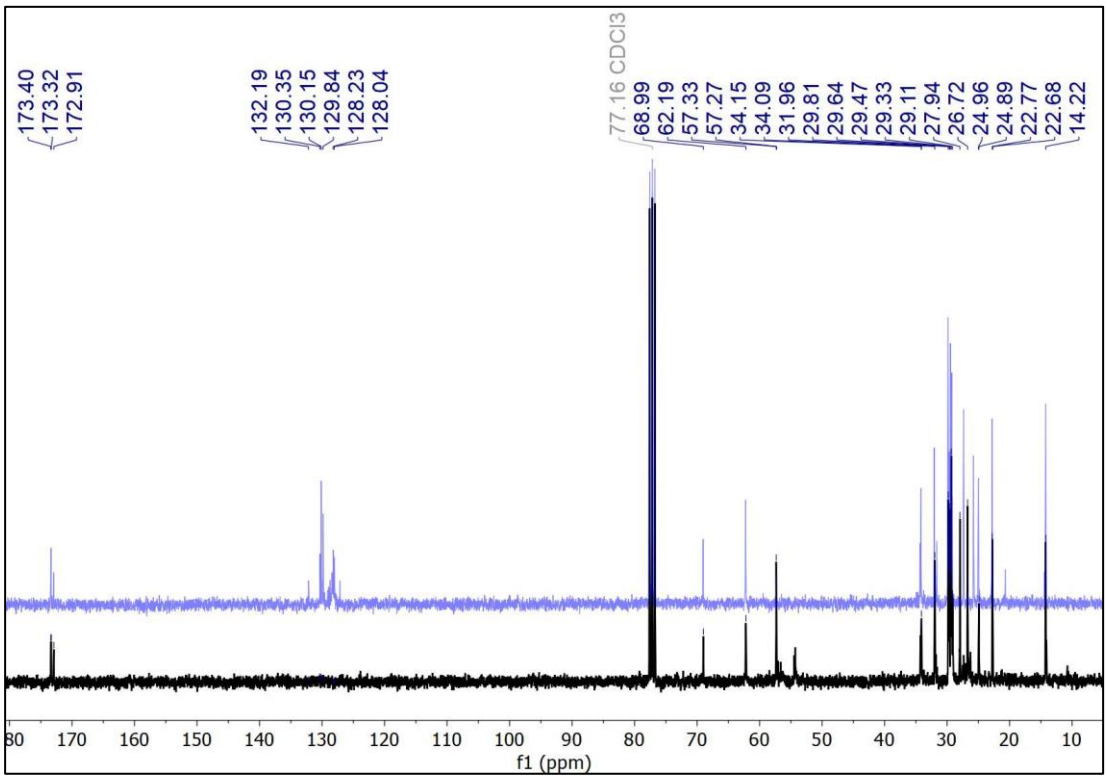

Figure 2.7. ^{13}C NMR spectra of waste-derived FO (top, blue) and EFO (bottom, black) in $CDCl_3$.

TFO used in this work, which contains only EPA and DHA, is spectroscopically similar in terms of ^{1}H and ^{13}C NMR data with the waste-derived FO used. The ^{1}H NMR spectrum for TFO, **Figure 2.8**, contains triplets at 0.86 and 0.97 ppm that correspond to the terminal methyl group of the fatty acid carbon chains for EPA and DHA, respectively. Peaks from 1.24 to 1.27 ppm correspond to protons of the methylene carbons of the fatty acid carbon chain. A peak at 1.77 ppm represents the protons on the carbon β to the carbonyl group. The peak centered on 2.05 ppm corresponds to the protons on the allylic carbons. A peak at 2.29 ppm corresponds to the protons on the carbon β to the carbonyl group for all

fatty acids except for DHA, which appears as a small peak at 2.38 ppm. Peaks around 2.82 ppm correspond to protons on allylic carbons between two double bonds, which shifts upfield after epoxidation. Peaks from 4.11 to 4.29 ppm and 5.24 ppm represent the protons in the glycerol chain of the triglyceride, on the methylene and methine carbons, respectively. The peaks around 5.36 ppm corresponds to the olefinic protons. The ^{1}H NMR spectrum for ETFO shows new peaks from 2.79 to 3.18 ppm, which corresponds to the formation of the epoxide. The conversion of double bonds to the corresponding epoxide was determined for both EFO and ETFO from the ratio of the epoxide protons, to the sum of the epoxide protons plus the remaining olefinic protons.

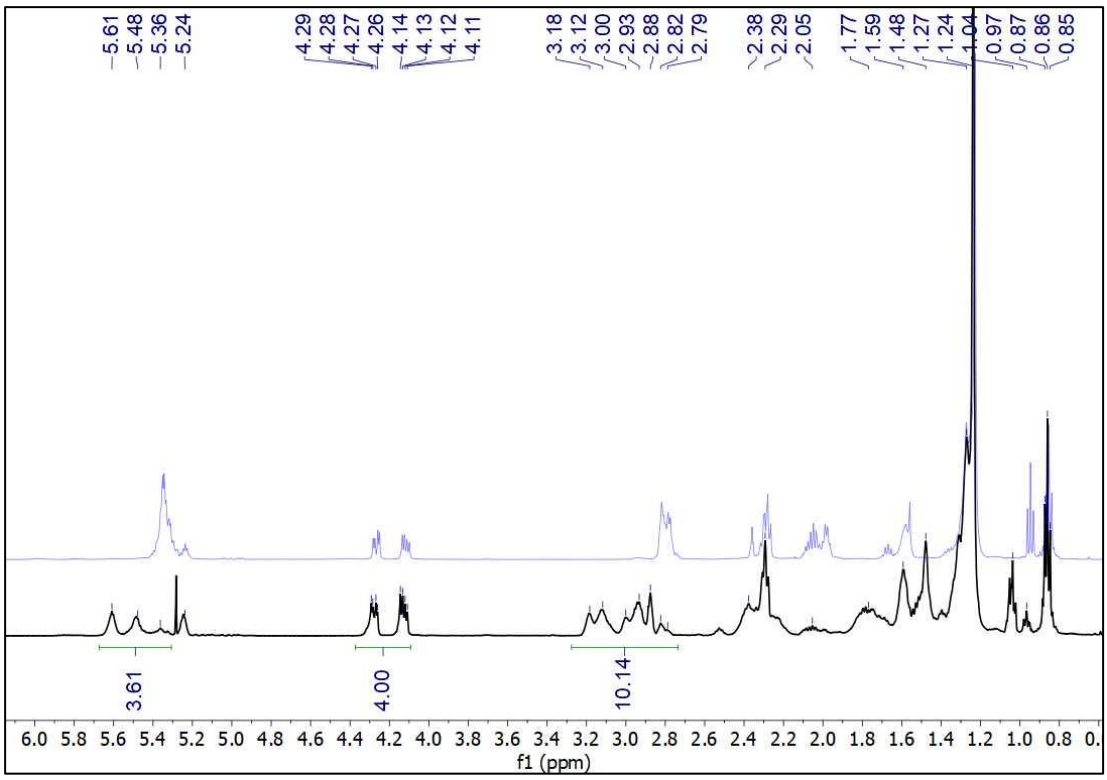

Figure 2.8. ^{1}H NMR spectra of TFO (top, blue) and ETFO (bottom, black).

The ^{13}C NMR spectrum for TFO, **Figure 2.9**, contains a peak at 14.2 ppm, which corresponds to the terminal methyl of the fatty acid carbon chain. Peaks from 20.7 to 34.1 ppm represent the methylene carbons. Peaks at 62.18 and 68.94 ppm represent the carbons in the glycerol of the triglyceride, the methylene and methine carbons, respectively. Peaks from 127.1 to 132.1 ppm represent the olefinic carbons in the fatty acid. Peaks from 173.0 to 173.4 ppm correspond to the carbonyl carbons. In the ^{13}C NMR spectrum for ETFO, new peaks occur at 57.3 and 58.4 ppm that correspond to the formation of the epoxide groups.

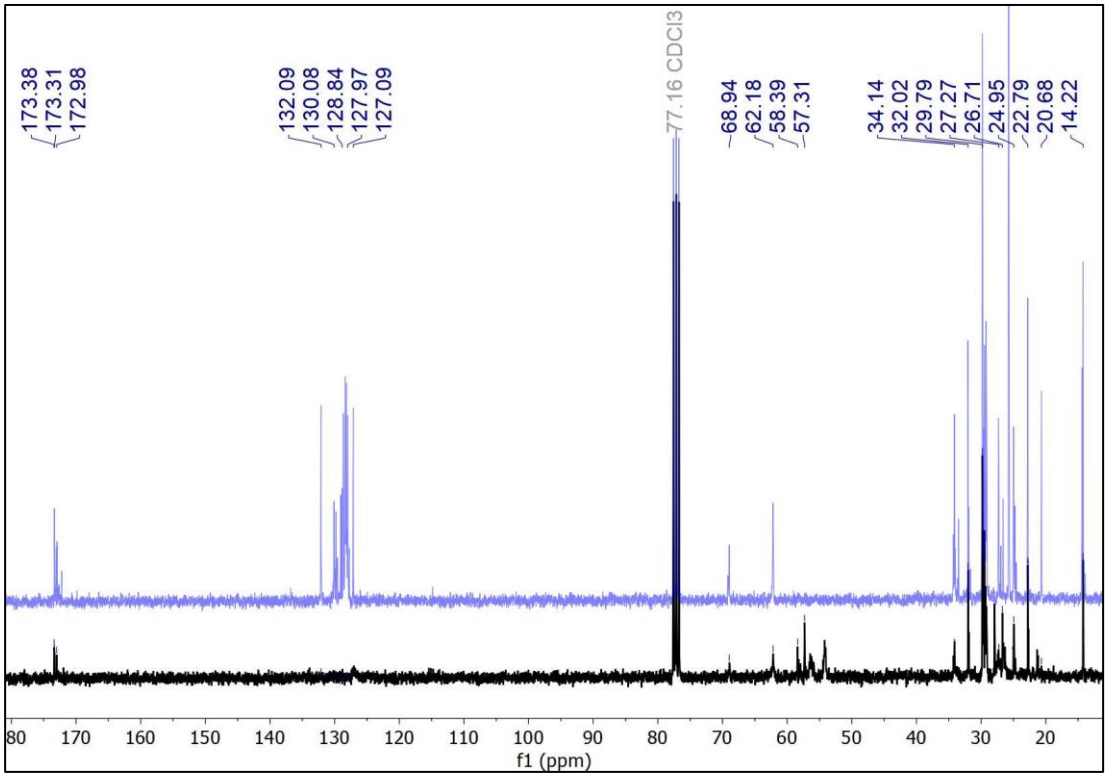

Figure 2.9. ^{13}C NMR spectra of TFO (top, blue) and ETFO (bottom, black).

2.2.2.2 Gas Chromatography-Mass Spectrometry

MO and EMO were analyzed by gas chromatography-mass spectrometry (GC-MS) to determine the conversion of double bonds to the epoxide and act as a confirmatory technique to complement the analysis performed using NMR data. For each GC run, the sample was dissolved in heptane with hexadecane as an internal standard (IS). The oven temperature was 150 °C and was increased to 300 °C at a rate of 10 °C min^{-1}. Helium was used as the carrier gas, set to a flow of 1 mL min^{-1} and experiments were performed in split-mode. Stock standard solutions of 10 mg mL^{-1} of MO and hexadecane were prepared and used to make a series of standards for the preparation of a calibration curve. The concentration of hexadecane was kept constant, while the amount of MO varied from 5% (v/v) to 40% (v/v). The ratio of the area of the MO peak to the IS peak was plotted against the concentration of MO in each standard to give a calibration curve, **Figure 2.10**. After epoxidation of MO using the acid catalyzed reaction with H_2O_2, 5 µL of the sample and 600 µL of hexadecane were made up to a 1 mL sample, and analyzed by GC-MS.

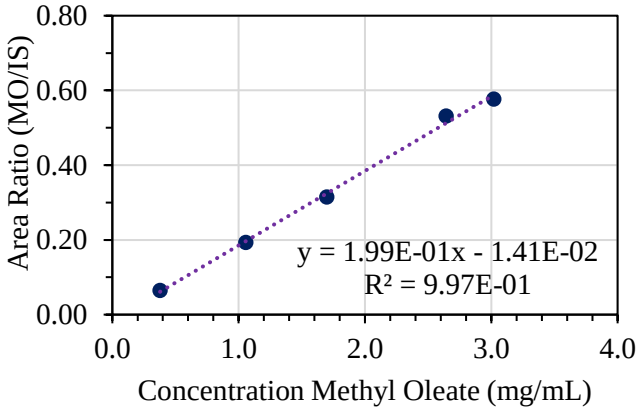

Figure 2.10. Calibration curve for determination of MO concentration by GC-MS.

Table 2.5. Conversion of MO to EMO from GC-MS calibration curve.

Run	Concentration Methyl Oleate (mg/mL)	Area Ratio (MO/IS)	MO (%)	Conversion (%)
1	160	6.234E-01	18.3	81.7
2	135	3.881E-01	15.4	84.6
3	151	4.383E-01	17.3	82.7

Average Conversion (%)	Standard Deviation (%)
83.0	1.5

A representative total ion chromatogram for an EMO sample is shown in **Figure 2.11**. It shows three main peaks, one at 4.8 min due to the IS, one at 9.8 min that represents MO, and one at 11.5 min which represents EMO. Representative mass spectra found for the MO and EMO peaks are given in **Figure 2.12** and **Figure 2.13**. **Figure 2.12** shows a molecular ion with a mass to charge ratio of 296.3, which correlates well with the molar mass of MO at 296.27 g mol^{-1}. **Figure 2.13** shows the molecular ion with a mass to charge ratio of 312.3, confirming the formation of EMO, which has a molar mass of 312.27 g mol^{-1}. Using the calibration curve, the concentration of MO remaining in the epoxidized sample could be determined, which could then be related to the percent conversion to the epoxide. The sample was run in triplicate, giving a conversion of 83.0 ± 1.5%. This agreed well with the conversion of 79% as determined from the ^{1}H NMR spectrum of the same sample. Therefore, ^{1}H NMR spectroscopy, as it is quicker and requires less preparation, was used to determine conversion for all samples in this thesis.

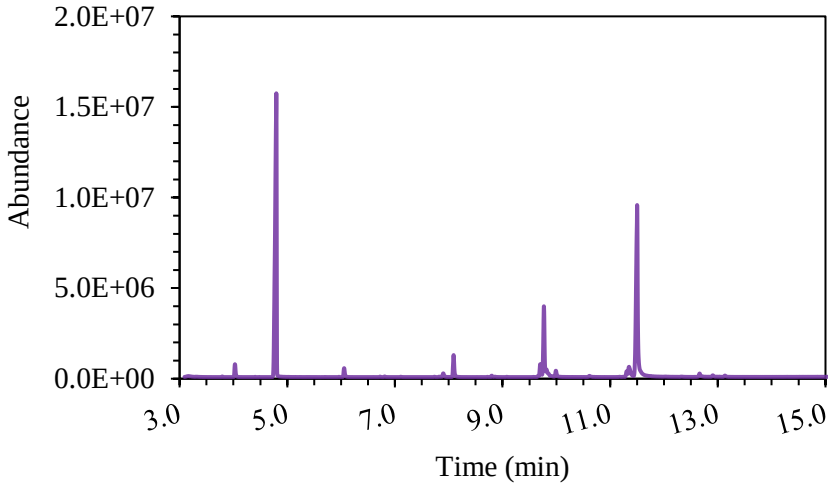

Figure 2.11. Total ion chromatogram of EMO sample with hexadecane internal standard.

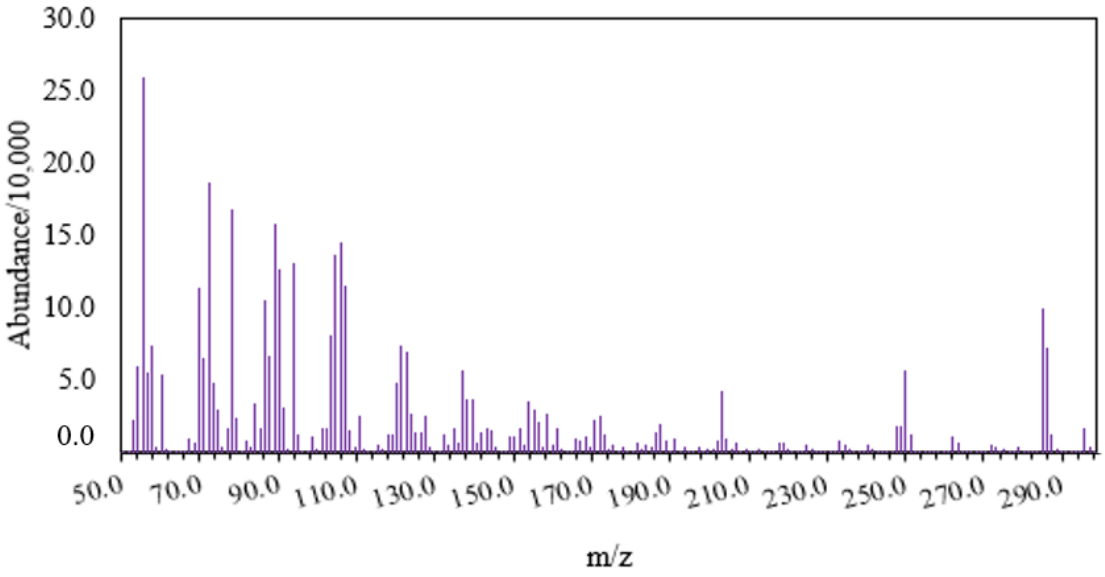

Figure 2.12. Mass spectrum for peak at 9.8 min, MO.

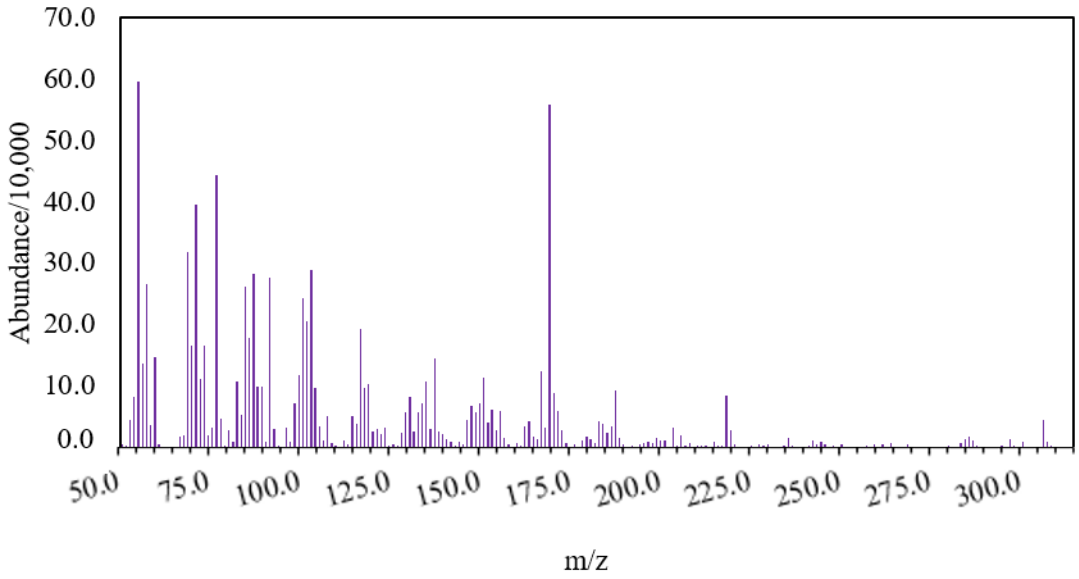

Figure 2.13. Mass spectrum for peak at 11.5 min, EMO.

2.2.2.3 Infrared Spectroscopy and Thermogravimetric Analysis

IR spectroscopy was performed on the starting FO and TFO as well as their corresponding epoxides. Their spectroscopic characterization is consistent with literature reports for vegetable oil epoxides.[11,18] Representative spectra for FO and EFO are shown in **Figure 2.14**. The spectrum for FO showed a characteristic band at 3009 cm^{-1} from the double bonds, which did not appear in the spectrum for EFO. The spectrum for EFO showed a characteristic band at 825 cm^{-1} from the epoxide group, that was not present in the FO spectrum. Bands at 1743 cm^{-1} and 1158 cm^{-1}, due to the ester group and bands at 1462 cm^{-1} and 1377 cm^{-1}, due to the methyl groups, were present in both spectra.

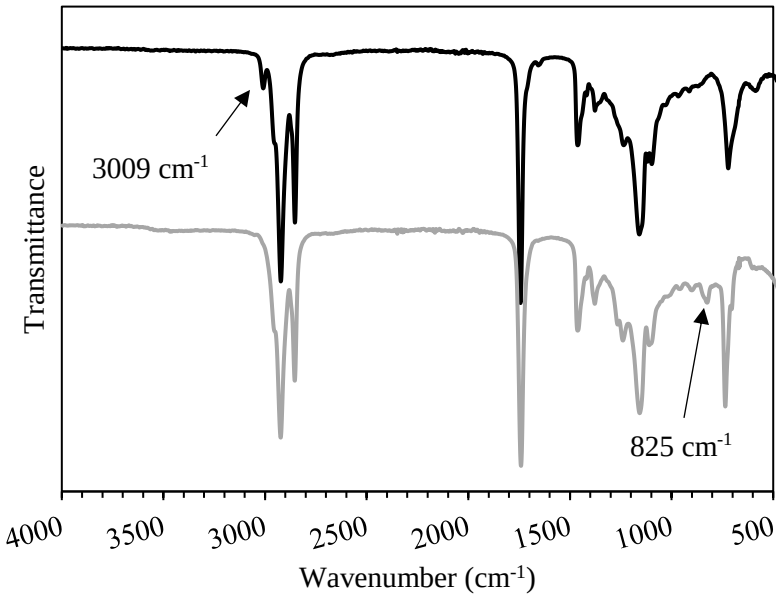

Figure 2.14. Infrared spectra of FO (black, top) and EFO (gray, bottom).

Representative spectra for TFO and ETFO are shown in **Figure 2.15**. The spectrum for TFO showed a characteristic band at 3012 cm^{-1} from the double bonds, which did not appear in the spectrum for ETFO. Bands at 1741 cm^{-1} and 1157 cm^{-1}, due to the ester group and bands at 1458 cm^{-1} and 1377 cm^{-1}, due to the methyl groups, were present in both spectra. The spectrum for ETFO showed a characteristic band at 827 cm^{-1} from the epoxide group, that was not present in the FO spectrum.

Through the acid catalyzed epoxidation of TFO with H_2O_2, a clear yellow oil was obtained after 18 h, which showed no conversion to the epoxide by ^1H NMR spectroscopy. IR spectroscopy was performed on this sample, giving the dashed spectrum in **Figure 2.15**. This spectrum contains bands due to methyl groups at 1459 cm^{-1} and 1377 cm^{-1}, as well bands due to the ester group at 1742 cm^{-1} and 1157 cm^{-1}, identical to those seen in the spectrum for TFO. The spectrum does not contain the desired band at 827 cm^{-1}, indicating

that no epoxide has formed, and instead contains a broad band around 3403 cm^{-1}. This broad band suggests that under the longer reaction time, the epoxide was converted to a diol.

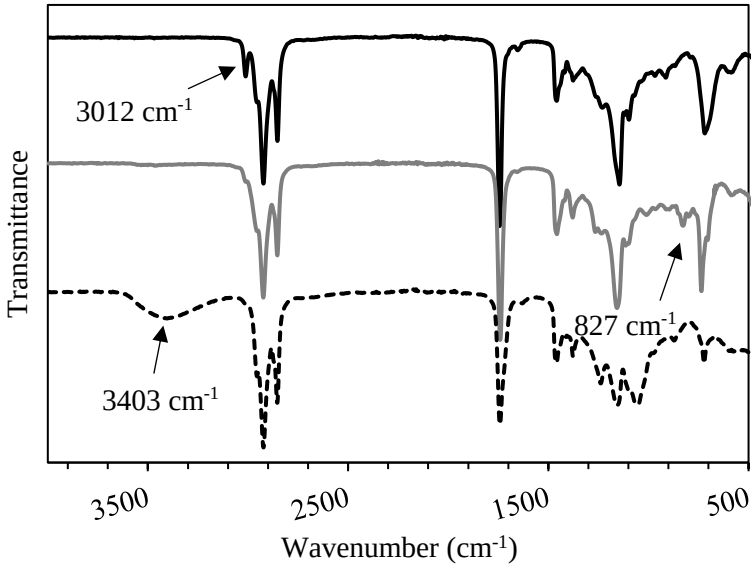

Figure 2.15. Infrared spectra of TFO (black, top), ETFO (gray, middle), over oxidized ETFO (dashed line, bottom).

EFO samples were analyzed by thermogravimetric analysis (TGA). Samples were heated from 20 °C to 800 °C at a heating rate of 10 °C/min, under a constant flow of nitrogen (50 mL/min). **Figure 2.16** shows a representative thermogram for EFO, with degradation of the epoxide beginning around 200 °C and the main degradation occurring above 330 °C.

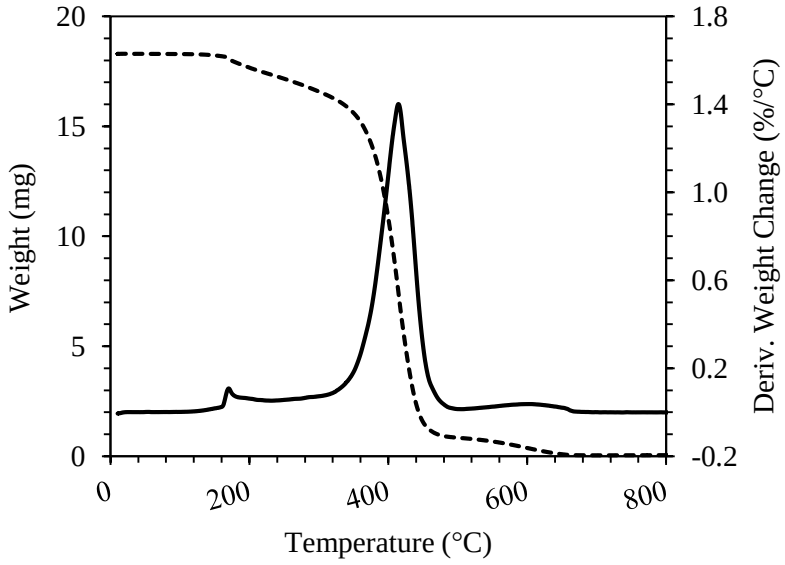

Figure 2.16. TGA plot of EFO, showing weight of sample (dashed line) and derivative weight change (continuous line) with heating.

2.2.3 Life Cycle Assessment of Epoxidation Methods

Using nine metrics, the different epoxidation methods were compared in a gate-to-gate LCA. These metrics were acidification potential (AP), ozone depletion potential (OD), smog formation potential (SF), global warming potential (GW), human toxicity by ingestion (INGTP) and inhalation (INHTP) potentials, persistence (PER), bioaccumulation (BIOACC), and abiotic resource depletion potential (ADP). For some of these metrics the concentration of each chemical in the soil, air, water, and sediment upon release to the environment is needed. To determine these concentrations a multimedia compartmental model was used. For this, the Henry's Law constant, octanol-water partition coefficient (K_{OW}), and soil sorption coefficient (K_{OC}), are required. The data for these calculations were sourced from the NIST Chemistry WebBook and safety data sheets. Values for K_{OC}

were approximated by using **Equation 1**. Values for ADP, GWP, and SFP were found in the literature.[19] In order to determine the persistence of a chemical, the Boethling Index was used and equation parameters were taken from the literature.[20] LC_{50} values used for the calculations were in units of g m^{-3} for rats with an exposure of 4 h. Values for 1 h were used if 4 h values were not available. LD_{50} values that were unavailable were estimated using the EPA Toxicity Estimation Software Tool, Version 4.2.1.[21]

$$K_{OC} = 0.41K_{OW} \quad \textbf{(1)}$$

For the determination of carbon dioxide (CO_2) produced from energy consumption, a heat capacity of 1.82 ± 0.37 J g^{-1} K^{-1} was used for the FO in solvent-free reactions.[22] FO is used in all reactions, so both FO and EFO are not included in the potential and impact tables. Individual indices for the chemicals used in each route are included in **Table 2.7** to **Table 2.10**, with the summary for each route shown in **Table 2.6**.

The first route, which uses *m*-CPBA, forms 3-chlorobenzoic acid (*m*-CBA) as a by-product of the reaction and so is included in the LCA table. This route has the highest ingestion potential due to the different salts used for washing solutions. The inhalation index for this route is the lowest, but no LC_{50} value, which is used to calculate the inhalation index, was found for *m*-CPBA. The inhalation of the fine particles can pose a serious health hazard, making the inhalation index not a representative depiction of the hazard. This route also uses a significant amount of CH_2Cl_2, making the smog formation and global warming indices the highest of all the routes assessed. CH_2Cl_2 is also an ozone depleting chemical that is not controlled by the Montreal Protocol, and is thought to have a negative impact on

the recovery of the ozone layer.[23] The calculated E-factor for this route is the highest, at 131.0.

All other routes use H_2O_2 and appear to be greener than the *m*-CPBA route based on the chosen metrics. The E-factors for the second route, using CH_3COOH, and third route, using HCOOH and ChCl-OxA, are also much lower at 26.38 and 25.22, respectively. The acidification potential is the highest for the second route due to the use of H_2SO_4. These routes have high inhalation and ingestion indices due to the use of H_2O_2. One impactful issue that is not accounted for in the gate-to-gate LCA, is the industrial synthesis of H_2O_2. This is a very energy intensive process that uses large amounts of solvent.[24] If the H_2O_2 required for the synthesis could be obtained in a more sustainable way, such as being generated *in situ* in tandem oxidation reactions[25,26] it would make these routes much more viable as truly green reactions for the epoxidation of alkenes. The HCOOH and ChCl-OxA route removes the use of H_2SO_4, a highly corrosive acid, and the bioaccumulation index is the lower as heptane is not used.

The fourth and final route, which also uses H_2O_2, removes the use of the DES catalyst, as it did not significantly improve the conversion of the FO to the desired epoxide. This reaction could be performed under otherwise identical conditions and optimized using DMC as the solvent used in purification of the product. The use of DMC over CH_2Cl_2 helps improve the environmental impact of the synthesis as CH_2Cl_2 is highly toxic and contributes to ozone depletion.[23] DMC is considered to be an environmentally friendly chemical that can be synthesized through many different chemical routes. A promising route for synthesizing DMC is a vapour-phase methyl nitrile carbonylation that has a low

cost, high efficiency, and is considered to be environmentally friendly.[27] An LCA was performed in 2016 by Garcia-Herrero et al. on six different routes to the formation of DMC, and showed that an electrochemical process could well exceed commercial processes with future development.[28] In 2019, DMC was shown to be synthesized using an electrochemically generated copper carbonyl catalyst that subsequently was used to form DMC.[29] The formation of DMC occurred slowly over 30 to 40 days, but is an example of an environmentally friendly synthesis of DMC. By using DMC and removing ChCl-OxA, many of the metrics in the LCA are improved on, making it the reaction with the greatest potential to be a green process.

Table 2.6. LCA comparison of epoxidation routes.

Route	I_A	I_{OD}	I_{SF}	I_{GW}	I_{INHT}	I_{INGT}	PER	BIOACC (log K_{ow})	I_{AD}
1	0	0.5	0.3	800	24	9.4E5	weeks	2.2	4.4E-1
2	20	0.1	0.1	192	2,500	9,200	weeks	4.7	2.8E-3
3	0	0.6	0.04	133	3,900	12,000	weeks	1.25	3.1E-3
4	0	0	0.2	54	4,120	12,000	weeks	0.35	3.2E-3

Route 1: *m*-CPBA epoxidation, route 2: H_2O_2/H_2SO_4 epoxidation, route 3: ChCl-OxA epoxidation, route 4: formic acid epoxidation.

Table 2.7. LCA indices for route 1, *m*-CPBA epoxidation.

Chemical	**I_A**	**I_{OD}**	**I_{SF}**	**I_{GW}**	**I_{INHT}**	**I_{INGT}**	**PER**	**BIOACC (log K_{ow})**	**I_{AD}**
CO_2	0	0	0	500	0	0	n/a	n/a	-
CH_2Cl_2	0	0.5	0.3	300	24	0.03	weeks	1.25	6.9E-4
m-CPBA	0	0	0	0	?	52	weeks	1.68	3.7E-6
m-CBA	0	0	0	0	?	240	weeks	2.15	9.2E-6
Na_2SO_3	0	0	0	0	0	2.4E5	n/a	-4.00	4.4E-1
$NaHCO_3$	0	0	0	0	0	2.5E5	n/a	-4.01	-
NaCl	0	0	0	0	0	4.5E5	n/a	-3.00	1.0E-4
$MgSO_4$	0	0	0	0	0	?	n/a	n/a	3.1E-3

Table 2.8. LCA indices for route 2, H_2O_2/H_2SO_4 epoxidation.

Chemical	**I_A**	**I_{OD}**	**I_{SF}**	**I_{GW}**	**I_{INHT}**	**I_{INGT}**	**PER**	**BIOACC (log K_{ow})**	**I_{AD}**
CO_2	0	0	0	122	0	0	n/a	n/a	-
H_2O_2	0	0	0	0	2500	7900	weeks	-1.50	-
Acetic Acid	0	0	0	0	0	1	weeks	-0.2	-
H_2SO_4	20	0	0	0	0	1300	n/a	n/a	-
Heptane	0	0	0	0	0	0	weeks	4.7	-
$MgSO_4$	0	0	0	0	0	?	n/a	n/a	2.8E-3
CH_2Cl_2	0	0.1	0.1	70	5	0	weeks	1.25	1.6E-4

Table 2.9. LCA indices for route 3, ChCl-OxA epoxidation.

Chemical	**I_A**	**I_{OD}**	**I_{SF}**	**I_{GW}**	**I_{INHT}**	**I_{INGT}**	**PER**	**BIOACC (log K_{ow})**	**I_{AD}**
CO_2	0	0	0	94	0	0	n/a	n/a	-
H_2O_2	0	0	0	0	3900	12000	weeks	-1.50	-
ChCl	0	0	0	0	0	2	n/a	n/a	4.4E-7
OxA	0	0	0	0	0	16	weeks	-1.70	-
Formic Acid	0	0	0	0	0	9	weeks	-0.54	-
CH_2Cl_2	0	0.6	0.04	39	3	0.004	weeks	1.25	8.8E-5
$MgSO_4$	0	0	0	0	0	?	n/a	n/a	3.1E-3

Table 2.10. LCA indices for route 4, formic acid epoxidation.

Chemical	I_A	I_{OD}	I_{SF}	I_{GW}	I_{INHT}	I_{INGT}	PER	BIOACC (log K_{ow})	I_{AD}
CO_2	0	0	0	36	0	0	n/a	n/a	-
H_2O_2	0	0	0	0	4000	12000	weeks	-1.50	-
Formic Acid	0	0	0	0	0	9	weeks	-0.54	-
$MgSO_4$	0	0	0	0	0	?	n/a	n/a	3.2E-3
DMC	0	0	0.2	19	120	18	weeks	0.35	-

2.3 Conclusions

FO-based epoxides derived from capelin oil have been previously reported,[4] but consideration was not given to the overall greenness of the process. The FO used in this thesis was epoxidized in high conversions using multiple methods. Using *m*-CPBA for the epoxidation of the waste-derived FO gave complete conversion to the desired epoxide, but uses large amounts of toxic solvents, and through the LCA performed, was found to be the least green method of those studied. To improve on the greenness of the epoxidation reaction H_2O_2 and CH_3COOH were used, with H_2SO_4 as the catalyst. Using this method, MO and OA were epoxidized in an 86% and 85% conversion, respectively. For the FO, an undesired polyol was formed at long reaction times (18 h) but reducing the reaction time to 12 h reduced polyol formation to 5% and conversion to the desired epoxide was 89%. Using the H_2SO_4 oxidation method for 15.25 h, a conversion of 65% was achieved for the TFO. This demonstrates that a relatively impure raw material (FO) can be converted potentially in higher yields than the purer TFO.

To further improve on the environmental impact of the epoxidation method used, a reaction using H_2O_2 and HCOOH was used, which through the LCA, was found to be the

greenest method of those used in this thesis. Using this method, FO and TFO could be epoxidized with high conversions of 94% and 84%, respectively. The use of CH_2Cl_2 could also be replaced by using DMC as the solvent, allowing for additional improvement on the environmental friendliness of the reaction. Using this green method, the desired epoxides were formed, which could be used for the formation of cyclic carbonates in Chapter 3.

2.4 Experimental

2.4.1 Materials

A modified fishmeal process was used to extract the fish oil used in this work from farmed Atlantic salmon (*Salmo salar Linnaeus*) offcuts as previously reported.[5] MO (70%), and *m*-CPBA (≤ 77%) were purchased from Sigma-Aldrich. OA dihydrate was purchased from A & C American Chemicals Ltd. ChCl (98%) was purchased from Alfa Aesar. CH_2Cl_2, glacial CH_3COOH and H_2SO_4 (all ACS grade) were purchased from Fisher Scientific. HCOOH was purchased from Fluka Analytical. H_2O_2 (30% w/w) was purchased from ACP chemicals. All reagents were used without further purification.

TFO was purchased from Jamieson Vitamins, containing triglycerides of EPA and DHA. The oil from the tablets was removed by cutting open the gelatin package and squeezing the oil into the reaction vessel. Similarly, the oil could be removed from the tablets by dissolving the gelatin tablets in hot water. Once dissolved, the oil can be separated from the water, collected, and dried.

2.4.2 Instrumentation

NMR spectra were recorded at 298 K on a Bruker Avance III 300 or Avance 500 MHz spectrometer in chloroform-d ($CDCl_3$). Chemical shifts, in ppm, for ^{1}H and ^{13}C NMR were referenced to the solvent signals or tetramethylsilane internal standard. GC-MS analyses were performed using an Agilent Technologies 7890 GC system equipped with a HP5-MS column coupled to an Agilent Technologies 5975C mass selective detector. IR spectra were recorded on a Bruker Alpha IR spectrophotometer using a platinum diamond ATR module, 36 scans at 4 cm^{-1} resolution in the spectral range of 400-4000 cm^{-1}. The thermal stability of samples was determined by TGA on a Q500 TGA from TA Instruments, heating from 20 to 800 °C at a heating rate of 20 °C min^{-1}. TGA analyses were performed under a constant flow of nitrogen gas (50 mL min^{-1}). Rheology measurements for the determination of the viscosity of the FO and EFO were measured on an Anton Parr Physica MCR 301. The measuring cone used was a D 50 mm, with an angle of 1° and gap of 0.100 mm. Water was analyzed for reference. Runs were performed in triplicate at 25.00 °C on 1 mL of sample. The viscosity was taken as the average of the slopes of the three shear stress versus shear rate plots (**A1-A3**).

2.4.3 General Procedure for Oxidation by 3-Chloroperoxybenzoic acid

Epoxidized Methyl Oleate

Prepared following a previously reported method,[7] with modification of the purification procedure. Methyl oleate (1.43 g, 3.4 mmol) was dissolved in 40 mL of CH_2Cl_2 in a round bottom flask equipped with a septum and needle, with stirring at 0 °C. 3-

Chloroperoxybenzoic acid (*m*-CPBA, 0.93 g, 4.1 mmol) was slowly added and left to stir at 25 °C for 11 h. The reaction mixture was cooled to 0 °C and filtered. The resulting solution was washed with 1 M Na_2SO_3 solution (3 × 20 mL), a saturated solution of $NaHCO_3$ (3 × 20 mL), and a 3 wt% solution of NaCl (15 mL). The organic phase was dried over anhydrous $MgSO_4$, filtered, and the solvent removed under reduced pressure to give a clear, colourless oil (1.37 g).

Epoxidized Fish Oil

Prepared following a previously reported method,[7] with modification to the purification procedure and equivalents of reagents. In a typical reaction, waste-derived fish oil (1.50 g) was dissolved in 40 mL of CH_2Cl_2 in a round bottom flask equipped with a septum and a needle, cooled to 0 °C and stirred. *m*-CPBA (1.99 g, 8.9 mmol) was slowly added and the mixture was left to stir at 25 °C for 12 h. The mixture was cooled to 0 °C and filtered. The resulting solution was washed with 1 M Na_2SO_3 solution (3 × 20 mL), a saturated solution of $NaHCO_3$ (3 × 20 mL), and a saturated solution of NaCl (15 mL). The organic phase was dried over anhydrous $MgSO_4$, filtered, and the solvent removed under reduced pressure to give a clear, colourless oil (1.56 g).

2.4.4 General Procedure for Oxidation Catalyzed by Sulfuric Acid

Epoxidized Methyl Oleate

Prepared following a previously reported method,[9] with modification of the solvent used. Methyl oleate (7.78 g) and CH_3COOH (0.46 g, 7.7 mmol) were dissolved in heptane (1.43 g) and heated in an oil bath to 60 °C. An acidified hydrogen peroxide solution (3.13

g, 28 mmol H_2O_2, 30% wt/wt; 0.047 g conc. H_2SO_4) was added dropwise to the reaction over 1 h. Upon complete addition, the reaction was stirred for 18 h at 60 °C. The reaction mixture was cooled to 0 °C and washed with deionized water (3 × 10 mL). Combined aqueous phase was extracted with 5 mL of heptane. Combined organic phase was dried over anhydrous $MgSO_4$ and the solvent removed under reduced pressure to give a clear, colourless oil (6.44 g).

Epoxidized Oleic Acid

Prepared following a previously reported method,[9] with modification of the solvent used. Oleic acid (5.77 g) and CH_3COOH (0.46 g, 7.7 mmol) were dissolved in heptane (1.45 g) and heated in an oil bath to 60 °C. An acidified hydrogen peroxide solution (3.24 g, 29 mmol H_2O_2, 30% wt/wt; 0.048 g conc. H_2SO_4) was added dropwise to the reaction over 1 h. Upon complete addition, the reaction was stirred for 18 h at 60 °C. The orange reaction mixture was cooled to 0 °C and washed with deionized water (3 × 10 mL). The combined aqueous phase was extracted with 5 mL CH_2Cl_2. The combined organic phase was dried over anhydrous $MgSO_4$ and the solvent removed under reduced pressure to give a clear, colourless oil (5.52 g).

Epoxidized Fish Oil

Prepared following a previously reported method,[9] with modification of the reaction time, solvent, and equivalents of reagents. Waste-derived fish oil (3.00 g) and CH_3COOH (0.45 g, 7.6 mmol) was dissolved in heptane (0.65 g) and heated in an oil bath to the reaction temperature. An acidified hydrogen peroxide solution (2.60 g, 23 mmol H_2O_2, 30% wt/wt; 0.026 g conc. H_2SO_4) was added dropwise to the reaction over 1 h. Upon complete addition,

the reaction was stirred for 12 h at the desired temperature. The reaction mixture was cooled to 0 °C, dissolved in 5 mL CH_2Cl_2, and washed with deionized water (3 × 10 mL). The organic phase was dried over anhydrous $MgSO_4$ and the solvent removed under reduced pressure to give a clear, colourless oil (1.66 g).

Epoxidized Tablet Fish Oil

Prepared by a previously reported method,[9] with modification of the reaction time, solvent, and equivalents of reagents. Tablet fish oil (3.23 g) and CH_3COOH (0.66 g, 11.07 mmol) was dissolved in heptane (0.68 g) and heated in an oil bath to 60 °C. An acidified hydrogen peroxide solution (3.37 g, 30 mmol H_2O_2, 30% wt/wt; 0.024 g conc. H_2SO_4) was added dropwise to the reaction over 1 h. Upon complete addition, the reaction was stirred for the indicated time at 60 °C. The light orange reaction mixture was cooled to 0 °C, dissolved in 5 mL CH_2Cl_2, and washed with deionized water (3 × 10 mL). The organic phase was dried over anhydrous $MgSO_4$ and the solvent removed under reduced pressure to give a clear, orange or yellow oil (2.04 g).

2.4.5 General Procedure for Oxidation Catalyzed by Formic Acid

Epoxidized Methyl Oleate

Methyl oleate (2.01 g), and HCOOH (0.17 g, 3.62 mmol), were heated to 40 °C. For experiments using a deep eutectic mixture of choline chloride and oxalic acid (1:1 molar ratio, 0.056 g), it was also added before heating to 40 °C. Hydrogen peroxide (0.92 g, 8.1 mmol, 30% wt/wt) was added dropwise over 1 h then heated to 50 °C and stirred for 8 h. Once complete, the reaction was cooled to 0 °C, the organic phase was washed with

deionized water (3 × 10 mL), and dried over anhydrous $MgSO_4$ to give a clear, colourless oil (0.41 g).

Epoxidized Oleic Acid

Oleic acid (2.55 g), and HCOOH (0.27 g, 5.90 mmol), were heated to 40 °C. Hydrogen peroxide (1.53 g, 13.5 mmol, 30% wt/wt) was added dropwise over 1 h then heated to 50 °C and stirred for 5 h. Once complete, the reaction was cooled to 0 °C, dissolved in CH_2Cl_2, and the organic phase was washed with deionized water (3 × 10 mL), and dried over anhydrous $MgSO_4$ to give a light pink, opaque oily solid (1.74 g).

Epoxidized Fish Oil

Waste-derived fish oil (2.00 g) and HCOOH (0.36 g, 7.79 mmol) were heated to 40 °C. For experiments using a deep eutectic mixture of choline chloride and oxalic acid (1:1 molar ratio, 0.10 g), it was also added before heating to 40 °C. Hydrogen peroxide (1.96 g, 17 mmol, 30% wt/wt) was added dropwise over 1 h then heated to 50 °C and stirred for 5 h. The reaction was cooled to 0 °C and dissolved in 5 mL CH_2Cl_2, or 8 mL DMC. The organic phase was washed with deionized water (3 × 10 mL), and the aqueous phase extracted with 10 mL DMC when used as the solvent, dried over anhydrous $MgSO_4$, and the solvent removed under reduced pressure to give a clear, colourless oil (1.54 g).

Epoxidized Tablet Fish Oil

Tablet fish oil (1.90 g) and HCOOH (0.53 g, 11.42 mmol) were heated to 40 °C. For experiments using a deep eutectic mixture of choline chloride and oxalic acid (1:1 molar ratio, 0.12 g), it was also added before heating to 40 °C. Hydrogen peroxide (1.84 g,

16 mmol, 30% wt/wt) was added dropwise over 1 h then heated to 50 °C and stirred for 5-8 h. The reaction was cooled to 0 °C and dissolved in 5 mL of CH_2Cl_2. The organic phase was washed with deionized water (3 × 10 mL), and the combined aqueous phase extracted with 6 mL CH_2Cl_2. The combined organic phase was dried over anhydrous $MgSO_4$, and the solvent removed under reduced pressure to give a clear, orange oil (1.95 g).

2.5 References

(1) Lligadas, G.; Ronda, J. C.; Galia, M.; Cadiz, V. Renewable Polymeric Materials from Vegetable Oils: A Perspective. *Mater. Today*. **2013**, *16* (9), 337–343.

(2) Bhalerao, M. S.; Kulkarni, V. M.; Patwardhan, A. V. Ultrasound-Assisted Chemoenzymatic Epoxidation of Soybean Oil by Using Lipase as Biocatalyst. *Ultrason. Sonochem*. **2018**, *40*, 912–920.

(3) Jalilian, S.; Yeganeh, H. Preparation and Properties of Biodegradable Polyurethane Networks from Carbonated Soybean Oil. *Polym. Bull*. **2015**, *72* (6), 1379–1392.

(4) Marks, D. W.; Larock, R. C. The Conjugation and Epoxidation of Fish Oil. *J. Am. Oil Chem. Soc*. **2002**, *79* (1), 65–68.

(5) Adeoti, I. A.; Hawboldt, K. Comparison of Biofuel Quality of Waste Derived Oils as a Function of Oil Extraction Methods. *Fuel*. **2015**, *158*, 183–190.

(6) U.S. Department of Agriculture. Oil, soybean, salad or cooking https://fdc.nal.usda.gov/fdc-app.html#/food-details/171411/nutrients (accessed July 2, 2019).

(7) Peña Carrodeguas, L.; Cristòfol; Fraile, J. M.; Mayoral, J. A.; Dorado, V.; Herrerías, C. I.; Kleij, A. W. Fatty Acid Based Biocarbonates: Al-Mediated Stereoselective Preparation of Mono-, Di- and Tricarbonates under Mild and Solvent-Less Conditions. *Green Chem*. **2017**, *19* (15), 3535–3541.

(8) Rubio, M.; Ramírez-Galicia, G.; Jovany López-Nava, L. Mechanism Formation of Peracids. *J. Mol. Struct. THEOCHEM.* **2005**, *726* (1–3), 261–269.

(9) Langanke, J.; Greiner, L.; Leitner, W. Substrate Dependent Synergetic and Antagonistic Interaction of Ammonium Halide and Polyoxometalate Catalysts in the Synthesis of Cyclic Carbonates from Oleochemical Epoxides and CO_2. *Green Chem.* **2013**, *15* (5), 1173–1182.

(10) Wang, J.; Liu, Y.; Zhou, Z.; Fu, Y.; Chang, J. Epoxidation of Soybean Oil Catalyzed by Deep Eutectic Solvents Based on the Choline Chloride-Carboxylic Acid Bifunctional Catalytic System. *Ind. Eng. Chem. Res*. **2017**, *56* (29), 8224–8234.

(11) Audic, J. L.; Lemiègre, L.; Corre, Y. M. Thermal and Mechanical Properties of a Polyhydroxyalkanoate Plasticized with Biobased Epoxidized Broccoli Oil. *J. Appl. Polym. Sci.* **2014**, *131* (6), 39983.

(12) Campanella, A.; La Scala, J. J.; Wool, R. P. Fatty Acid-Based Comonomers as Styrene Replacements in Soybean and Castor Oil-Based Thermosetting Polymers. *J. Appl. Polym. Sci*. **2010**, *119*, 1000–1010.

(13) Hazmi, A. S. A.; Aung, M. M.; Abdullah, L. C.; Salleh, M. Z.; Mahmood, M. H. Producing Jatropha Oil-Based Polyol via Epoxidation and Ring Opening. *Ind. Crops Prod*. **2013**, *50*, 563–567.

(14) Meadows, S.; Hosur, M.; Celikbag, Y.; Jeelani, S. Comparative Analysis on the Epoxidation of Soybean Oil Using Formic and Acetic Acids. *Polym. Polym. Compos.* **2018**, *26* (4), 289–298.

(15) Aursand, M.; Rainuzzo, J. .; Grasdalen, H. Quantitative High-Resolution ^{13}C and ^{1}H Nuclear Magnetic Resonance of Ω3 Fatty Acids from White Muscle of Atlantic Salmon (Salmo Salar). *J. Am. Oil Chem. Soc.* **1993**, *70* (10), 971–981.

(16) Büttner, H.; Grimmer, C.; Steinbauer, J.; Werner, T. Iron-Based Binary Catalytic System for the Valorization of CO_2 into Biobased Cyclic Carbonates. *ACS Sustain. Chem. Eng.* **2016**, *4* (9), 4805–4814.

(17) Zhang, J.; Tang, J. J.; Zhang, J. X. Polyols Prepared from Ring-Opening Epoxidized Soybean Oil by a Castor Oil-Based Fatty Diol. *Int. J. Polym. Sci.* **2015**, *2015*.

(18) Téllez, G. L. Characterization of Linseed Oil Epoxidized at Different Percentages. *Superf. y Vacío.* **2009**, *22* (1), 5–10.

(19) Guinée, J. B. *Handbook on Life Cycle Assessment*; Kluwer Academic Publishers: Dordrecht, 2002.

(20) Boethling, R. S.; Howard, P. H.; Meylan, W.; Stiteler, W.; Beauman, J.; Tirado, N. Group Contribution Method for Predicting Probability and Rate of Aerobic Biodegradation. *Environ. Sci. Technol.* **1994**, *28*, 459–465.

(21) United States Environmental Protection Agency. Toxicity Estimation Software Tool (TEST) https://www.epa.gov/chemical-research/toxicity-estimation-software-tool-test (accessed July 2, 2019).

(22) Jayasinghe, P. Biofuels from Fish Waste From Remote Fish Processing Plants in Newfoundland and Labrador, B. Sc. Eng. (Hons), Memorial University of Newfoundland, St. John's, NL, November 2010.

(23) Hossaini, R.; Chipperfield, M. P.; Montzka, S. A.; Leeson, A. A.; Dhomse, S. S.; Pyle, J. A. The Increasing Threat to Stratospheric Ozone from Dichloromethane. *Nat. Commun*. **2017**, *8*.

(24) Campos-Martin, J. M.; Blanco-Brieva, G.; Fierro, J. L. G. Hydrogen Peroxide Synthesis: An Outlook beyond the Anthraquinone Process. *Angew. Chem. Int. Ed*. **2006**, *45* (42), 6962–6984.

(25) Puértolas, B.; Hill, A. K.; García, T.; Solsona, B.; Torrente-Murciano, L. In-Situ Synthesis of Hydrogen Peroxide in Tandem with Selective Oxidation Reactions: A Mini-Review. *Catal. Today*. **2015**, *248*, 115–127.

(26) Chen, Q.; Beckman, E. J. One-Pot Green Synthesis of Propylene Oxide Using in Situ Generated Hydrogen Peroxide in Carbon Dioxide. *Green Chem*. **2008**, *10* (9), 934–938.

(27) Tan, H.-Z.; Wang, Z.-Q.; Xu, Z.-N.; Sun, J.; Xu, Y.-P.; Chen, Q.-S.; Chen, Y.; Guo, G.-C. Review on the Synthesis of Dimethyl Carbonate. *Catal. Today.* **2018**, *316*, 2–12.

(28) Garcia-Herrero, I.; Cuéllar-Franca, R. M.; Enríquez-Gutiérrez, V. M.; Alvarez-Guerra, M.; Irabien, A.; Azapagic, A. Environmental Assessment of Dimethyl Carbonate Production: Comparison of a Novel Electrosynthesis Route Utilizing CO_2 with a Commercial Oxidative Carbonylation Process. *ACS Sustain. Chem. Eng*. **2016**, *4* (4), 2088–2097.

(29) Davies, B. J. V.; Šarić, M.; Figueiredo, M. C.; Schjødt, N. C.; Dahl, S.; Moses, P. G.; Escudero-Escribano, M.; Arenz, M.; Rossmeisl, J. Electrochemically Generated Copper Carbonyl for Selective Dimethyl Carbonate Synthesis. *ACS Catal*. **2018**, 859–866.

Chapter 3: Coupling of Epoxidized Fish Oil with Carbon Dioxide

3.1 Introduction

The chemical fixation of carbon dioxide (CO_2) is an attractive area of research as CO_2 is an inexpensive, non-toxic, non-depleting and renewable resource.[1–3] Using CO_2 as a feedstock for reactions is also highly attractive as it utilizes the main chemical product of fossil fuel burning. While many reactions involve using CO_2 as a starting material, including the production of urea, methanol, salicylic acid, as well and organic and inorganic carbonates, the amount of CO_2 consumed by these reactions is a very small fraction of the CO_2 generated by human activity today.[1] Furthermore, the capture and utilization of CO_2 requires a considerable amount of energy, as it is the lowest in energy of all carbon-containing binary neutral species.[4] The energy needed to capture CO_2 leads to further emissions of CO_2 and other greenhouses gases, making the environmental benefit of CO_2 utilization difficult to define. Therefore, the goal for making cyclic carbonates is not to greatly reduce the amount of CO_2 in the atmosphere, but to access more environmentally friendly routes to products that would otherwise be produced using petroleum-derived or toxic reagents. The first reactions to produce cyclic carbonates used diols and phosgene.[5,6] Phosgene is toxic and has a large environmental impact. Therefore, using CO_2 and biomass-derived epoxides to form organic cyclic carbonates could greatly decrease the environmental impact of their production.

Cyclic carbonates derived from soybean oil-derived epoxides were first reported in 2004 by Tamami et al., which were further used to make non-isocyanate polyurethanes (NIPU).[7] The reaction could be performed on a large scale, using 5 mol% (with respect to

the epoxy groups) of tetrabutylammonium bromide (TBAB) as the catalyst and achieved a 94% yield of carbonated soybean oil (CSBO). The reaction was performed at 110 °C at atmospheric pressure with a flow of CO_2, and was complete after 70 h.

As was demonstrated in Chapter 2, FO-based epoxides can be synthesized with high conversions and are spectroscopically similar to those of epoxides derived from soybean oil. Several catalysts were used in this thesis, with the reaction conditions optimized for both the model substrates, epoxidized methyl oleate (EMO) and epoxidized oleic acid (EOA) (**Scheme 3.1**), as well as the two FO substrates, epoxidized fish oil (EFO) and epoxidized tablet fish oil (ETFO) (**Scheme 3.2**). The optimization and catalyst screening will be outlined and discussed in Section 3.2.

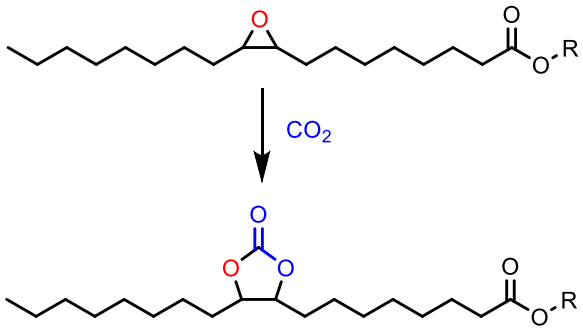

Scheme 3.1. Schematic for the conversion of EMO (R = Me) and EOA (R = H) to their respective cyclic carbonates.

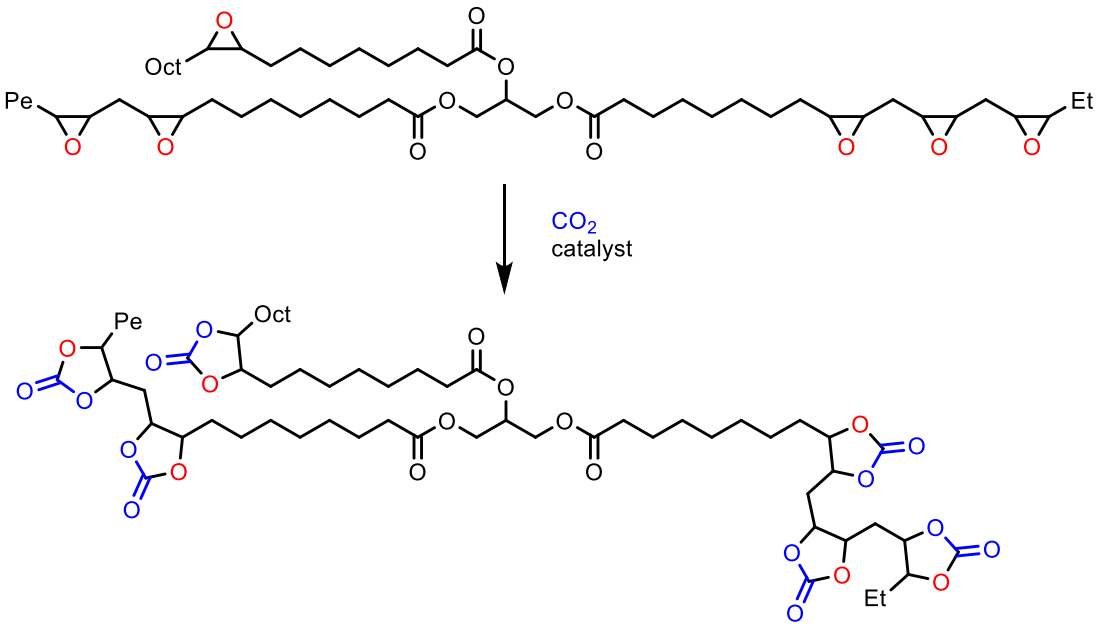

Scheme 3.2. Schematic for the conversion of EFO triglycerides to organic cyclic carbonates.

3.2 Results and Discussion

3.2.1 Catalyst Screening and Parameter Optimization

The formation of cyclic carbonates from the epoxidized oils was performed using several catalysts with CO_2 in a pressure vessel. The epoxide, catalyst, and co-catalyst were added to a pressure vessel, the vessel was sealed, and the mixtures stirred by a magnetic stirrer. The vessel was then pressurized to 10 bar with CO_2 and heated to the desired reaction temperature. Once the reaction was complete, the vessel was cooled to room temperature, the pressure was slowly released, and the carbonated oil collected. When biochar was used as a catalyst, the carbonated product was dissolved in CH_2Cl_2, filtered through a glass frit, and the solvent removed to give the carbonated product. In all other

cases, the carbonated product was not further purified. This gave high conversions of the epoxide to the desired cyclic carbonate, as determined by ^{1}H nuclear magnetic resonance (NMR) spectroscopy.

Summarized reaction conditions for the formation of carbonated fish oil (CFO) from EMO are presented in **Table 3.1**. Reactions with EMO were ran for 24 h at 110 °C at a pressure of 10 bar CO_2. When bis(triphenylphosphine)iminium chloride (PPNCl) was used, reaction conditions were changed to 100 °C and 20 bar CO_2. Entry 1 was performed using a two-component catalyst system of oxidized biochar,[8] a material produced from the pyrolysis of biomass under a limited supply of oxygen,[9] with TBAB. The biochar activates the epoxide through hydrogen bonding with hydroxyl groups on the surface of the biochar, allowing for nucleophilic attack by the chloride from TBAB. Using 5 wt.% of biochar and 5.9 mol% of TBAB gave almost complete conversion to the desired cyclic carbonate, as determined from the ^{1}H NMR spectrum (**Figure 3.2**) and confirmed by the ^{13}C NMR spectrum (**Figure 3.3**). In entry 2, an iron(III) amino-bis(phenolate) complex FeCl(O_2N_2) was used, shown in **Figure 3.1**, along with TBAB. Using 1.2 mol% of FeCl(O_2N_2) and 5.0 mol% of TBAB, almost complete conversion was also achieved. This reaction proceeds through the mechanism shown in **Scheme 3.3**. The Lewis acidic metal center activates the epoxide group, allowing for nucleophilic attack by the bromide, forming a metal-alkoxide intermediate. Insertion of the CO_2 then occurs, followed by closing of the ring to form the cyclic carbonate.

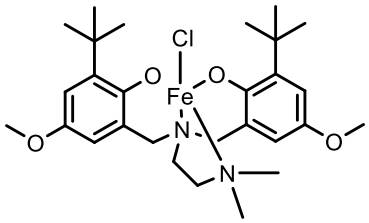

Figure 3.1. Iron(III) amino-bis(phenolate) complex, $FeCl(O_2N_2)$ used for the coupling of epoxides and CO_2.[10]

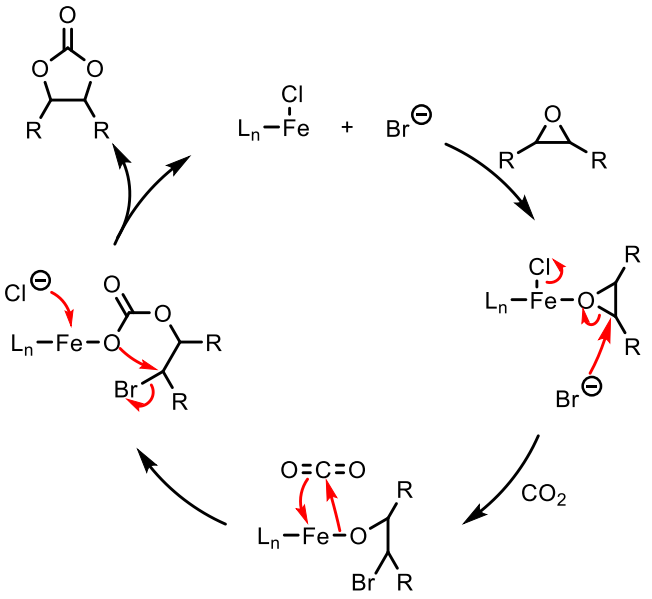

Scheme 3.3. Mechanism for the formation of cyclic carbonates from epoxides, catalyzed by $FeCl(O_2N_2)$ and TBAB.[11]

Changing the second component to PPNCl instead of TBAB reduced the conversion to only 10%. Triphenylborane (BPh_3), which has been previously used in the Kerton group for the formation of cyclic and polycarbonates,[12] was used for the formation of cyclic

carbonates from EMO. Using 0.7 mol% of BPh_3 and 2.9 mol% of PPNCl, a conversion of 61% was achieved.

TBAB is a catalyst commonly used in the literature for the formation of cyclic carbonates from vegetable oil-based epoxides and CO_2,[7,13–16] and so a reaction was performed using TBAB alone. With a catalyst loading of 5 mol%, a high conversion of 86% was achieved. Since the reaction using just TBAB as the catalyst gave high conversions, it was used for the optimization reactions with EFO. Experiments were performed using EOA under similar conditions using TBAB and showed no conversion to the cyclic carbonate by ^{1}H NMR or infrared (IR) spectroscopy, potentially due to the presence of the free carboxylic acid group (**A5**, **A6**).

Table 3.1. Catalytic coupling of EMO and CO_2 at 110 °C.

Entry	Catalyst System		Mol%[a]		Pressure (bar CO_2)	Conversion to Cyclic Carbonate (%)[b]
	1	2	1	2		
1	Biochar	TBAB	5.0[c]	5.9	10	99
2	$FeCl(O_2N_2)$	TBAB	1.2	5.0	10	99
3[d]	$FeCl(O_2N_2)$	PPNCl	0.7	3.0	20	10
4[d]	BPh_3	PPNCl	0.7	2.9	20	61
5	TBAB	N/A	5.0	0	10	86

[a]Relative to moles of epoxide groups. [b]Determined by ^{1}H NMR spectroscopy. [c]Weight % relative to mass of oil used. [d] Performed at 100 °C.

Summarized reaction conditions for the formation of cyclic carbonates from EFO are presented in **Table 3.2**. Entry 1, using 6.7 mol% of TBAB, afforded a high conversion of 92%. Formation of the desired cyclic carbonate was confirmed by IR spectroscopy,

which is presented in Section 3.2.2.2. The synthesized CFO showed an increase of viscosity from 0.0962 ± 0.0017 Pa·s for EFO, to 5.19 ± 0.14 Pa·s (**A4**). Following a method reported in the literature,[17] ascorbic acid was used with TBAB for a two-component catalyst system. Ascorbic acid, or vitamin C, is a natural compound that is produced industrially from many sustainable methods, and is renewably sourced,[18] making it an ideal catalyst component for a green reaction. Using 8.7 mol% of TBAB and 8.3 mol% of ascorbic acid increased the conversion slightly to almost complete conversion (Entry 2). Reducing the amount of ascorbic acid to 4.1 mol% did not lower the conversion (Entry 3). Entry 4 reduced the amount of TBAB to 4.1 mol% and saw a drop in the conversion to 79%. Using a similar loading of TBAB and reducing the loading of ascorbic acid to 2.0 mol% increased the conversion to 90%, using lower catalyst loadings than in entries 2 and 3. Finally, ascorbic acid was used at a catalyst loading of 3.0 mol%, with no TBAB, giving no conversion to the desired cyclic carbonate, indicating that ascorbic acid alone cannot activate the epoxide for reaction.

Reactions of biomass-derived epoxides and CO_2 can be very energy intensive due to the high temperatures and pressures required to achieve high conversion. In order to make the reactions as green and environmentally friendly as possible, lower reaction temperatures were tested to see if the energy required for the reaction could be lowered. Reactions were therefore performed at 90 °C to reduce the energy used for heating the reaction. TBAB was used alone at catalyst loadings of 4.2 mol% and 2.3 mol% at this reduced temperature, giving much lower conversions of 49% and 23%, respectively.

Reducing the temperature significantly reduced the conversion, so the higher temperature of 110 °C was maintained for all other reactions.

Table 3.2. Catalytic coupling of EFO and CO_2 at 110 °C.

Entry	Catalyst System		Mol%[a]		Conversion to Cyclic Carbonate (%)[b]
	1	2	1	2	
1	TBAB	N/A	6.7	0	92
2	TBAB	Ascorbic acid	8.7	8.3	99
3	TBAB	Ascorbic acid	8.7	4.1	99
4	TBAB	Ascorbic acid	4.1	5.4	79
5	TBAB	Ascorbic acid	3.9	2.0	90
6	N/A	Ascorbic acid	0	3.0	-
7	TBAB	N/A	3.3	0	70
8[c]	TBAB	N/A	4.2	0	49
9[c]	TBAB	N/A	2.3	0	23

[a]Relative to moles of epoxide groups. [b]Determined by ^{1}H NMR spectroscopy. [c]Performed at 90 °C.

Cyclic carbonates were synthesized under similar catalyst loadings using epoxidized tablet fish oil (ETFO), giving thick brown oils that could not be fully characterized by ^{1}H NMR spectroscopy to determine conversion. By IR spectroscopy, the carbonated tablet fish oil (CTFO) was identical spectroscopically to the CFO materials with almost complete conversion. The spectrum of a representative sample is shown in **Figure 3.6** in Section 3.2.2.2.

Similar methods using TBAB for the formation of vegetable oil-derived cyclic carbonates have been reported.[7,13–16] The conditions used in these methods are presented in **Table 3.3** for comparison with the TBAB and ascorbic acid catalyzed reaction with EFO.

The optimized conditions for the formation of CFO occurs at 110 °C, at a pressure of 10 bar, for 48 h. High temperatures and pressures are very common for the formation of cyclic carbonates from vegetable oils. In order to reduce the reaction time to 10 h or less, Zheng et al., Samanta et al., and Doley et al., require 5 to 10 times the pressure of CO_2, while still maintaining a high temperature.[14–16] The first cyclic carbonate based on soybean oil was synthesized by Tamami et al., with the reaction performed at atmospheric pressure with a constant flow of CO_2.[7] Due to the low pressure used, the reaction required 70 h to achieve high conversions to the product.

Bähr and Mülhaupt performed a reaction using epoxidized soybean or linseed oil, at 140 °C, 10 bar CO_2, for over 40 h, with a catalyst loading of 3.5 wt.% TBAB.[13] Optimized conditions in this thesis use 4 mol% TBAB, which corresponds to 2.7 wt.% TBAB, with 2 mol% ascorbic acid. The catalyst loading of TBAB used is lower than that reported in the literature, while using a lower temperature and the same pressure, for a similar reaction time, achieving a high conversion to the desired CFO.

Table 3.3. Comparison of literature conditions for the formation of bio-based cyclic carbonates using TBAB.

Reference	Substrate	T (°C)	P (bar CO_2)	t (h)	Catalyst Loading
Tamami et al., 2004	Soybean oil	110	atm	70	TBAB, 5 mol%
Bähr & Mülhaupt, 2012	Soybean and linseed oil	140	10	>40	TBAB, 3.5 wt%
Zheng et al., 2015	Cottonseed oil	130	50	7	TBAB, 3.5 mol%
Samanta et al., 2016	Soybean oil	140	104	6	TBAB, 6 wt%
Doley et al., 2018	Sunflower oil	110	50	10	TBAB, 3.5 mol%
This Work	Fish Oil	110	10	48	TBAB, 4 mol% Ascorbic acid 2 mol%

Ascorbic acid was previously reported as a hydrogen-bond donor for the synthesis of cyclic carbonates from epichlorohydrin using tetrabutylammonium iodide (TBAI) as the nucleophile, with a catalyst loading of 2 mol% ascorbic acid and 4 mol% of TBAI.[17] The reaction was performed for 23 h at 1 bar CO_2 and 40 °C, giving a 94% conversion. Under similar catalyst loadings of ascorbic acid and TBAB, the FO-based epoxides used in this work were synthesized in a similar conversion of 90%, under a higher temperature and pressure, but this is often required for internal epoxides. All subsequent reactions were therefore performed using 3.9 mol% TBAB and 2.0 mol% ascorbic acid, as it uses lower catalyst loadings than other catalyst systems studied, while still achieving a high conversion to the product.

3.2.2 Characterization of Cyclic Carbonates

3.2.2.1 ^{1}H and ^{13}C NMR Data

Cyclic carbonates of the model compound, MO, synthesized in this work have been previously reported and data obtained for this thesis are consistent with both ^{1}H and ^{13}C NMR data reported in the literature.[11] Representative ^{1}H and ^{13}C NMR spectra for CMO are shown in **Figure 3.2** and **Figure 3.3**. The ^{1}H NMR spectrum for CMO, **Figure 3.2**, contains identical peaks to that for EMO, with a triplet at 0.87 ppm representing the terminal methyl group (H_{18}). A complex pattern of peaks appearing from 1.2 to 1.7 ppm represents the methylene protons within the carbon chain, with the protons on the carbon β to the carbonyl (H_2) represented by a triplet centered at 2.30 ppm. A broad peak at 2.01 ppm represents the allylic protons (H_8 and H_{11}) in the molecule. A singlet at 3.66 ppm represents the hydrogens (H_{19}) from the methyl ester group. The ^{1}H NMR spectrum for CMO has new peaks appearing at 4.21 ppm and 4.60 ppm, which represents the formation of the *trans*- and *cis*-oriented cyclic carbonates, respectively (H_9, H_{10}). The conversion of the epoxide to the corresponding cyclic carbonate was determined from the ratio of the two cyclic carbonate peaks to the remaining epoxide peak at 2.89 ppm.

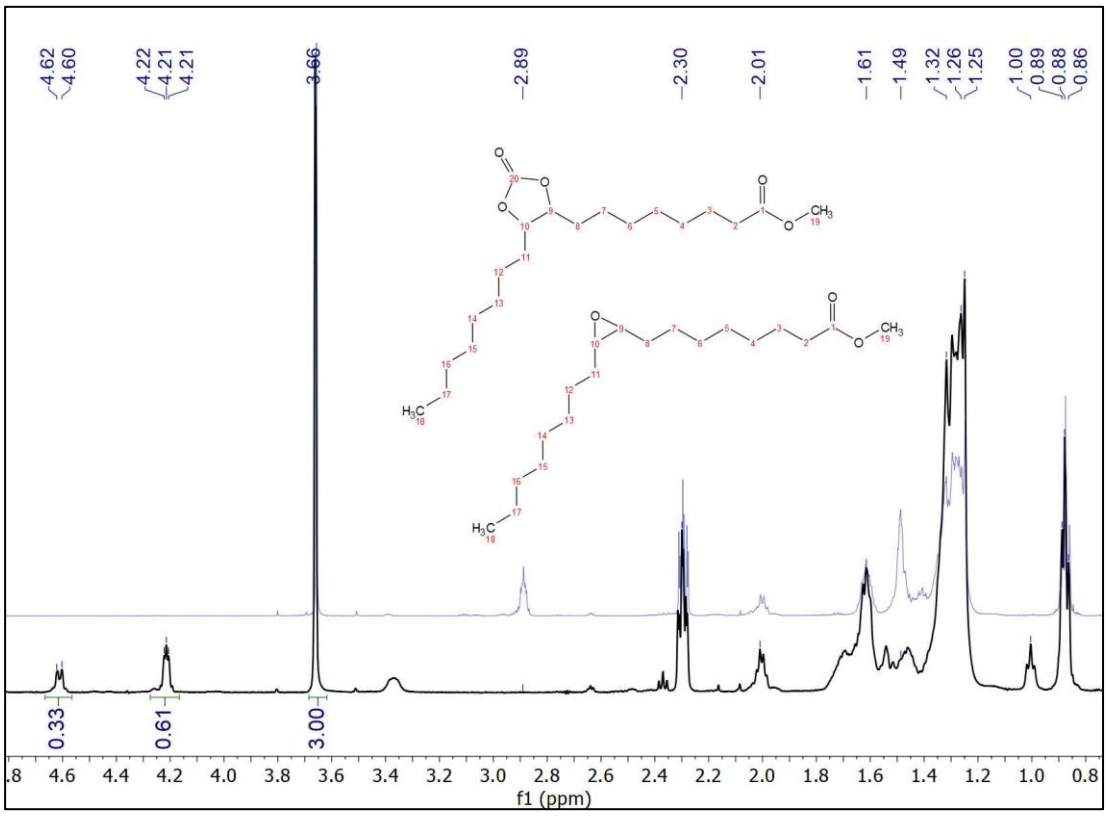

Figure 3.2. ^{1}H NMR spectra of EMO (top, blue) and CMO (bottom, black).

The ^{13}C NMR spectrum for CMO, **Figure 3.3**, contains a peak at 14.2 ppm, corresponding to the terminal methyl of the carbon chain (C_{18}). Peaks from 22.7 to 34.1 ppm represent the methylene carbons in the carbon chain (C_2-C_8, C_{11}-C_{17}). The peak at 51.5 ppm corresponds to the methyl of the ester group (C_{19}). New peaks appear at 80.1 ppm and 82.1 ppm, corresponding to the formation of cis- and trans- oriented cyclic carbonates, respectively (C_9, C_{10}). The peaks at 129.8 ppm and 130.1 ppm represent the olefinic protons (C_9, C_{10}) that did not react during the formation of the epoxide previously. A new peak appears at 154.8 ppm, which corresponds to the carbonyl group of the cyclic carbonate

(C_{20}), indicating the formation of the cyclic carbonate. The peak at 174.3 ppm corresponds to the carbonyl carbon present in both EMO and CMO (C_1).

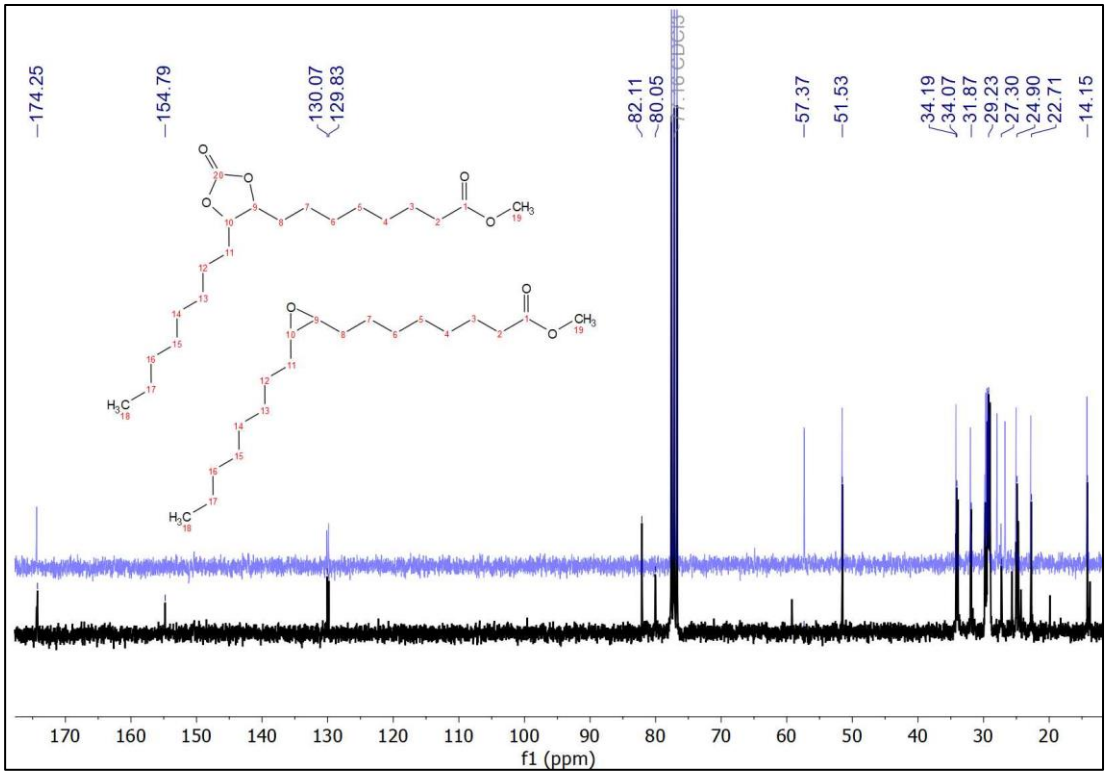

Figure 3.3. ^{13}C NMR spectra of EMO (top, blue) and CMO (bottom, black).

Fish oil derived cyclic carbonates synthesized in this work have similar ^{1}H and ^{13}C NMR spectra to those reported in the literature for vegetable oil-based cyclic carbonates.[11,13] Representative ^{1}H and ^{13}C NMR spectra for CFO are presented in **Figure 3.4** and **Figure 3.5**, respectively. The ^{1}H NMR spectrum for CFO, **Figure 3.4**, contains a triplet at 0.88 ppm that corresponds to the terminal methyl group for all fatty acids except ω-3 fatty acids, which appear at 1.01 ppm. Peaks around 1.25 ppm correspond to protons of the methylene groups. A peak at 1.61 ppm represents the protons on the carbon β to the

carbonyl group for all fatty acids except DHA. The peak centered on 2.04 ppm corresponds to the protons on the allylic carbons. Peaks at 2.31 ppm correspond to the protons on the carbon β to the carbonyl group for all fatty acids except for DHA. Peaks between 2.90 and 3.20 ppm correspond to unreacted epoxide groups present. A new peak appears at 3.35 ppm and is due to the presence of TBAB in the crude reaction mixture. Peaks from 4.12 to 4.30 ppm and 5.26 ppm represent the protons in the glycerol chain of the triglyceride, on the methylene and methine carbons, respectively. The ^{1}H NMR spectrum for CFO shows several new peaks from 4.49 to 4.92 ppm, which indicate the formation of the cyclic carbonate.

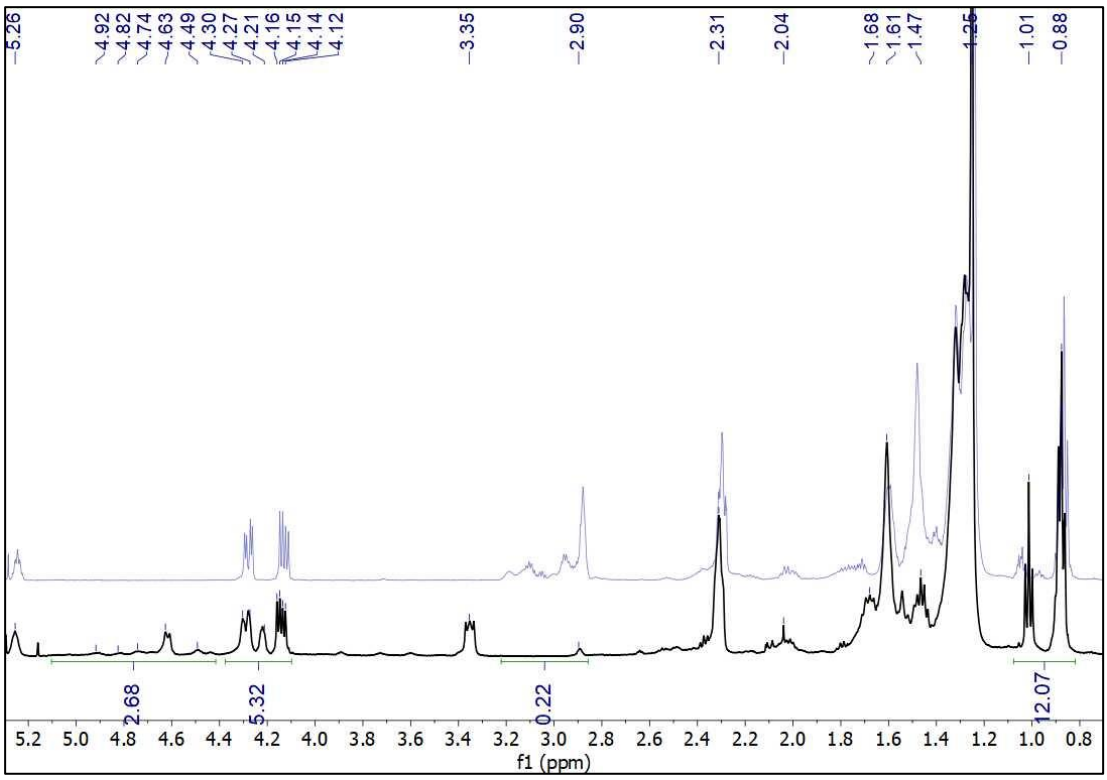

Figure 3.4. ^{1}H NMR spectra of EFO (top, blue) and CFO (bottom, black).

The ^{13}C NMR spectrum for CFO, **Figure 3.5**, contains a peak at 14.1 ppm, which corresponds to the terminal methyl of the fatty acid carbon chain. Peaks from 19.7 to 34.0 ppm represent the methylene carbons of the carbon chain. Peaks at 57.2 ppm and 58.9 ppm correspond to the remaining epoxide groups that were unreacted. The peaks at 62.1 ppm and 68.9 ppm represent the carbons in the glycerol of the triglyceride, the methylene and methine carbons, respectively. New peaks appear at 80.0 ppm and 82.0 ppm, which represent the formation of the cyclic carbonates. Another new peak is present at 154.7 ppm that is indicative of the carbonyl carbon of the cyclic carbonate, confirming the formation of the desired cyclic carbonate. Peaks which occur between 172.8 ppm and 173.2 ppm correspond to the carbonyl carbons of different fatty acids present in the FO.

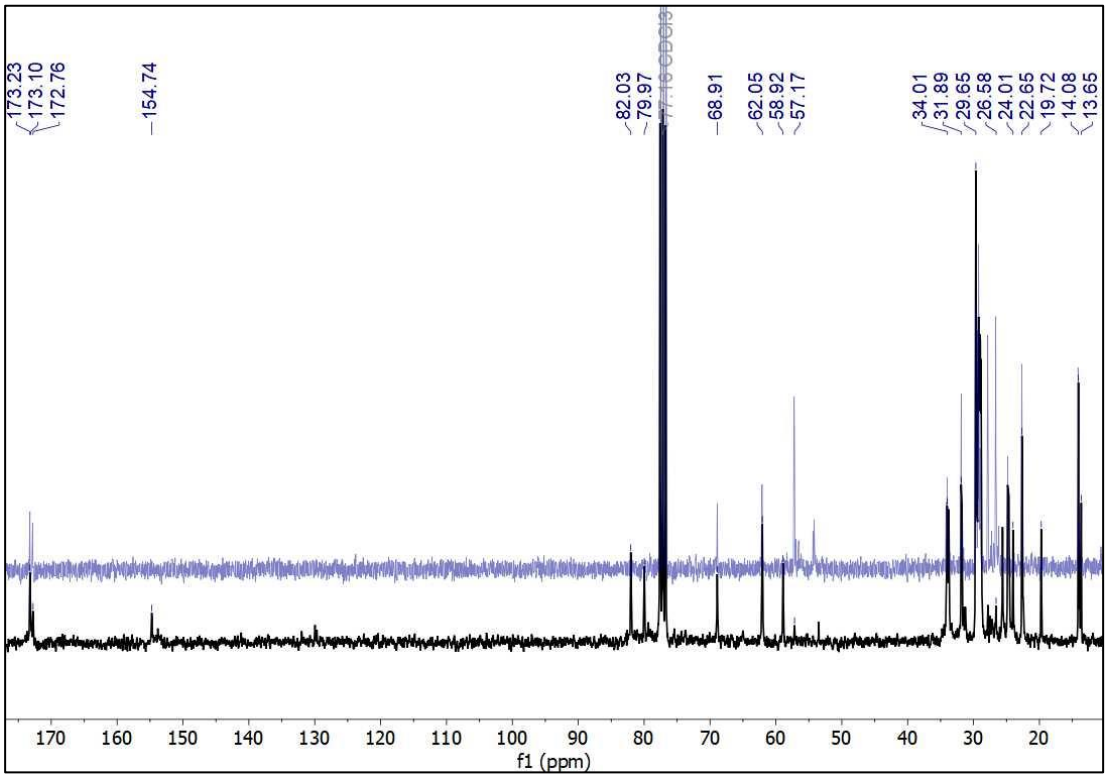

Figure 3.5. ^{13}C NMR spectra of EFO (top, blue) and CFO (bottom, black).

3.2.2.2 Infrared Spectroscopy and Thermogravimetric Analysis

IR spectra were obtained on the isolated CFO and CTFO, and compared to epoxides, reported in Chapter 2. Their spectroscopic characterization is consistent with literature reports for vegetable oil-derived cyclic carbonates.[19,20] Representative spectra for CFO and CTFO are presented in **Figure 3.6**. The spectrum for both CFO and CTFO showed a characteristic band at 1797 cm^{-1} from the carbonyl of the cyclic carbonate ring, and a band at 1046 cm^{-1}, due to the C-O bonds of the cyclic carbonate. These bands confirm the formation of the desired cyclic carbonate, which for CTFO, could not be determined by ^{1}H NMR spectroscopy.

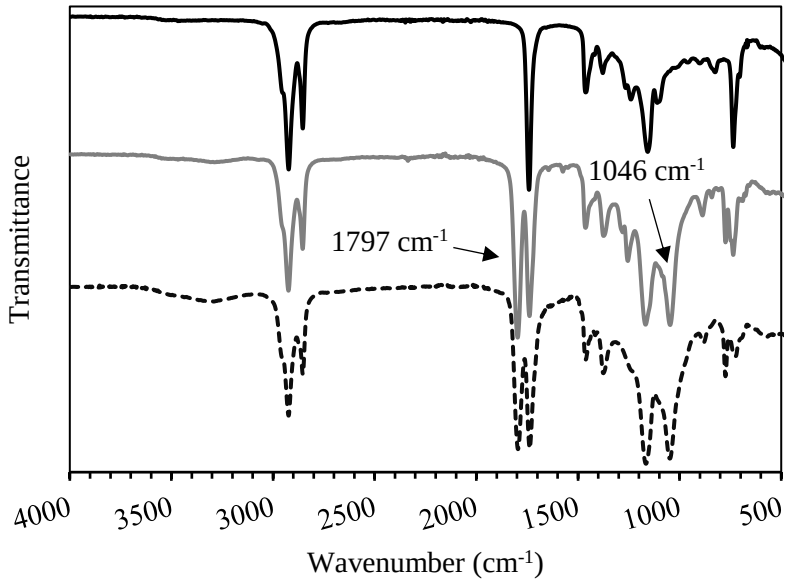

Figure 3.6. Infrared spectra of EFO (black, top), CFO (gray, middle), CTFO (black dashed, bottom).

CFO samples were analyzed by thermogravimetric analysis (TGA). Samples were heated from 20 °C to 1000 °C at a heating rate of 10 °C/min, under a constant flow of nitrogen (50 mL/min). **Figure 3.7** shows a representative thermogram for CFO, with degradation of the cyclic carbonate beginning at 260 °C. A smaller peak in the derivative weight change curve is apparent at 150 °C, which is likely due to residual TBAB[14] in the sample as the TGA was performed on the crude product.

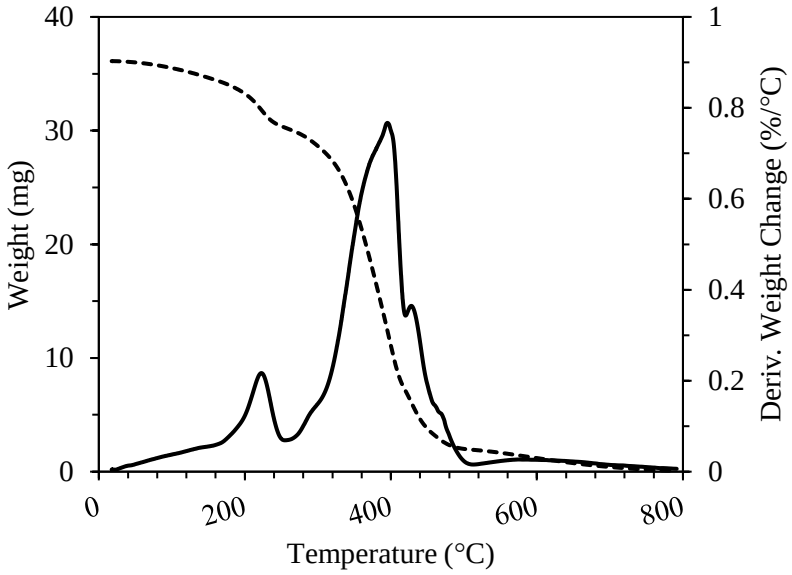

Figure 3.7. TGA plot of CFO, showing weight of sample (dashed line) and derivative weight change (continuous line) with heating.

CTFO samples were analyzed by thermogravimetric analysis (TGA) and were heated from 20 °C to 600 °C at a heating rate of 10 °C/min, under a constant flow of nitrogen (50 mL/min). **Figure 3.8** shows a representative thermogram for CTFO, with degradation of the cyclic carbonate beginning at 260 °C and another large weight loss

beginning around 470 °C, higher than that for CFO. The small weight loss around 150 °C is also likely due to residual TBAB[14] in the sample as the TGA was performed on the crude product.

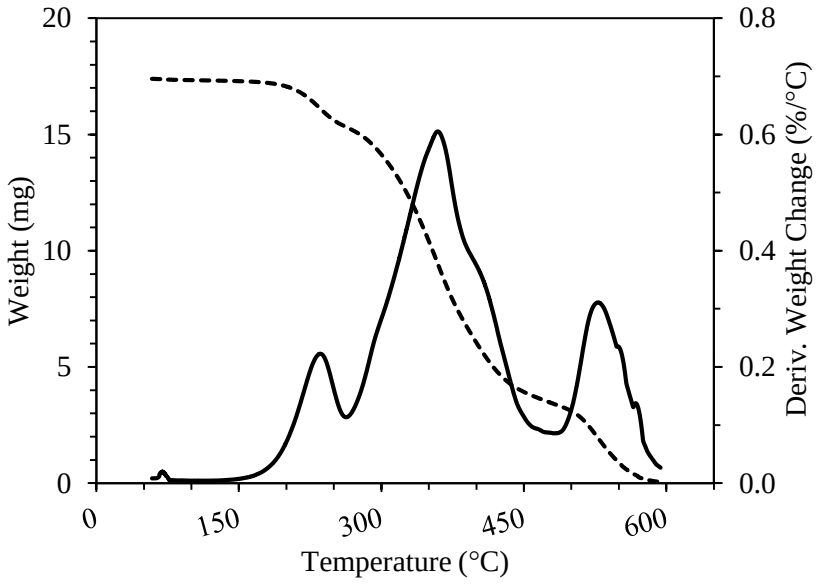

Figure 3.8. TGA plot of CTFO, showing weight of sample (dashed line) and derivative weight change (continuous line) with heating.

3.4 Conclusions

FO-based cyclic carbonates were synthesized for the first time, which were spectroscopically similar to their vegetable oil-based analogues. Using 6.7 mol% TBAB with the EFO, cyclic carbonates were obtained in a 92% conversion. Using less TBAB, at 3.9 mol%, and adding 2.0 mol% ascorbic acid, a natural product, the desired cyclic carbonates could still be synthesized in a high conversion, at 90%. Cyclic carbonates synthesized from the TFO were highly viscous and were not able to be analyzed by ^{1}H

NMR spectroscopy to determine their conversion. Instead, their formation was confirmed by IR spectroscopy, which showed they are spectroscopically identical to CFO. These cyclic carbonates, which are formed at lower temperatures and pressures than what is seen in the literature for vegetable oil cyclic carbonates, will be used for the formation of NIPU materials in Chapter 4.

3.5 Experimental

3.5.1 Materials

TBAB (99%) was purchased from Sigma-Aldrich. CO_2 (99.998%, supercritical fluid grade) was purchased from Praxair Canada. L-ascorbic acid (99+%), and bis(triphenylphosphine)iminium chloride (PPNCl) was purchased from Alfa Aesar. Iron(III) amino-bis(phenolate) complex, $FeCl(O_2N_2)$, was previously synthesized by Ms. Erika Butler at Memorial University[10] and used without further purification. Oxidized biochar was provided by Ms. Juliana Vidal at Memorial Univeristy.[8]

3.5.2 Instrumentation

NMR spectra were recorded at 298 K on a Bruker Avance III 300 or Avance 500 MHz spectrometer in chloroform-d ($CDCl_3$). Chemical shifts, in ppm, for ^{1}H and ^{13}C NMR were referenced to the residual deuterated solvent signals. IR spectra were recorded on a Bruker Alpha IR spectrophotometer using a platinum diamond ATR module, 36 scans at 4 cm^{-1} resolution in the spectral range of 400-4000 cm^{-1}. The thermal stability of samples was determined by thermogravimetric analysis (TGA) on a Q500 TGA from TA Instruments,

heating from 20 to 800 °C at a heating rate of 20 °C min^{-1}. TGA analyses were performed under a constant flow of nitrogen gas (50 mL min^{-1}). Rheology measurements for the determination of the viscosity of the FO and EFO were measured on an Anton Parr Physica MCR 301. The measuring cone used was a D 50 mm, with an angle of 1° and gap of 0.100 mm. Water was analyzed for reference. Runs were performed in triplicate at 25.00 °C on 1 mL of sample. The viscosity was taken as the average of the slopes of the three shear stress versus shear rate plots (**A4**).

3.5.3 General Procedure for Cyclic Carbonate Synthesis

For the conversion of the epoxide to cyclic carbonates, EFO (0.40 g), ascorbic acid (0.003 g, 0.018 mmol), and TBAB (0.011 g, 0.034 mmol) were added to a 3.7 mL glass vial. The mixture was stirred using a small stir bar and placed in a 300 mL series 5500 High Pressure Compact Laboratory Reactor (Parr Instrument Co.). The pressure vessel was modified by removing the impellor from the equipped overhead stirrer so that 5 vials could be added to the vessel at a time for batch reactions (**Figure 3.9**). The sealed vessel was pressurized to 10 bar of CO_2,[1] heated to the required temperature in an oil bath, and stirred on a hot plate-stirrer for 48 h. Once complete, the pressure vessel was cooled to room temperature and vented in a fume hood. The crude product, a viscous brown oil, was collected and used without further purification for the formation of NIPU materials.

[1] CAUTION: Care must be taken when using pressures above atmospheric.

Figure 3.9. Modified 300 mL pressure vessel used for batch reactions to form CFO.

Equipped stirrer with removed impellor outlined on lid.

3.6 References

(1) Lu, X.-B.; Darensbourg, D. J. Cobalt Catalysts for the Coupling of CO_2 and Epoxides to Provide Polycarbonates and Cyclic Carbonates. *Chem. Soc. Rev*. **2012**, *41* (4), 1462–1484.

(2) von der Assen, N.; Bardow, A. Life Cycle Assessment of Polyols for Polyurethane Production Using CO_2 as Feedstock: Insights from an Industrial Case Study. *Green Chem*. **2014**, *16* (6), 3272–3280.

(3) von der Assen, N.; Jung, J.; Bardow, A. Life-Cycle Assessment of Carbon Dioxide Capture and Utilization: Avoiding the Pitfalls. *Energy Environ. Sci*. **2013**, *6* (9), 2721.

(4) Aresta, M.; Dibenedetto, A. Utilisation of CO_2 as a Chemical Feedstock: Opportunities and Challenges. *Dalton Trans*. **2007**, No. 28, 2975–2992.

(5) Baizer, M. M.; Clark, J. R.; Swidinsky, J. Monocarbamates of 1,2-Dihydroxy-3-Aryloxypropanes. *J. Org. Chem*. **1957**, *22* (12), 1595–1599.

(6) Aresta, M.; Dibenedetto, A. Carbon Dioxide as Building Block for the Synthesis of Organic Carbonates - Behavior of Homogeneous and Heterogeneous Catalysts in the Oxidative Carboxylation of Olefins. *J. Mol. Catal. A Chem*. **2002**, *182–183*, 399–409.

(7) Tamami, B.; Sohn, S.; Wilkes, G. L. Incorporation of Carbon Dioxide into Soybean Oil and Subsequent Preparation and Studies of Nonisocyanate Polyurethane Networks. *J. Appl. Polym. Sci*. **2004**, *92* (2), 883–891.

(8) Vidal, J. L.; Andrea, V. P.; MacQuarrie, S. L.; Kerton, F. M. Oxidized Biochar as a Simple, Renewable Catalyst for the Production of Cyclic Carbonates from Carbon Dioxide and Epoxides. *ChemCatChem,* **2019**, In Press.

(9) Liu, W. J.; Jiang, H.; Yu, H. Q. Development of Biochar-Based Functional Materials: Toward a Sustainable Platform Carbon Material. *Chem. Rev*. **2015**, *115* (22), 12251–12285.

(10) Butler, E. D. Iron Amino-Phenolate Complexes as Catalysts for CO_2 Activation, M. Sc., Memorial University of Newfoundland, St. John's, NL, March 2018.

(11) Büttner, H.; Grimmer, C.; Steinbauer, J.; Werner, T. Iron-Based Binary Catalytic System for the Valorization of CO_2 into Biobased Cyclic Carbonates. *ACS Sustain. Chem. Eng*. **2016**, *4* (9), 4805–4814.

(12) Andrea, K. A.; Kerton, F. M. Triarylborane-Catalyzed Formation of Cyclic Organic Carbonates and Polycarbonates. *ACS Catal*. **2019**, *9*, 1799–1809.

(13) Bähr, M.; Mülhaupt, R. Linseed and Soybean Oil-Based Polyurethanes Prepared via the Non-Isocyanate Route and Catalytic Carbon Dioxide Conversion. *Green Chem*. **2012**, *14* (2), 483–489.

(14) Zheng, J. L.; Burel, F.; Salmi, T.; Taouk, B.; Leveneur, S. Carbonation of Vegetable Oils: Influence of Mass Transfer on Reaction Kinetics. *Ind. Eng. Chem. Res*. **2015**, *54* (43), 10935–10944.

(15) Samanta, S.; Selvakumar, S.; Bahr, J.; Wickramaratne, S.; Sibi, M. P.; Chisholm, B. J.; Sibi, M. P.; Chisholm, B. J.; Wickramaratne, D. S.; Sibi, M. P.; et al. Synthesis and Characterization of Polyurethane Networks Derived from Soybean Oil-Based Cyclic Carbonates and Bio-Derivable Diamines Synthesis and Characterization of

Polyurethane Networks Derived from Soybean Oil-Based Cyclic Carbonates and Bio-Derivable Diamines. *ACS Sustain. Chem. Eng*. **2016**, *4* (12), 1–7.

(16) Doley, S.; Dolui, S. K. Solvent and Catalyst-Free Synthesis of Sunflower Oil Based Polyurethane through Non-Isocyanate Route and Its Coatings Properties. *Eur. Polym. J*. **2018**, *102*, 161–168.

(17) Arayachukiat, S.; Kongtes, C.; Barthel, A.; Vummaleti, S. V. C.; Poater, A.; Wannakao, S.; Cavallo, L.; D'Elia, V. Ascorbic Acid as a Bifunctional Hydrogen Bond Donor for the Synthesis of Cyclic Carbonates from CO_2 under Ambient Conditions. *ACS Sustain. Chem. Eng*. **2017**, *5* (8), 6392–6397.

(18) Pappenberger, G.; Hohmann, H.-P. Industrial Production of L-Ascorbic Acid (Vitamin C) and D-Isoascorbic Acid. In Biotechnology of Food and Feed Additives. *Advances in Biochemical Engineering/Biotechnology*; Zorn, H., Czermak, P., Eds.; Springer: Berlin, 2013; Vol. 143, pp 143–188.

(19) Doll, K. M.; Erhan, S. Z. The Improved Synthesis of Carbonated Soybean Oil Using Supercritical Carbon Dioxide at a Reduced Reaction Time. *Green Chem*. **2005**, *7* (12), 849–854.

(20) Alves, M.; Grignard, B.; Gennen, S.; Detrembleur, C.; Jerome, C.; Tassaing, T. Organocatalytic Synthesis of Bio-Based Cyclic Carbonates from CO_2 and Vegetable Oils. *RSC Adv*. **2015**, *5* (66), 53629–53636.

Chapter 4: Synthesis of Non-Isocyanate Polyurethane Materials from Fish Oil-Based Cyclic Carbonates

4.1 Introduction

Non-isocyanate polyurethane (NIPU) materials based on biomass-derived chemicals are highly attractive due to their inherently greener synthesis and a desire to produce potentially biodegradable materials.[1–3] In this thesis, for the synthesis of the NIPU material, the fish oil (FO) derived cyclic carbonate, or carbonated FO (CFO), is reacted with an amine. The formation of NIPU materials from soybean oil was first reported in 2004 by Tamami et al., in which they reacted the carbonated soybean oil (CSBO) with ethylenediamine, hexamethylenediamine, or tris(2-aminoethyl)amine.[4] The produced polymeric materials had a range of glass transitions temperatures (T_g), with the highest being 43 °C.

The reaction for the formation of the NIPU materials proceeds through the mechanism shown in **Scheme 4.1**. In the first step, a tetrahedral intermediate is formed after nucleophilic attack of an amine on the carbonyl of the cyclic carbonate. In the second step, a second amine deprotonates this tetrahedral intermediate, and in the final step, the electron density on the oxygen initiates the breaking of one of the carbon-oxygen bonds, leading to the formation of the NIPU. This forms a urethane linkage with an extra hydroxyl functional group, which are specifically called polyhydroxyurethanes. The cyclic carbonates typically used are 5-membered cyclic carbonates, which are less reactive than other 6-, 7-, and 8-membered carbonates, as well as related thiocarbonates. Despite this, the 5-membered cyclic carbonates are preferentially used, as the other cyclic carbonates are

synthesized using phosgene derivatives or carbon disulfide, both of which are harmful substances.[5]

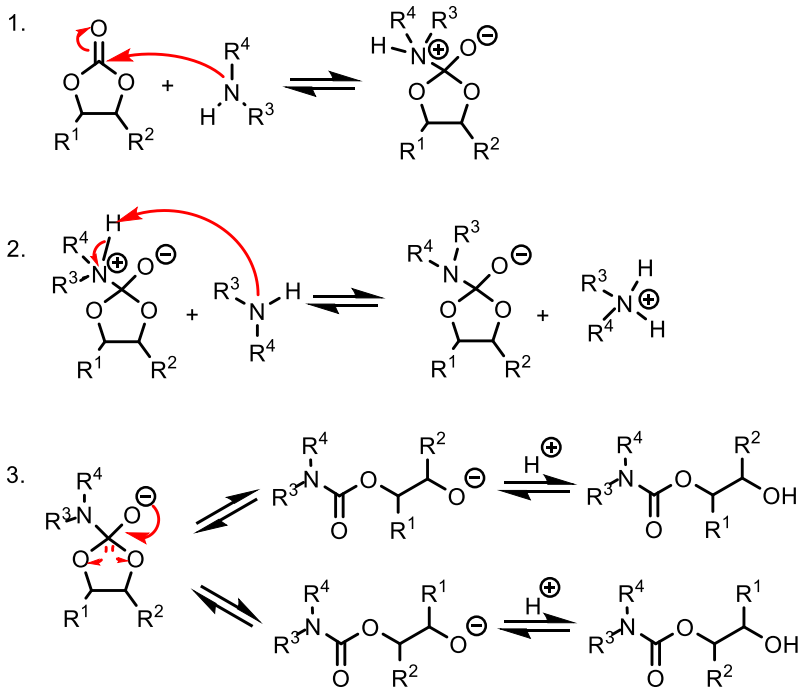

Scheme 4.1. Mechanism for the formation of non-isocyanate polyurethanes from a cyclic carbonate and amine.[5]

As demonstrated in Chapter 1, NIPU materials can be synthesized from biomass-derived materials through green methods, and as demonstrated in Chapter 3, waste-derived FO can be used to synthesize organic cyclic carbonates that are spectroscopically similar to cyclic carbonates derived from soybean oil. The goal for this chapter was to synthesize NIPU materials from the FO-derived cyclic carbonates. Although this has been performed with other biomass-derived chemicals, NIPU materials have not previously been

synthesized using ocean-based biomass such as FO. For comparison with the FO-derived NIPU materials, reactions were also performed with cyclic carbonates derived from a nutritional tablet FO (TFO). Using the cyclic carbonates derived from FO, the NIPUs produced have the representative structure shown in **Scheme 4.2**. The route to their synthesis will be outlined in Section 4.2, along with the characterization of the produced materials.

Using biomass-derived amines with the FO-derived cyclic carbonates for the production of NIPU materials produces a 100% bio-derived material that may show an improved biodegradability over conventional polyurethane materials. The degradability of the NIPUs is especially important for the end of life of the material. As a material that could potentially replace petroleum derived polymers, having a material that also persists in the environment is not desired. Ideally, the material will show an enhanced degradability, with innocuous degradation products. The degradability of the NIPU material will be explored in Section 4.2.2.

Two different amines were used in this thesis for the ring-opening polymerization of the FO-derived cyclic carbonates: 4,7,10-trioxa-1,13-tridecanediamine (**Figure 4.1**), and a commercially available bio-derived amine mixture, NC-540 (**Figure 4.2**). This bio-derived amine is synthesized from cashew nut shell liquid, a by-product of the cashew kernel industry, which accounts for 20-25% of the nut's weight.[6] Bio-derived NC-540 has previously been reported for the formation of NIPU materials using cyclic carbonates derived from linseed oil,[7,8] producing films that showed good performance in terms of coating properties.

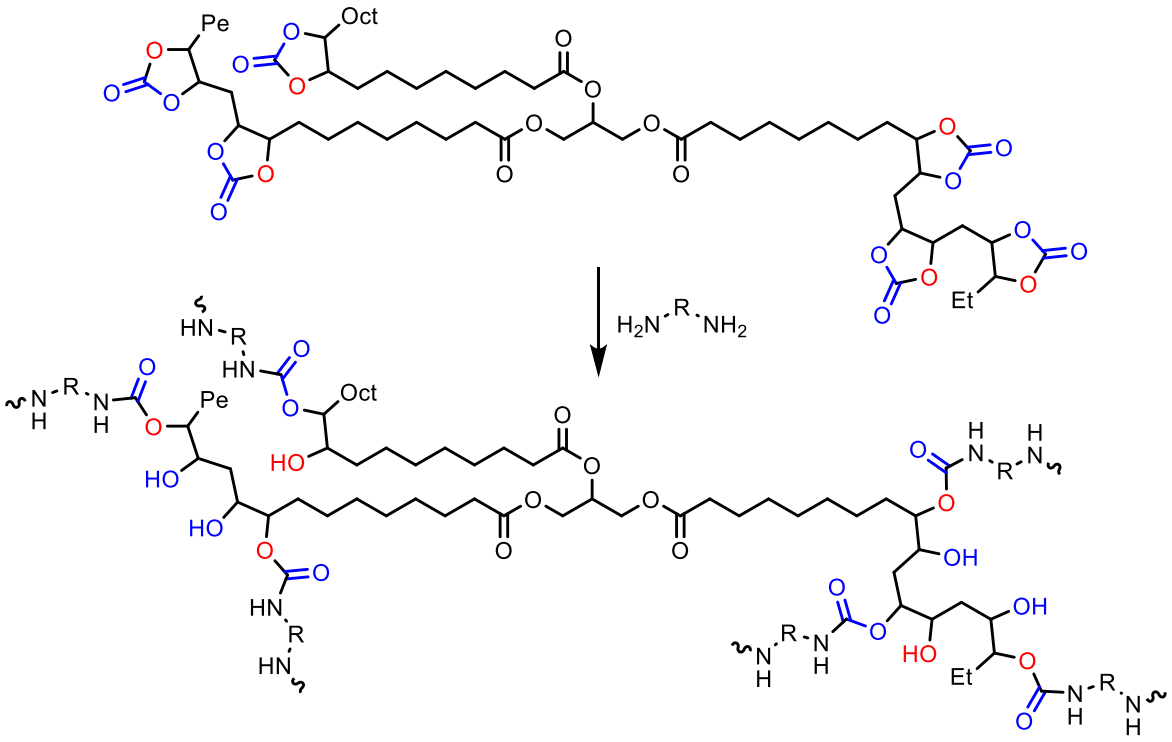

Scheme 4.2. Schematic for the conversion of FO-based cyclic carbonates to NIPU.

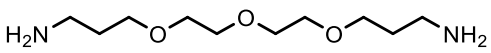

Figure 4.1. 4,7,10-Trioxa-1,13-tridecanediamine.

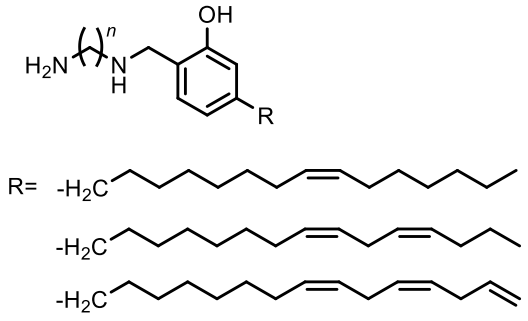

Figure 4.2. Representative structure of amine mixture, NC-540.[7]

4.2 Results and Discussion

4.2.1 Synthesis of Non-Isocyanate Polyurethanes from Fish Oil

The formation of the FO-based NIPU was performed by mixing the amine and the CFO on a glass Petri dish and heating to 40 °C. The Petri dish was then placed uncovered in an oven at 100 °C for 24 h to cure. The dish was then removed from the oven, cooled to 20 °C, and the film removed from the glass dish using a scalpel blade. The resulting film was then characterized and compared with results from different mixing ratios (weight CFO:weight amine) and a NIPU material made using the carbonated TFO (CTFO). Summarized reaction conditions are presented in **Table 4.1**.

Table 4.1. Summary of experimental conditions for the formation of NIPU films.

Entry	Carbonated Fish Oil (g)	NC-540 (g)	Carbonate:Amine
1	0.16	0.17	1:1.1
2	0.20	0.26	1:1.3
3	0.12	0.22	1:1.8
4	0.10	0.20	1:2.0
5[a]	0.12	0.06	1:0.5
6[b]	0.19	0.20	1:1.1

[a]4,7,10-trioxa-1,13-tridecanediamine used. [b]CTFO used.

The different mixing ratios of the CFO and amine produced materials with different appearances and physical properties, each shown in **Figure 4.3**. Using NC-540, a mixing ratio of the carbonate to amine of 1:2 gave flexible films which were 50 µm thick and were red, transparent, and shiny (**Figure 4.3-A**). Elemental analysis was performed on the film, showing it was 5.88% nitrogen, confirming incorporation of the amine. A mixing ratio of

approximately 1:1 gave a 1.0 mm thick flexible film, which was also red, transparent, and shiny (**Figure 4.3-B**). Using the TFO and NC-540, a brittle reddish-brown shiny solid was obtained, which was also fairly flexible (**Figure 4.3-C**). When 4,7,10-trioxa-1,13-tridecanediamine was used instead of NC-540 with CFO, a thin, light brown, sticky film was obtained (**Figure 4.3-D**).

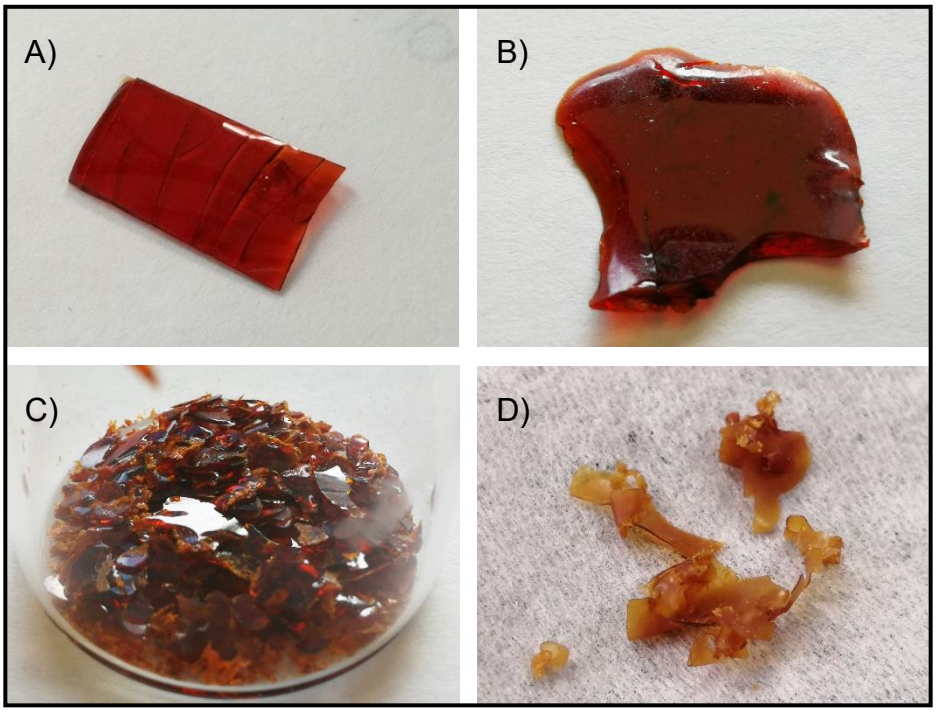

Figure 4.3. FO-derived NIPU films. A) 1:2 mixing ratio, B) 1:1 mixing ratio, C) TFO-derived NIPU film, and D) 4,7,10-trioxa-1,13-tridecanediamine film, entries 4, 1, 6 and 5 respectively in Table 4.1.

Each NIPU material was analyzed by infrared (IR) spectroscopy to confirm the formation of the desired urethane linkage. Their spectroscopic characterization is consistent with literature reports for vegetable oil-derived NIPU materials.[4,9,10] Representative spectra

for a FO-derived NIPU and a TFO-derived NIPU are presented in **Figure 4.4**, with a spectrum for CFO presented for comparison to the NIPU materials. Both NIPU spectra show weakening of the band at 1797 cm^{-1}, due to the carbonyl of the cyclic carbonate, indicating ring-opening. A new band at 1654 cm^{-1} and a broad band at 3294 cm^{-1} appear in both spectra, which are characteristic of an N-H bend and O-H/N-H stretching, respectively. These bands confirm the formation of the desired NIPU material from both CFO and CTFO.

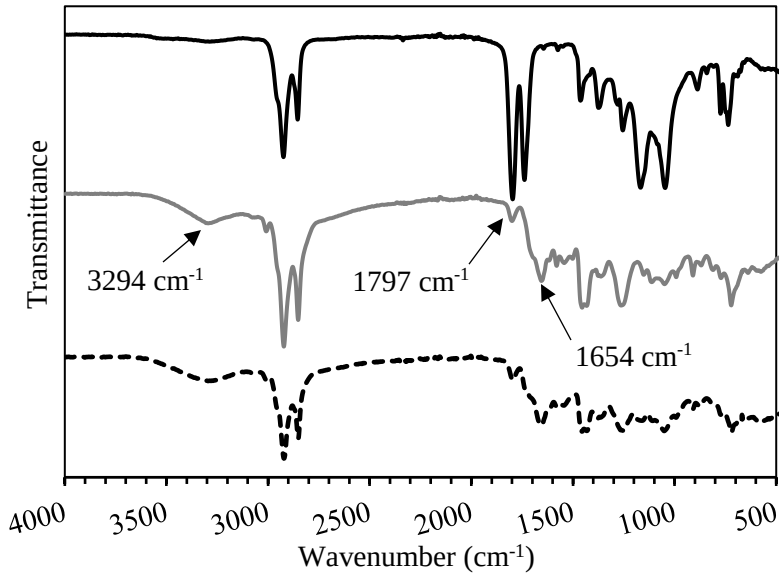

Figure 4.4. Infrared spectra of CFO (black, top), FO-NIPU (gray, middle), and TFO-NIPU (black dashed, bottom).

The NIPU materials were analyzed by thermogravimetric analysis (TGA). Samples were heated from 20 °C to 700 °C at a heating rate of 10 °C/min, under a constant flow of nitrogen (50 mL/min). **Figure 4.5** shows a representative thermogram for a FO-NIPU material, with degradation beginning at 200 °C and the main weight loss occurring after

360 °C. The peak beginning at 200 °C is likely due to the NC-540 amine used to cure the film, which has a boiling point of 207 °C.[11]

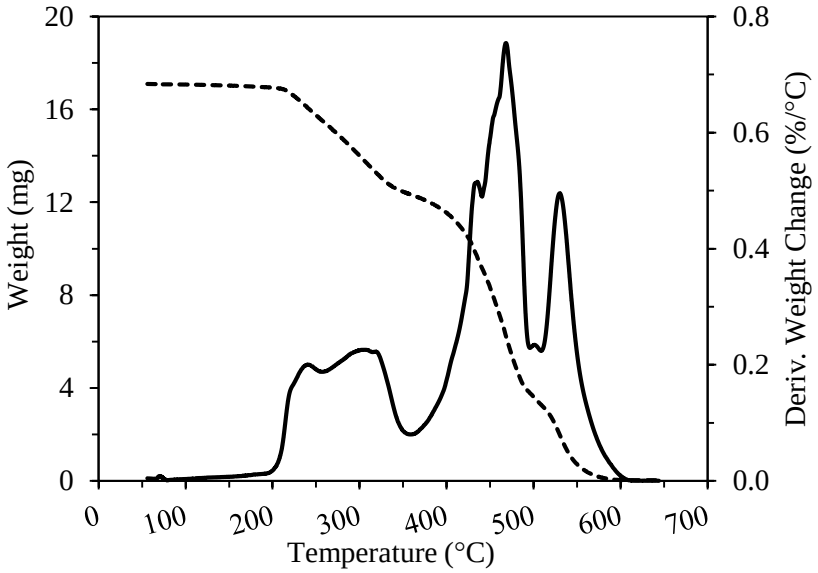

Figure 4.5. TGA plot of FO-NIPU, showing weight of sample (dashed line) and derivative weight change (continuous line) with heating.

The TFO-derived NIPU material was also analyzed by TGA. Samples were heated from 20 °C to 650 °C at a heating rate of 10 °C/min, under a constant flow of nitrogen (50 mL/min). **Figure 4.6** shows a representative thermogram for a TFO-NIPU material, with degradation beginning at 180 °C and a small amount of weight loss occurring between 375 °C and 400 °C. Weight loss continues from 400 °C to 500 °C, and from 500 °C to the final temperature of 650 °C. The difference in degradation temperatures between the FO and TFO-derived NIPUs is due to the different fatty acids present in each oil. The FO contains mostly oleic acid, a monounsaturated fatty acid, while the TFO is composed of only

eicosapentaenoic acid (EPA) and docosahexaenoic acid (DHA), which have 5 and 6 double bonds, respectively.

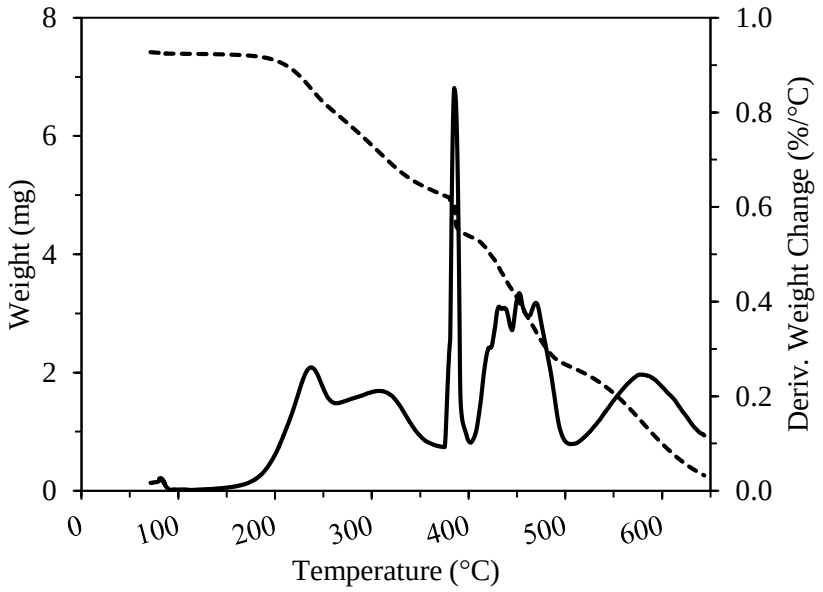

Figure 4.6. TGA plot of TFO-NIPU, showing weight of sample (dashed line) and derivative weight change (continuous line) with heating.

The samples were analyzed by differential scanning calorimetry (DSC) to potentially find a T_g for the polymer samples. In the DSC plot for the FO-NIPU film, the sample was cooled and heated in several loops, showing no endo- or exotherms between −70 °C and 50 °C (**Figure 4.7**). The NIPU material is soft and flexible, therefore the T_g may be lower than the lower limit of the instrument, −70 °C. In another run, the material was heated from 20 °C to 300 °C, the sample began degrading at higher temperatures, and no T_g was observed in this range.

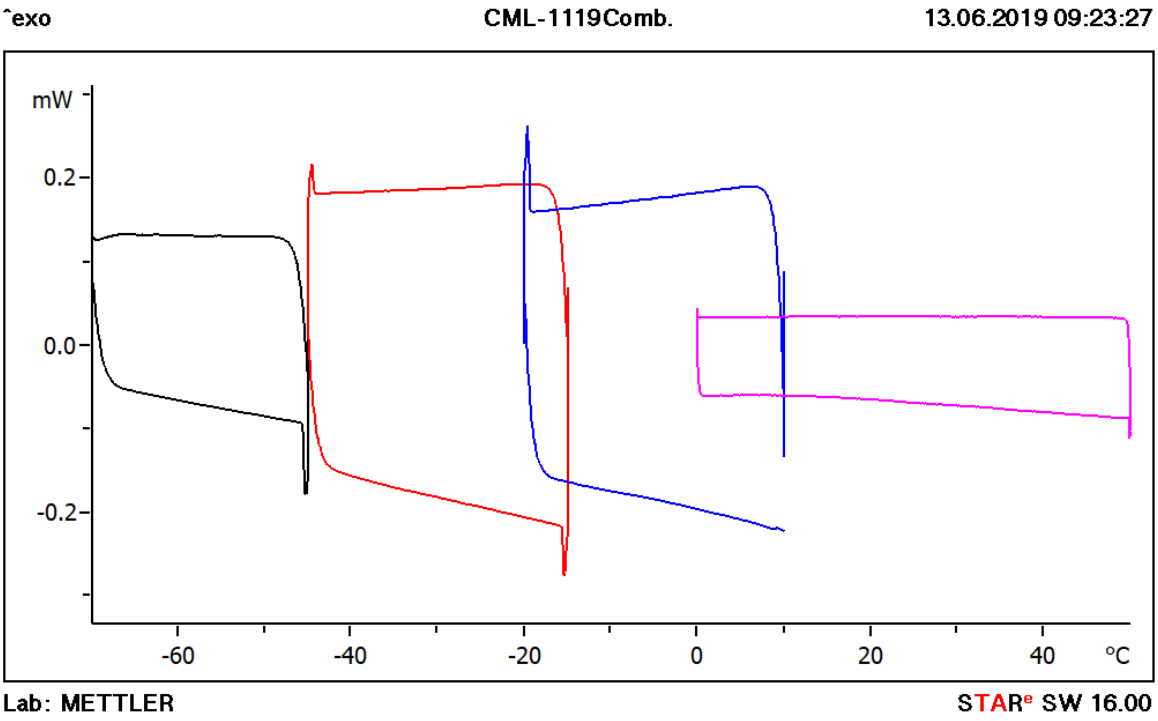

Figure 4.7. DSC plot of FO-NIPU.

The TFO-derived NIPU material was also analyzed by DSC. The sample was heated from 25 °C to 150 °C, cooled back to 25 °C, and repeated for two cycles. This was performed again between –70 °C and 25 °C. Within this full temperature range studied, no T_g was observed (**Figure 4.8**). The sample was heated from –70 °C to –10 °C at a slower heating rate of 5 °C/min, with no endo- or exotherms observed (**Figure 4.9**). As with the FO-NIPU, the material is flexible and the T_g is likely below the temperature range of the instrument used for the TFO-NIPU. The existence of a low temperature T_g indicates that these materials could have potential low temperature applications.

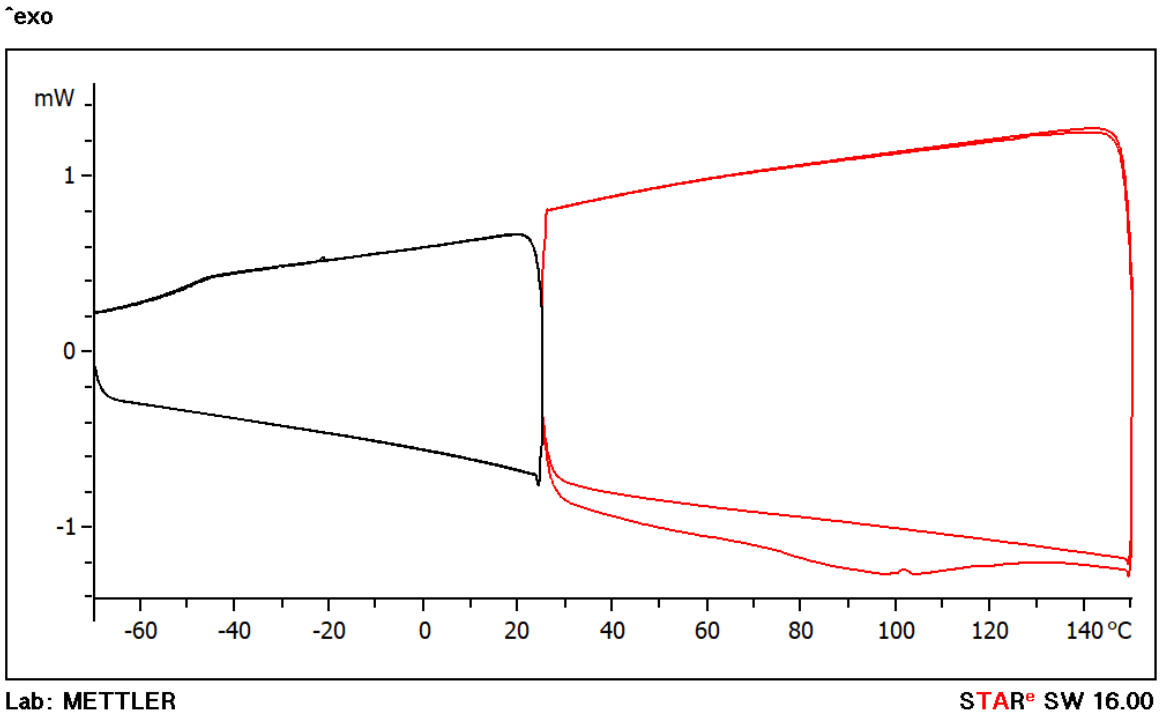

Figure 4.8. DSC plot of TFO-NIPU, –70 °C to 150 °C.

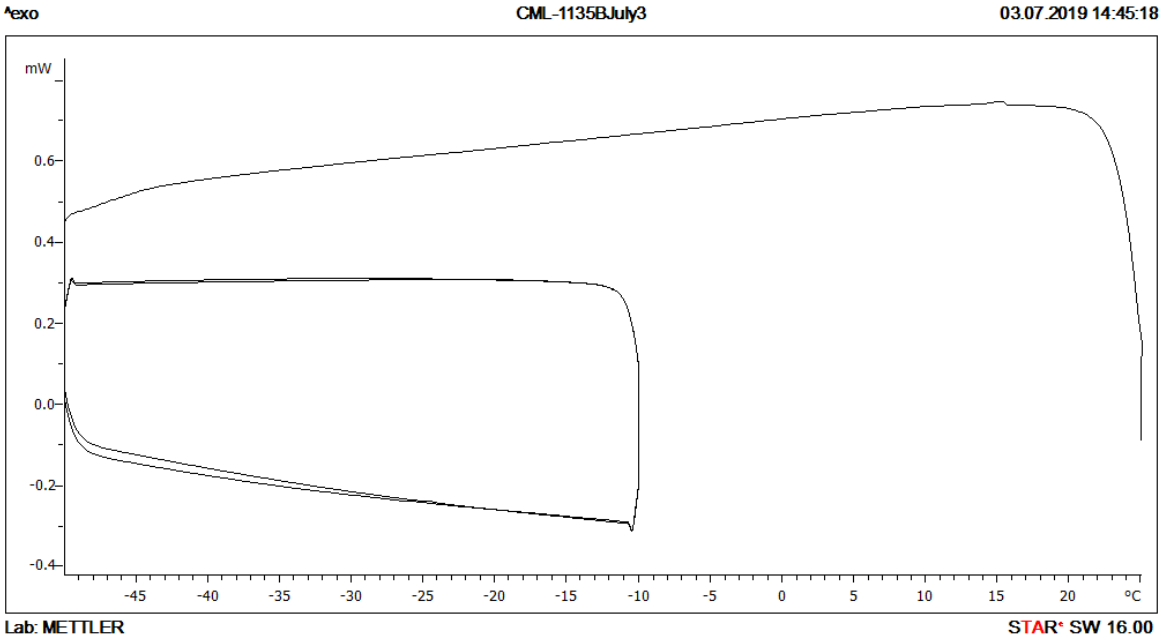

Figure 4.9. DSC plot of TFO-NIPU, –50 °C to –10°C, 5 °C/min.

4.2.2 Behaviour of Non-Isocyanate Polyurethane Materials in Water and Enzymatic Degradation Studies

4.2.2.1 Behaviour of films in various aqueous environments

To study the degradability of the FO-NIPU material in aqueous solutions, pieces of the film were stirred in deionized water, synthetic seawater, and seawater collected from Middle Cove Beach, NL. Squares of the film (**Figure 4.3-A.**) were placed in an Erlenmeyer flask, each with 100 mL of the appropriate aqueous solution, sealed and shaken at 290 rotations/min. The synthetic seawater used was made to a concentration of 33 g/L, the global average salinity of seawater, with sea salts. The resulting synthetic seawater had the approximate concentration of ions presented in **Table 4.2**.

Table 4.2. Ion concentrations in synthetic seawater for aqueous degradation studies.

Ion	Concentration (mg/L)
Chloride	17000
Sodium	9500
Magnesium	1100
Potassium	350
Calcium	350
Carbonate	170

After 28 days of stirring, the NIPU films were removed from the aqueous solutions, resulting in the films shown in **Figure 4.10**. Changes in the masses of the films are shown in **Table 4.3** below. The film in deionized water was light orange and opaque (**Figure 4.10-A**), and its mass after stirring was 187% its original mass, indicating that there was a large uptake of deionized water. After leaving the film to dry overnight in the open air, the film

lost a large portion of this water, and was 120% its original mass. When replicate experiments were performed, similar weight changes were obtained, even when using a smaller piece of NIPU film.

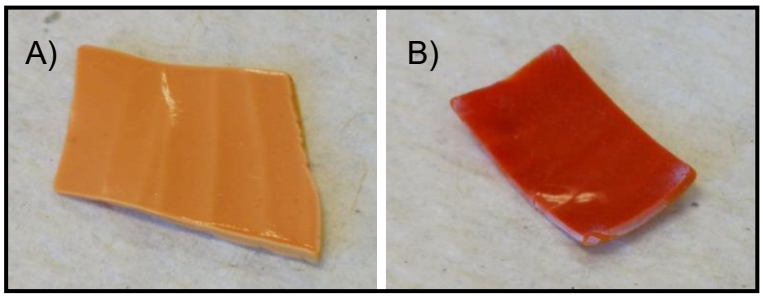

Figure 4.10. FO-NIPU films after stirring for 28 days in, A) deionized water and, B) seawater.

For the synthetic seawater film, after stirring for 28 days, the film remained the same reddish-orange colour, but turned opaque (**Figure 4.10-B**). Its mass when removed from the seawater was 112% its original mass, indicating a much smaller amount of water was absorbed by the film compared to in deionized water. After drying in air overnight, the film returned to its original mass, indicating that it lost all the water that was absorbed. When repeated, similar weight changes were obtained. The film that was exposed to real seawater collected from Middle Cove Beach, NL, also remained reddish-orange and became opaque. The weight changes seen with the film were similar to those of the synthetic seawater film, with its mass being 120% its original mass after stirring and losing all of the absorbed water after drying in the air overnight.

Table 4.3. FO-NIPU masses before and after shaking in water or seawater for 28 days.

	Starting Mass (g)	Weight After Stirring (%)	Weight After Drying (%)
Deionized Water	0.0310	187	120
	0.0106	168	112
Synthetic Seawater	0.0316	112	100
	0.0370	123	103
Seawater, MC	0.0287	120	102

MC = Middle Cove Beach, NL.

A scanning electron microscope (SEM) was used to analyse the surface of the films after shaking in the aqueous solutions. The original film (**Figure 4.11 A-B**) shows small wrinkles throughout the surface, as well as flat regions. The film shaken in deionized water (**Figure 4.11 C-D**) contains small holes, potentially due to the large uptake of water and its subsequent release. The film shaken in synthetic seawater (**Figure 4.11 E-F**) has long needle-like salt crystals throughout the surface of the film, which are slightly embedded into the surface. These crystals appear in large agglomerates regularly over the surface. When reproduced, the films in deionized water and seawater were identical in appearance.

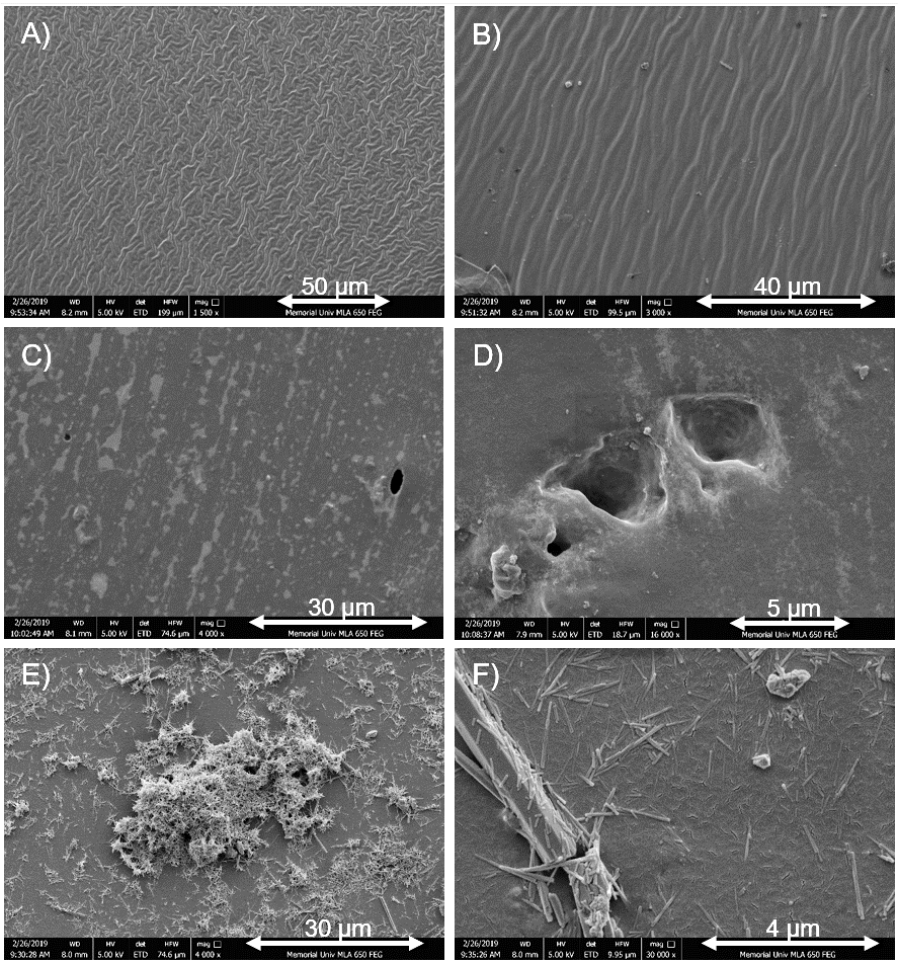

Figure 4.11. Selected, typical SEM micrographs of FO-NIPU films exposed to water for 28 days, A-B) original film, C-D) deionized water NIPU film, and E-F) synthetic seawater NIPU film.

To determine the elemental composition of the crystals on the surface of the film exposed to synthetic seawater, energy dispersive X-ray (EDX) analysis was performed on the film. This was performed using the same facility as the SEM experiments. An EDX spectrum, shown in **Figure 4.12** below, was generated by analyzing the center of one of the agglomerates of crystals. The spectrum shows large amounts of calcium and oxygen

with some potassium, chlorine, sodium, and minimal amounts of magnesium. From the concentration of ions in the synthetic seawater (**Table 4.2**), the chlorine, sodium, and magnesium are expected to be much higher than observed due to their high concentrations in the water, but instead, calcium and oxygen are the highest in the crystals.

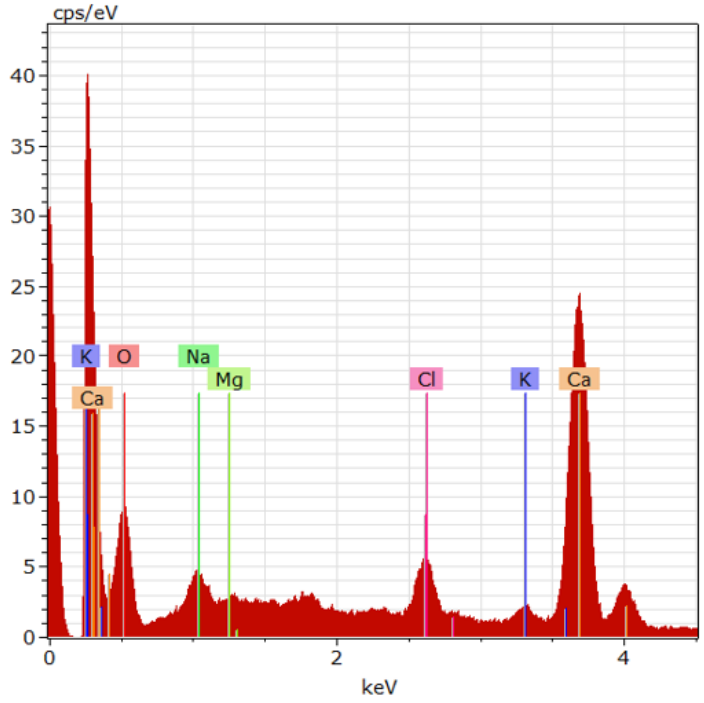

Figure 4.12. EDX spectrum of crystals on film exposed to synthetic seawater.

Elemental maps of the elements of interest were generated for the same agglomerate of crystals and are shown in **Figure 4.13** below. On the surface of the film, there is some sodium and chlorine present but not localized to the crystals. As with the EDX spectrum, there are large amounts of calcium and oxygen present, which is localized within the crystals, indicating that calcium carbonate ($CaCO_3$) may have formed on the film. From the elemental map for magnesium, there appears to be some magnesium present in small

regions that correspond to larger crystals on the surface of the film, which may correspond to either $MgCO_3$ or mixed group 2 carbonates ($Mg_xCa_yCO_3$).

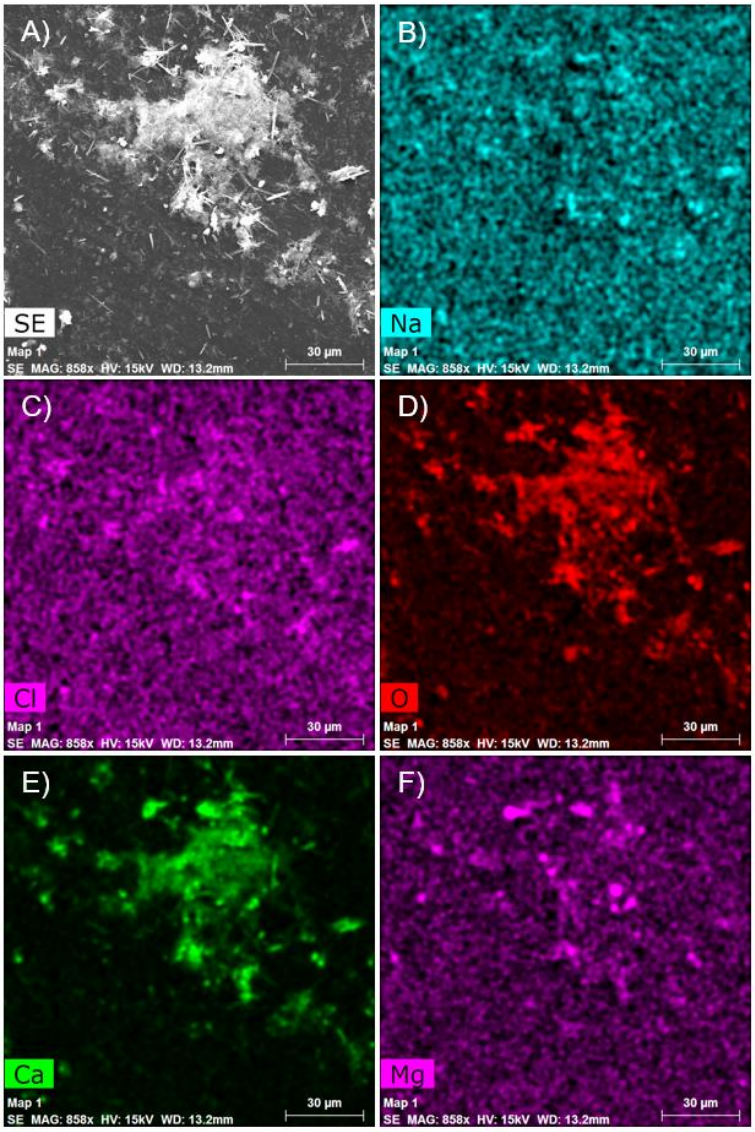

Figure 4.13. Elemental maps of crystals on synthetic seawater film, A) SEM micrograph of agglomerate, B) sodium, C) chlorine, D) oxygen, E) calcium, and F) magnesium.

SEM micrographs of the FO-NIPU film that was shaken in real seawater were also taken, along with elemental maps (**Figure 4.14**). The film is covered with some needle-like crystals, like those on the film exposed to synthetic seawater, but it is mostly covered with a different material that appears regularly over the surface. From the elemental maps, this appears to be mostly sodium and chlorine, with some magnesium throughout. There is some calcium and oxygen present, but they are present mostly in particles around the regions where sodium and chlorine are present. The material is therefore likely sodium chloride (NaCl) with small amounts of magnesium chloride ($MgCl_2$) and $CaCO_3$.

The difference in the surface appearance of the films exposed to natural seawater versus synthetic seawater is possibly due to differences in salinity. The synthetic seawater is made to the global average concentration of seawater, whereas the seawater collected from Middle Cove Beach has a much lower salinity than the global average, due to the fresh-water streams that reach the ocean nearby in the cove. As well, the real seawater contains many microorganisms that are not present in the synthetic seawater, which is produced in a lab with deionized water and is therefore sterile. These two factors appear to have an impact on the salt that crystallizes on the surface of the film, causing mostly $CaCO_3$ to form on the surface when in synthetic seawater, but NaCl to form on the surface when in real seawater.

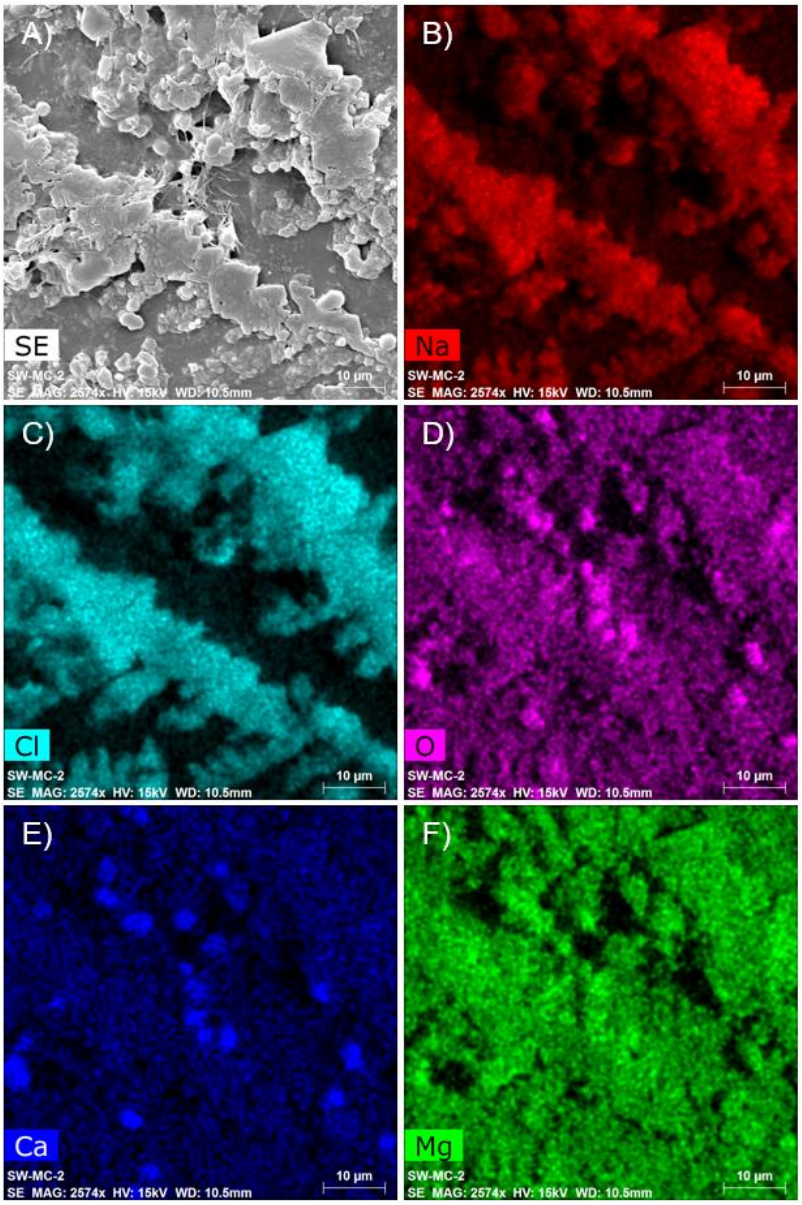

Figure 4.14. Elemental maps of surface of Middle Cove seawater film, A) SEM micrograph of film, B) sodium, C) chlorine, D) oxygen, E) calcium, and F) magnesium.

The films were analyzed by IR spectroscopy for comparison to the original FO-NIPU material before stirring in the aqueous solutions, with their spectra shown in **Figure 4.15**. The film shaken in deionized water shows an increase in the -OH region around 3290

cm^{-1}, due to the large amount of water present in the film even after drying. In the spectrum for the film exposed to seawater, new bands appear, one broad band around 1460 cm^{-1} and one sharp band at 874 cm^{-1}. The band at 1460 cm^{-1} is typical of amorphous $CaCO_3$, while the sharp band at 874 cm^{-1} suggests a calcite phase.[12] This agrees with that seen through the EDX spectrum and the elemental maps, indicating that $CaCO_3$ is present on the surface of the seawater film.

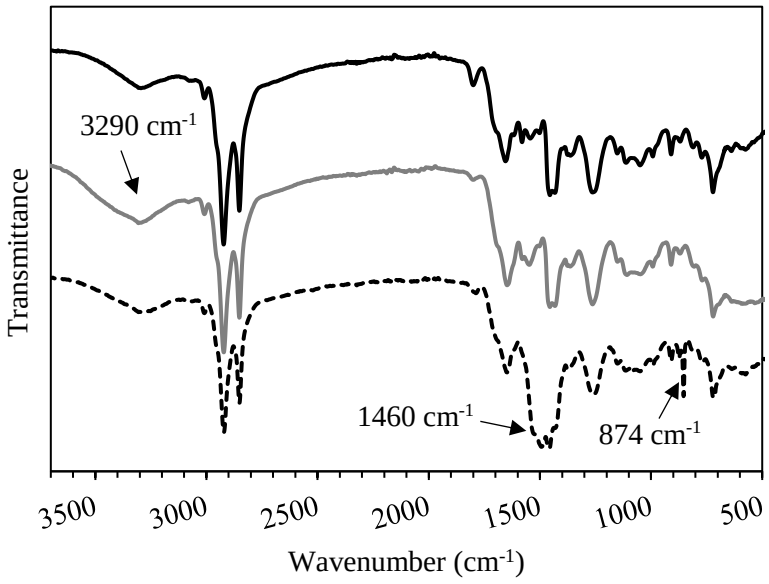

Figure 4.15. IR spectra of FO-NIPU (black, top), deionized water NIPU (gray, middle), and seawater NIPU (black dashed, bottom).

Both films exposed to real and synthetic seawater showed a decreased uptake of water compared to when films were shaken in deionized water only. While the film exposed to real seawater had mostly NaCl on the surface, the film exposed to synthetic seawater seems to have $CaCO_3$ on the surface. An SEM micrograph of the film shaken in synthetic

seawater, taken after 30 min of stirring (**Figure 4.16**), shows formation of crystals on the surface of the film. This early crystal growth potentially inhibits the uptake of water by the film, causing films to absorb less water in either type of seawater used. This may explain why the films show little deformation or degradation when compared to the film shaken in deionized water that contained holes.

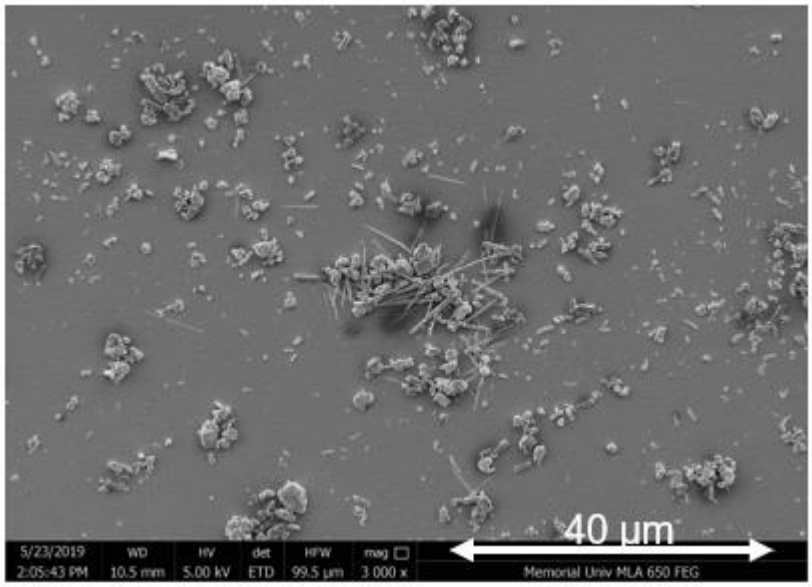

Figure 4.16. SEM micrograph of synthetic seawater FO-NIPU film after 30 minutes.

4.2.2.2 Enzymatic Degradation Studies

To study the enzymatic degradability of the FO-NIPU material, a 5 mm by 5 mm square piece was put in a buffered solution following a similar method that was previously reported in the literature.[13] 10.00 mL of a pH 7 phosphate buffered solution, containing 0.8 mol/L potassium chloride (KCl) was used for the studies. The solution was put in a 20 mL glass scintillation vial to which the square of FO-NIPU was added. After equilibrating for

3 days, 50 µL of a lipase, Novozym® 51032, was added. The vial was wrapped in paper towel to reduce the light entering the solution. This was performed in duplicate to test the reproducibility of the results.

After 14 days, the film had curled up, with brown mould appearing on the inner side of the film and within the solution. After 22 days, one film was removed from its solution and characterized. The film turned light beige in colour and remained curled up (**Figure 4.17-A**). A brownish-green mould covered only the inside surface of the film (**Figure 4.17-B**), while the outside remained shiny and smooth. The film had increased in mass and was now 2.8 times its original mass. After drying in the open air overnight the now dark red film was hard and brittle, indicating some degradation had probably occurred.

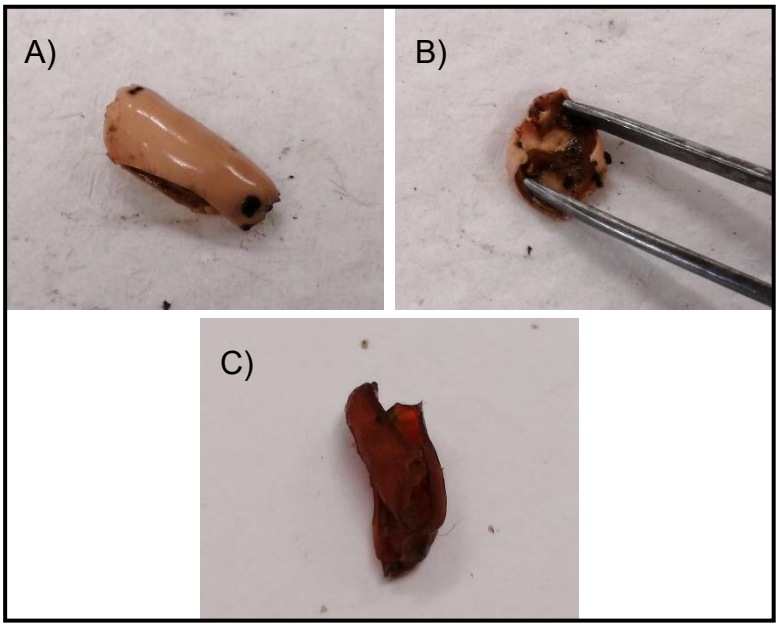

Figure 4.17. Enzyme degraded NIPU film, A) outside of film after removing from solution, B) inside of film, and C) after drying.

To further characterize the degraded film, SEM micrographs of the mould covered surface were taken (**Figure 4.18**). The film appears to be highly degraded and cracked throughout the surface of the film, with a stringy mass present throughout (**Figure 4.18-C**), which is potentially the hyphae from the mould. In many clusters throughout the film, small particles are present that could be bacteria and its produced spores (**Figure 4.18-D**). With further characterization, the identity of the bacteria on the surface of the film could be determined, and longer tests performed to test to what extent degradation will occur.

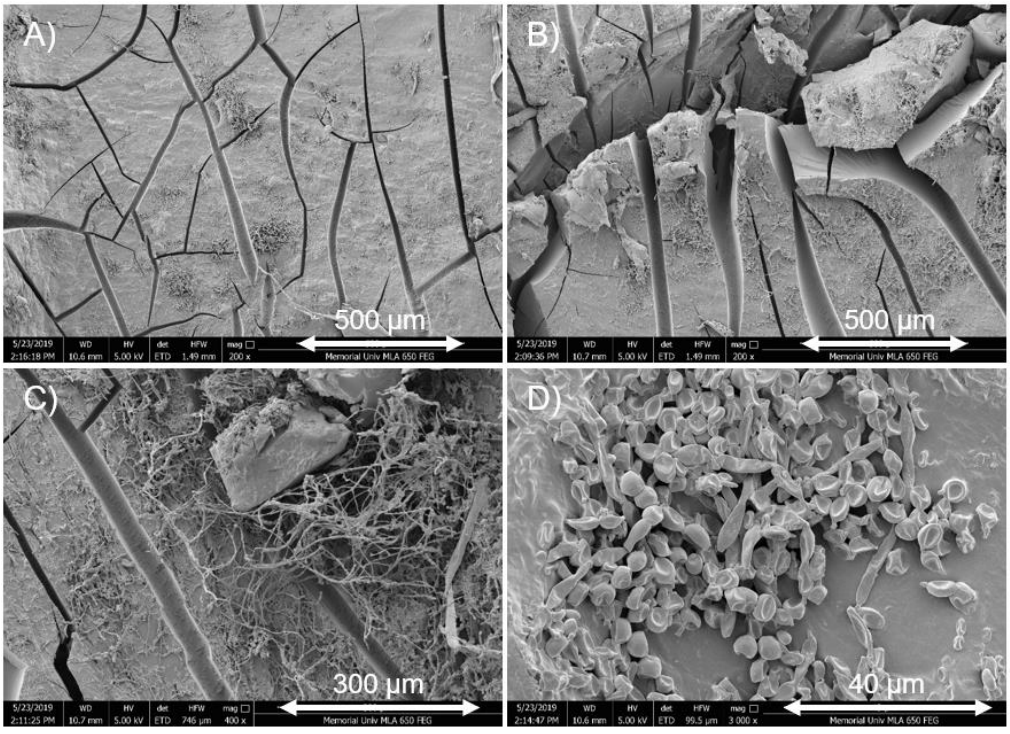

Figure 4.18. SEM micrograph of enzyme degraded NIPU film A-B) cracked surface of film, C) hyphae from mould, and D) bacteria on surface of film.

4.4 Conclusions

FO-based NIPU films were synthesized using CFO or CTFO and a bio-based amine mixture, NC-540. The resulting films are therefore 100% biomass and waste-derived. The formation of the urethane linkages was confirmed by IR spectroscopy. Using the CFO, a red shiny and flexible film, which showed no T_g between −70 °C and its degradation temperature of over 200 °C, was formed. When 4,7,10-trioxa-1,13-tridecanediamine was used instead of NC-540, a light brown, thin, flexible and sticky film was produced. Using the CTFO with NC-540, a brittle dark brown solid was formed that was still shiny and flexible. This material also showed no T_g between −70 °C and its degradation temperature.

The FO-NIPU film showed minimal degradation in deionized water. This was likely caused by the swelling of the polymer that led to the formation of small pores across the surface, and no degradation observed in seawater. When placed in synthetic or real seawater, salts such as NaCl and $CaCO_3$ crystallized on the surface of the film, and in some locations were slightly embedded into the surface of the film. These crystals may play a role in preventing uptake of water by the film.

The film shows some degradation by lipase enzymes, as indicated by the cracking on the surface and the brittle nature of the film once air dried. Mould that formed on the surface of the film may enhance the degradation of the film in aqueous solutions. Further testing of the mechanical properties of the films and degradation studies are required. In summary, the materials produced in this work are new, 100% biomass and waste-derived materials, that show promising results for degradation, which is important for the end of a materials life.

4.5 Experimental

4.5.1 Materials

Cashew nut shell liquid-derived amine, NC-540, was provided by the Cardolite Corporation. Sea salts used for the synthetic seawater (33 g/L) and potassium phosphate dibasic (K_2HPO_4, >98%) were purchased from Sigma-Aldrich. Potassium phosphate monobasic (KH_2PO_4) was purchased from Anachemia Science. Seawater was collected from Middle Cove Beach, Logy Bay, NL. For enzymatic degradation studies, Novozym® 51032 was purchased from Strem Chemicals, Incorporated.

4.5.2 Instrumentation

IR spectra were recorded on a Bruker Alpha IR spectrophotometer using a platinum diamond ATR module, performing 36 scans at 4 cm^{-1} resolution in the spectral range of 400-4000 cm^{-1}. The thermal stability of samples was determined by thermogravimetric analysis (TGA) on a Q500 TGA from TA Instruments, heating from 20 to 800 °C at a heating rate of 10 °C min^{-1}. Differential scanning calorimetry was performed on a Mettler Toledo DSC 1 in the temperature range of −70 to 500 °C at a heating rate of 10 °C min^{-1}. TGA and DSC analyses were performed under a constant flow of nitrogen gas (50 mL min^{-1}). SEM micrographs were obtained on a FEI MLA 650F, equipped with a high throughput EDX analytical system from Bruker. Samples were coated with gold for SEM imaging and coated with carbon for EDX analysis. Elemental analysis was performed by Guelph Chemical Laboratories Ltd. with the samples handled under nitrogen.

4.5.3 General Procedure for Non-Isocyanate Polyurethane Synthesis

For the conversion of the cyclic carbonates to a NIPU material, CFO (0.10 g) and NC-540 (0.20 g), were weighed into a Petri dish, heated to 40 °C, and stirred with a metal spatula. The resulting mixture was spread evenly on the Petri dish and placed in an oven at 100 °C for 24 h. The film was then cooled to 20 °C and scraped off the Petri dish using a scalpel blade, resulting in a shiny and flexible red film that was approximately 50 µm thick.

4.6 References

(1) Blattmann, H.; Fleischer, M.; Bähr, M.; Mülhaupt, R. Isocyanate- and Phosgene-Free Routes to Polyfunctional Cyclic Carbonates and Green Polyurethanes by Fixation of Carbon Dioxide. *Macromol. Rapid Commun*. **2014**, *35* (14), 1238–1254.

(2) Maisonneuve, L.; Lamarzelle, O.; Rix, E.; Grau, E.; Cramail, H. Isocyanate-Free Routes to Polyurethanes and Poly(Hydroxy Urethane)s. *Chem. Rev*. **2015**, *115*, 12407–12439.

(3) Datta, J.; Włoch, M. Progress in Non-Isocyanate Polyurethanes Synthesized from Cyclic Carbonate Intermediates and Di- or Polyamines in the Context of Structure–Properties Relationship and from an Environmental Point of View. *Polym. Bull*. **2016**, *73* (5), 1459–1496.

(4) Tamami, B.; Sohn, S.; Wilkes, G. L. Incorporation of Carbon Dioxide into Soybean Oil and Subsequent Preparation and Studies of Nonisocyanate Polyurethane Networks. *J. Appl. Polym. Sci*. **2004**, *92* (2), 883–891.

(5) Cornille, A.; Blain, M.; Auvergne, R.; Andrioletti, B.; Boutevin, B.; Caillol, S. A Study of Cyclic Carbonate Aminolysis at Room Temperature: Effect of Cyclic Carbonate Structures and Solvents on Polyhydroxyurethane Synthesis. *Polym. Chem*. **2017**, *8* (3), 592–604.

(6) Scaldaferri, C. A.; Pasa, V. M. D. Green Diesel Production from Upgrading of Cashew Nut Shell Liquid. *Renew. Sustain. Energy Rev*. **2019**, *111*, 303–313.

(7) Mahendran, A. R.; Aust, N.; Wuzella, G.; Müller, U.; Kandelbauer, A. Bio-Based Non-Isocyanate Urethane Derived from Plant Oil. *J. Polym. Environ*. **2012**, *20* (4), 926–931.

(8) Mahendran, A. R.; Wuzella, G.; Aust, N.; Müller, U. Synthesis, Characterization, and Properties of Isocyanate-Free Urethane Coatings from Renewable Resources. *J. Coatings Technol. Res*. **2014**, *11* (3), 329–339.

(9) Bähr, M.; Mülhaupt, R. Linseed and Soybean Oil-Based Polyurethanes Prepared via the Non-Isocyanate Route and Catalytic Carbon Dioxide Conversion. *Green Chem*. **2012**, *14* (2), 483–489.

(10) Pérez-Sena, W. Y.; Cai, X.; Kebir, N.; Vernières-Hassimi, L.; Serra, C.; Salmi, T.; Leveneur, S. Aminolysis of Cyclic-Carbonate Vegetable Oils as a Non-Isocyanate Route for the Synthesis of Polyurethane: A Kinetic and Thermal Study. *Chem. Eng. J.* **2018**, *346* (April), 271–280.

(11) Cardolite Corporation. Safety Data Sheet, NC-540. 2017.

(12) Cai, G.-B.; Chen, S.-F.; Liu, L.; Jiang, J.; Yao, H.-B.; Xu, A.-W.; Yu, S.-H. 1,3-Diamino-2-Hydroxypropane-N,N,N′,N′-Tetraacetic Acid Stabilized Amorphous Calcium Carbonate: Nucleation, Transformation and Crystal Growth. *CrystEngComm*, **2009**, *12* (1), 234–241.

(13) De Hoe, G. X.; Zumstein, M. T.; Tiegs, B. J.; Brutman, J. P.; McNeill, K.; Sander, M.; Coates, G. W.; Hillmyer, M. A. Sustainable Polyester Elastomers from Lactones: Synthesis, Properties, and Enzymatic Hydrolyzability. *J. Am. Chem. Soc*. **2018**, *140* (3), 963–973.

Chapter 5: Conclusions and Future Work

5.1 Conclusions

Fish oil (FO) derived from the by-products from fish processing plants, was used for the formation of epoxides using three different methods: (i) oxidation by 3-chloroperoxybenzoic acid, (ii) oxidation by hydrogen peroxide and acetic acid, catalyzed by sulfuric acid, and (iii) oxidation by hydrogen peroxide catalyzed by formic acid. A gate-to-gate life cycle assessment of these methods was performed, showing the reaction using formic acid and hydrogen peroxide is the greenest route to the formation of epoxidized FO (EFO). This reaction was optimized for the formation of EFO and epoxidized tablet FO (ETFO).

Using EFO and carbon dioxide (CO_2), with 3.9 mol% tetrabutylammonium bromide and 2.0 mol% ascorbic acid, cyclic carbonates were synthesized with a conversion of 90%. The products were characterized by ^{1}H and ^{13}C NMR spectroscopy, IR spectroscopy, and TGA. Using the ETFO, a highly viscous material was formed but its ^{1}H NMR spectrum was too difficult to interpret. The formation of the TFO-derived cyclic carbonate was confirmed by IR spectroscopy.

The FO-based cyclic carbonates were used to produce sustainable and fully bio-sourced non-isocyanate polyurethanes (NIPUs). Using a cashew nut shell liquid-derived amine mixture, NIPU materials were synthesized. Using carbonated FO (CFO) a shiny, red, flexible film was produced. With the carbonated tablet FO (CTFO) a shiny, dark brown, brittle film was formed that was still highly flexible. Scientific measurements to determine

flexibility and brittleness in an accurate fashion still need to be performed, as equipment to make such measurements was not accessible during my studies.

The degradation of the FO-NIPU materials in aqueous solutions was studied. A large uptake of deionized water was observed after stirring for 28 days at room temperature, whereas in saltwater, less water was absorbed potentially due to the salt that crystallized on the surface of the film. The material also shows promising preliminary results towards degradation by enzymes. The NIPU material prepared in the current work is 100% bio-derived, with both components derived from waste streams that do not compete with food production. Synthesis and use of this material could lead to new opportunities in waste management, producing valuable materials from resources that are currently underutilized.

5.2 Future Work

The process used to extract the fish oil determines the fatty acid profile. By using oils extracted using different methods, materials with different properties may be synthesized. The NIPU materials produced vary depending on their mixing ratios and the amine used. Simpler amines, which are similar to the bio-based amine used, would be interesting to try in order to determine if it is the long fatty acid chains that make the material so flexible. As well, other bio-based amines, such as L-lysine (i.e. amino acids), may give entirely different properties to the NIPU material, while remaining a 100% bio-derived material. As well, the cyclic carbonates used in the reactions were all obtained in high conversions. Synthesizing cyclic carbonates at lower conversions so that many

epoxide groups remain could lead to the formation of different materials that could potentially be functionalized post-NIPU synthesis.

The materials need to be further studied regarding their ability to degrade in the environment, whether that be in aqueous or terrestrial environments. The degradation studies performed showed promising results. In the enzymatic degradation reactions, mould grew on the film, but only on one side. The shiny outside of the film did not appear to have any mould on it, whereas the other side of the film, which was scratched from scraping the film off the glass after its formation, had mould grow on it. The mould and potential degradation products would need to be characterized to test if the film is degrading to innocuous chemicals that would be harmless if released into the environment.

Chapter 6: Appendix

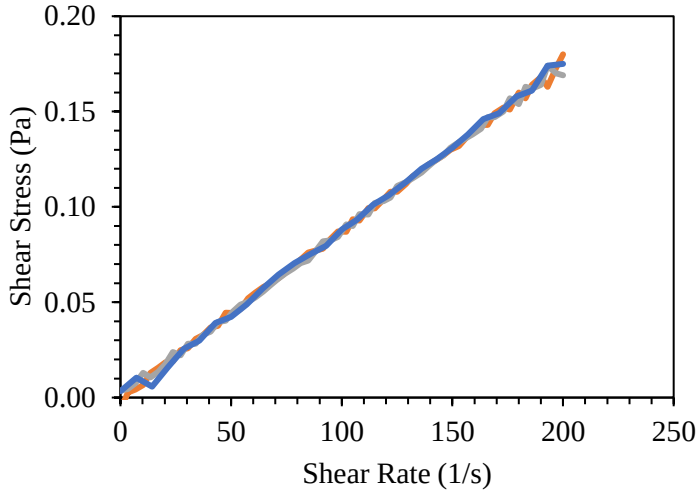

A1. Rheology measurements of water used for calibration of the instrument, with three runs, average slope 0.000875 ± 0.000007 Pa·s.

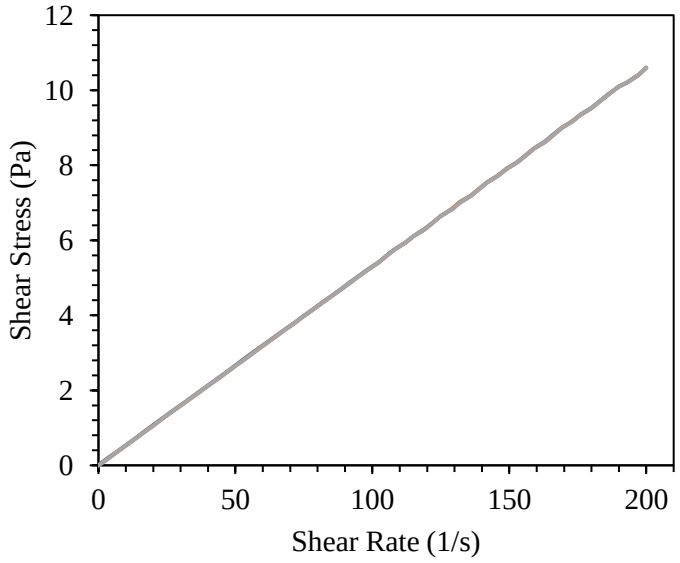

A2. Rheology measurements of fish oil, with three runs, average slope 0.0530 ± 0.0001 Pa·s.

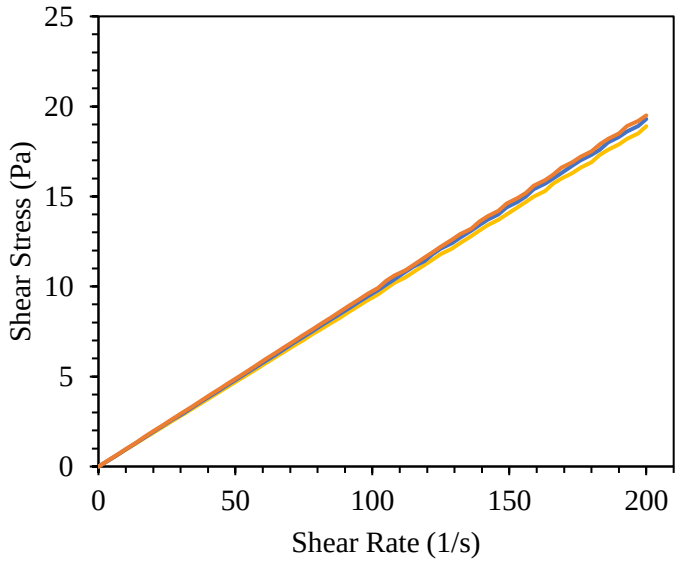

A3. Rheology measurements of epoxidized fish oil, with three runs, average slope 0.0962 ± 0.0017 Pa·s.

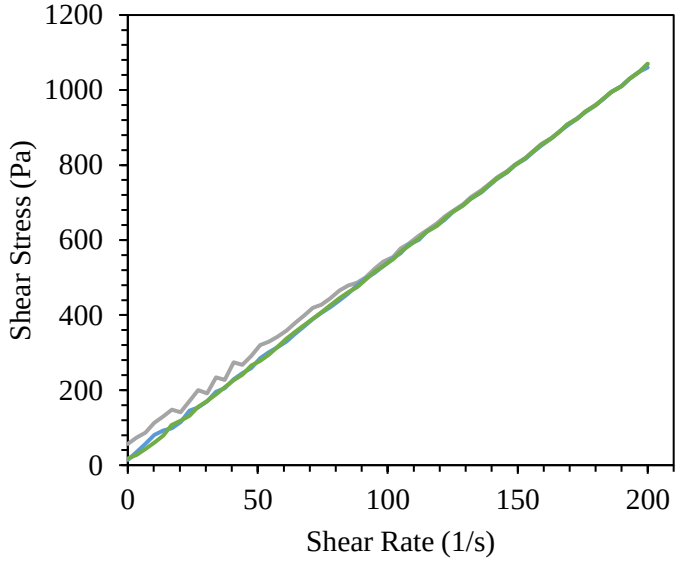

A4. Rheology measurements of carbonated fish oil, with three runs, average slope 5.19 ± 0.14 Pa·s.

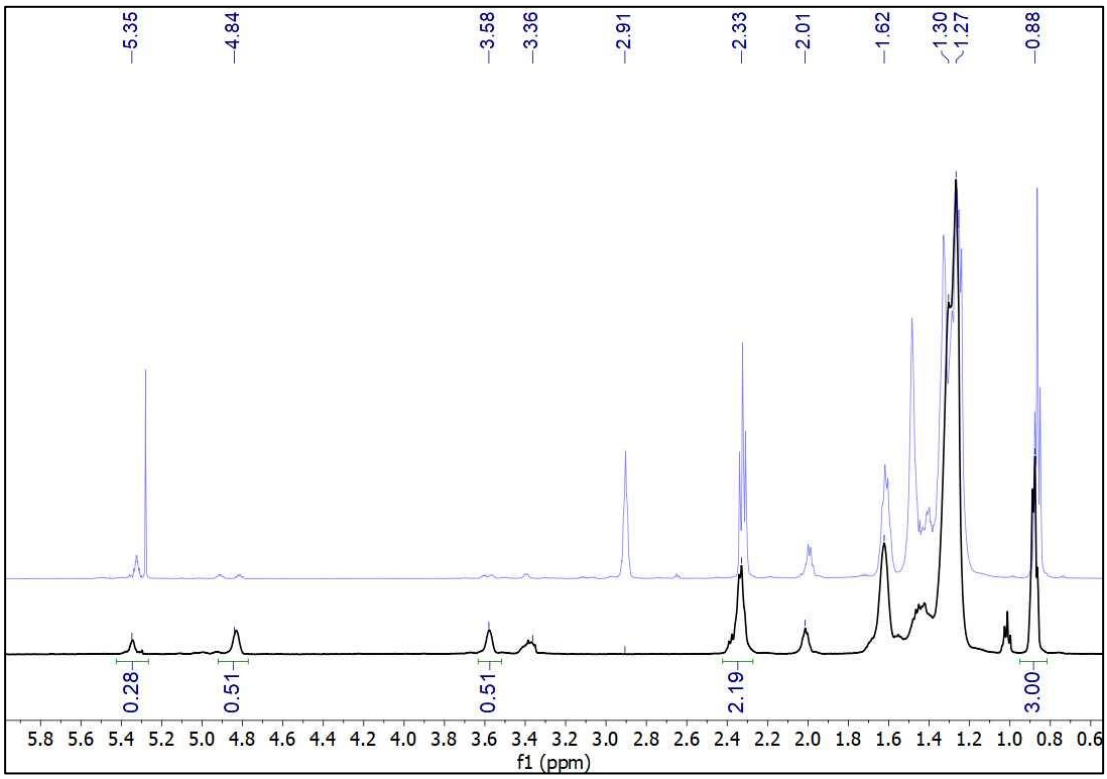

A5. ^{1}H NMR spectra of epoxidized oleic acid (top, blue) and carbonated oleic acid (bottom, black) in $CDCl_3$ at 25 °C.

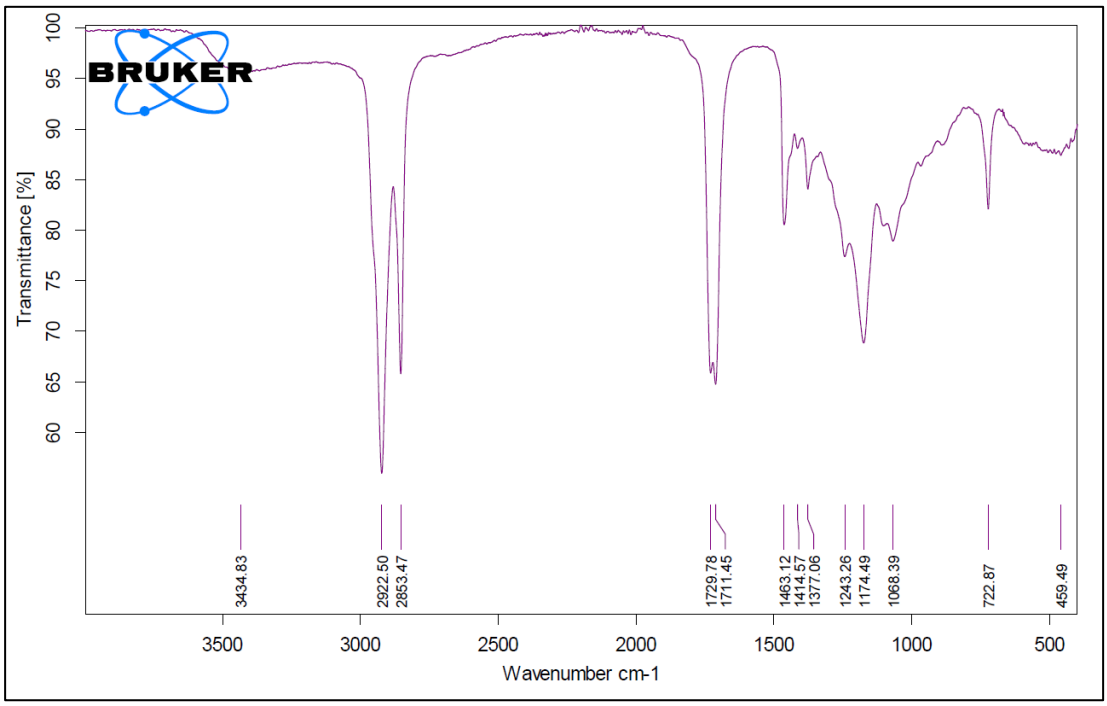

A6. IR spectrum of product from coupling reaction of epoxidized oleic acid and CO_2.